Classification of spin-$\frac{1}{2}$ fermionic quantum spin liquids on the trillium lattice

Ming-Hao Li,[1] Sounak Biswas,[1,2] and S. A. Parameswaran[1]
[1]*Rudolf Peierls Centre for Theoretical Physics, Parks Road, Oxford OX1 3PU, United Kingdom*
[2]*Institut für Theoretische Physik und Astrophysik, Universität Würzburg, 97074 Würzburg, Germany*

(Received 14 November 2024; revised 9 June 2025; accepted 17 July 2025; published 19 September 2025)

We study fermionic quantum spin liquids (QSLs) on the three-dimensional trillium lattice of corner-sharing triangles. We are motivated by recent experimental and theoretical investigations that have explored various classical and quantum spin liquid states on similar networks of triangular motifs with strong geometric frustration. Using the framework of projective symmetry groups (PSG), we obtain a classification of all symmetric Z_2 and $\mathsf{U}(1)$ QSLs on the trillium lattice. We find two Z_2 spin-liquids, and a single $\mathsf{U}(1)$ spin-liquid that is proximate to one of the Z_2 states. The small number of solutions reflects the constraints imposed by the nonsymmorphic symmetries in the space group of the trillium lattice. Using self-consistency conditions of the mean-field equations, we obtain the spinon band-structure and spin structure factors corresponding to these states. All three of our spin liquids are gapless at their saddle points: one of the two Z_2 QSLs is nodal, while the $\mathsf{U}(1)$ case hosts a spinon Fermi surface. One of our Z_2 spin liquids hosts a stable gapless nodal star that is protected by projective symmetries against additions of further neighbor terms in the mean-field ansatz. We comment on directions for further work.

DOI: 10.1103/3nmp-1vt2

I. INTRODUCTION

Spin liquids are magnetic systems that fail to order at the temperatures expected on the basis of their exchange energy scale, while exhibiting cooperative behavior that distinguishes them from high-temperature paramagnet [1,2]. A natural ingredient leading to such lack of ordering is geometric frustration, wherein the lattice structure eliminates simple ground-state configurations that minimize the exchange interaction energy between magnetic moments [3,4], and which would typically lead to symmetry breaking in the thermodynamic limit. This is manifest, for instance, in a system of three classical spins with pairwise antiferromagnetic Heisenberg interactions: the lowest-energy state of the triangle cannot be described in terms of minimal-energy configurations of each of the individual bonds. Frustrated lattices can be assembled by tiling space with such elementary units—typically triangles or tetrahedra—in order to form edge-sharing or corner-sharing structures: common examples are the triangular and kagome lattices in two dimensions (2D), and the pyrochlore and hyperkagome lattices in 3D. Classical ground states of antiferromagnets on such lattices are macroscopically degenerate [5]. These degeneracies can often be understood in the exactly solvable large-N limit: frustration is signaled by a macroscopically degenerate manifold of continuously connected ordering wavevectors [6–10]. Such "classical spin liquids" often order at very low temperatures T (much lower than the scale set by exchange couplings), in accord with the third law of thermodynamics, which forbids the finite $T \to 0$ entropy associated with an extensive ground-state degeneracy. Typically, thermal or quantum fluctuations select an ordering wave vector out of this manifold, in a phenomenon termed "order by disorder" [9,11,12]. However, in some cases the system is sufficiently frustrated that the quantum mechanical ground state selected as $T \to 0$ continues to exhibit no broken symmetries, and instead is a quantum spin liquid characterized by an emergent deconfined gauge structure. The resulting quantum spin liquid (QSL) is often strikingly characterized by the appearance of fractionalized excitations, whereas its gauge structure is more subtly encoded in certain long-range entanglement properties of the ground-state wavefunction.

A powerful framework to understand QSL ground states of quantum spin systems is provided by the projective symmetry group [13]. This framework, which makes the emergent gauge structure especially transparent, builds on the so-called "parton construction" [14–19], and proceeds by representing each spin in terms of auxiliary fermionic "spinons", $\vec{S} = \frac{1}{2} f_i^\dagger \vec{\sigma}_{ij} f_j$. The physical Hilbert space of quantum spins is recovered via the projection, i.e., by imposing the constraint that there is exactly one fermion per site. The resulting Hamiltonian of these auxiliary (or Abrikosov) fermions is generically quartic and can then be studied within a mean-field decoupling wherein operators corresponding to fermion hopping, fermion-pair creation, and fermion-pair annihilation are self-consistently determined, leading to a quadratic mean-field "ansatz". By construction, ground states of such ansatzes correspond to symmetric, disordered wavefunctions, i.e., candidate QSL states.

This parton (or "projective") construction suggests low-energy effective descriptions for these phases in terms of spinons coupled to gauge fields. Of course, the resulting

Published by the American Physical Society under the terms of the Creative Commons Attribution 4.0 International license. Further distribution of this work must maintain attribution to the author(s) and the published article's title, journal citation, and DOI.

strongly coupled problem can be challenging to treat in a controlled fashion, particularly in cases where the spinon degrees of freedom are gapless. Nevertheless, a key feature of the parton approach is that it provides a systematic framework to enumerate and classify candidate variational wavefunctions in terms of their topological structure, in much the same way that the Landau-Ginzburg formalism provides a useful starting point to investigate broken symmetries as captured by conventional mean-field wavefunctions. Such a classification is facilitated by the projection of the mean-field Hamiltonian from the large Hilbert space of auxiliary fermions back to the physical spin Hilbert space—essential in order to obtain a sensible spin wave function—which confers a "gauge structure" to the fermion Hilbert space. Specifically, mean-field ansatzes that correspond to the same physical wave function after projection are related by a gauge transformation. Consequently, the mean-field fermion ansatzes are only required to be invariant under physical symmetries up to an associated gauge transformation. In other words, the mean-field ansatz is invariant under a *projective symmetry group* (PSG) that is usually larger than the physical symmetry group of the QSL wave function. However, there exists a group of pure gauge transformations—typically Z_2, $\mathsf{U}(1)$ or $\mathsf{SU}(2)$—termed the invariant gauge group (IGG), which leaves the mean-field ansatz invariant. The IGG and PSG together characterize the low-energy, long-wavelength fluctuations around the mean-field ansatz: these involve fermions coupled to gauge fields, with the gauge group specified precisely by the IGG, and fermions in a mean-field dispersion classified by representations of the PSG.

In other words, different PSGs capture distinct "quantum orders" of QSL phases with a specified IGG, in much the same way that the physical symmetry groups characterize broken symmetries.

Notably, there can be distinct PSGs corresponding to the same physical symmetry manifest in the spin wavefunction, underscoring the fact that these "quantum orders" can be richer than their classical counterparts.

Experimental evidence for QSLs and the resulting need to characterize their emergent low-energy properties has driven a systematic program of applying the projective construction to a variety of frustrated lattices [13,20–35]. The resulting mean-field ansatzes provide starting points for more refined calculations where the projected fermion wavefunctions can be calculated variationally using Monte Carlo approaches [36–42]. The parton construction and the consequent study of QSLs and their gauge structures has been extended to higher-spin ($S > 1/2$) moments [43–45]. (Alternative parton constructions that split the spins into bosons [46–49] offer a complementary set of insights into the phenomenology of possible QSLs and their possible proximate phases.)

In this work, we continue this program by classifying symmetric spin liquid states on the trillium lattice [50], a three-dimensional network of corner-sharing triangles displayed in Fig. 1. A natural theoretical motivation of this problem is that the motif of corner-sharing triangles is expected to seed significant magnetic frustration, like the better-known kagome and hyperkagome lattices. At a more experimentally grounded level, trillium is the magnetic lattice of MnSi, or that of the Ce moments in CeIrSi, which has

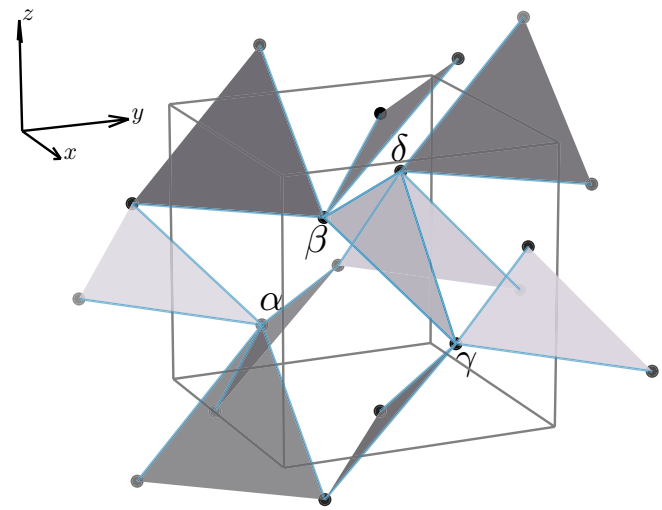


FIG. 1. The three-dimensional trillium lattice of corner-sharing triangles. Each site is shared by three triangular plaquettes. The Bravais lattice is cubic, with a basis of four sublattice sites labeled α, β, δ and γ.

been considered before in the context of frustrated magnetism [9]. Recent characterizations of the quantum spin liquid material $K_2Ni_2(SO_4)_3$ [51–53] show that the magnetic Ni^{2+} ions, with $S = 1$, lie on two interconnected trillium lattices, having exactly the same set of symmetries as single trillium lattice—implying that these structures share the classification of symmetric spin liquid states in terms of projective symmetry groups. Another compound $KSrFe_2(PO_4)_3$ with structures similar to $K_2Ni_2(SO_4)_3$, with $S = 5/2$, has been shown to exhibit no long-range order down to $T = 0.19$ K [54]. Our interest in trillium is also seeded by its remarkable similarity to the hyperhyperkagome (HHK) lattice that describes the network of coupled Cu^{2+} ions in $PbCuTe_2O_6$, which was shown to host a QSL ground state in a series of recent experiments [55–57], leading to theoretical work on spin liquid states on the underlying HHK structure [29,48]. Both trillium and HHK are three-dimensional networks of corner-sharing triangles with a cubic Bravais lattice where each site belongs to three corner-sharing triangles. Classical frustrated magnets on these lattices share similar phenomenology [9]: a large regime with classical spin liquid behavior, eventually yielding to co-planar ordering at very low temperatures. For both lattices, large-N approaches yield "partial ordering" [8,9,58,59], characterized by a macroscopic but sub-extensive set of ordering wave vectors, whose manifold forms a line (HHK) or surface (trillium) in three-dimensional reciprocal space. This is distinct from the large-N signatures of a classical spin liquid, where this manifold would be extensive [6,7,10], as obtained, e.g., for the pyrochlore, kagome and hyperkagome lattices. [Note that a recent study of classical Ising models with three-spin interactions on the trillium and HHK showed that both host very similar classical fractal spin liquids, with "fractonic" glassy behavior arising out of kinetic constraints [60]; however, this is unlikely to be directly relevant to the QSL problem studied here.]

The HHK lattice has the same space group and hence the same classification of PSGs as the three-dimensional

hyperkagome lattice [29], in which each site is shared by two (rather than three) corner sharing triangles. The latter has been the subject of numerous theoretical investigations of its ordered and spin-liquid states [10,27,28,48,61,62] motivated by its relevance to the candidate QSL material $Na_4Ir_3O_8$ [63–66].

The corresponding $P4_132$ space group has both twofold and threefold rotations and twofold, threefold, and fourfold nonsymmorphic screw rotations, with the screw symmetries known to cause a drastic reduction of the total number of QSL states [28]. In contrast, the $P2_13$ space group of trillium has threefold rotations, along with twofold and threefold nonsymmorphic screw rotations [9].

In the light of the preceding discussion, it is natural to ask what QSL phases are consistent with symmetries of the trillium lattice. To this end, in this paper we undertake a classification of PSGs for spin-1/2 QSLs on this lattice. Although experiments [51–53] indicate that $K_2Ni_2(SO_4)_3$ is best understood as an effective spin-1 system, understanding the simpler spin-1/2 case is an important first step towards a more comprehensive study of the higher-spin problem. Accordingly, we hope that the present work will guide the interpretation of results of future experiments, and add to our theoretical understanding of QSL phases in three dimensions.

The rest of this paper is organized as follows. In Sec. III A, we introduce the crystal structure of the trillium lattice and the symmetry generators of its space group. In Sec. III B, we present the symmetry group relations of trillium, and outline the classification of its PSGs using them. We also present the gauge transformations accompanying physical symmetries for all of the PSGs. The details are relegated to Appendices A and B.

II. BACKGROUND: PROJECTIVE SYMMETRY GROUP FORMALISM

We briefly review the projective symmetry group classification of parton mean-field theories, as applied to spin models with Heisenberg exchange interactions. Readers familiar with the parton approach can jump ahead to the next section, but may wish to quickly skim this section to orient themselves with our notation and conventions. We begin with the Heisenberg model on a given spatial lattice,

$$H = \sum_{\{i,j\}} J_{ij} \vec{S}_i \cdot \vec{S}_j. \tag{1}$$

In order to implement the PSG, we first enlarge the Hilbert space by decomposing spins into Abrikosov fermions as follows:

$$\vec{S}_i = \sum_{\alpha,\beta} \frac{1}{2} f^\dagger_{i\alpha} \vec{\sigma}_{\alpha\beta} f_{i\beta}. \tag{2}$$

The above equation maps the spin Hilbert space to the subspace of the Abrikosov fermion Hilbert space in which the fermion occupation number on each site is 1. This means that, on the operator level, we strictly have $\sum_\alpha f^\dagger_{i\alpha} f_{i\alpha} = \mathrm{Id}$. Indeed, by using the identity, we can verify that $[S^m, S^n] = i\epsilon_{lmn} S^l$. In fact, a second constraint, is also introduced as a consequence of the first: $\sum_{\alpha,\beta} f_{i\alpha} f_{i\beta} \epsilon_{\alpha\beta} = 0$. (One can verify by considering $\sum_{\alpha,\beta} f_{i\alpha} f_{i\beta} \epsilon_{\alpha\beta} \sum_\gamma f^\dagger_{i\gamma} f_{i\gamma} |\psi\rangle$, where $\sum_\gamma f^\dagger_{i\gamma} f_{i\gamma} |\psi\rangle = |\psi\rangle$ by virtue of single occupancy.)

In terms of the Abrikosov fermions, the Heisenberg Hamiltonian reads (up to some constants)

$$\begin{aligned} H &= \sum_{\{i,j\}} \sum_{\alpha\beta\mu\nu} J_{ij} \frac{1}{4} (f^\dagger_{i\alpha} \vec{\sigma}_{\alpha\beta} f_{i\beta}) \cdot (f^\dagger_{j\mu} \vec{\sigma}_{\mu\nu} f_{j\nu}) \\ &= \sum_{\{i,j\}} \sum_{\alpha\beta} -\frac{1}{2} J_{ij} \left(f^\dagger_{i\alpha} f_{j\alpha} f^\dagger_{j\beta} f_{i\beta} + \frac{1}{2} f^\dagger_{i\alpha} f_{i\alpha} f^\dagger_{j\beta} f_{j\beta} \right). \end{aligned} \tag{3}$$

We now study H within a mean-field approximation, by introducing parameters for expectation values of operators

$$\eta_{ij} \epsilon_{\alpha\beta} = -2\langle f_{i\alpha} f_{j\beta} \rangle, \quad \chi_{ij} \delta_{\alpha\beta} = 2\langle f^\dagger_{i\alpha} f_{j\beta} \rangle, \tag{4}$$

where $\eta_{ij} = \eta_{ji}$ and $\chi_{ij} = \chi^\dagger_{ji}$.

As is usual, we expand operators in Eq. (3) in terms of fluctuations about their expectation values and ignore terms that are quadratic in fluctuations, leading to

$$\begin{aligned} H_{\mathrm{MFT}} = &- \sum_{\langle i,j \rangle} \frac{3}{8} J_{ij} (\chi_{ji} f^\dagger_{i\mu} f_{j\mu} + \eta_{ij} \epsilon_{\mu\nu} f^\dagger_{i\mu} f^\dagger_{j\nu} + \mathrm{H.c.} \\ &- |\chi_{ij}|^2 - |\eta_{ij}|^2) + \sum_i \Big(\mu^3_i (f^\dagger_{i\uparrow} f_{i\uparrow} - f_{i\downarrow} f^\dagger_{i\downarrow}) \\ &+ \frac{1}{2} (\mu^1_i + i\mu^2_i) f_{i\mu} f_{i\nu} \epsilon_{\mu\nu} + \mathrm{H.c.} \Big), \end{aligned} \tag{5}$$

where we have introduced the Lagrange multipliers $\mu^{1,2,3}_i$ to impose the one-fermion-per-site constraint at a mean-field level. These, as well as the parameters χ_{ij} and η_{ij}, are determined self consistently.

To discuss the SU(2) gauge structure of the mean-field Hamiltonian, it is convenient to introduce a spinor representation

$$\psi \equiv \begin{bmatrix} \psi_1 \\ \psi_2 \end{bmatrix} \equiv \begin{bmatrix} f_\uparrow \\ f^\dagger_\downarrow \end{bmatrix}. \tag{6}$$

In terms of these spinors, the H_{MFT} can be be compactly rewritten as

$$\begin{aligned} H_{\mathrm{MFT}} = &\sum_{\langle i,j \rangle} \frac{3}{8} J_{ij} \left[\frac{1}{2} \mathrm{Tr}(U^\dagger_{ij} U_{ij}) - (\psi^\dagger_i U_{ij} \psi_j + \mathrm{H.c.}) \right] \\ &+ \sum_{i,l} \mu^l_i \psi^\dagger_i \tau^l \psi_i, \end{aligned} \tag{7}$$

where the matrix U_{ij} captures both mean-field parameters via

$$U_{ij} \equiv \begin{bmatrix} \chi^\dagger_{ij} & \eta_{ij} \\ \eta^\dagger_{ij} & -\chi_{ij} \end{bmatrix}. \tag{8}$$

The constraint implementing projection into the spin Hilbert space at the mean-field level now has the form

$$\langle \psi^\dagger_i \tau^l \psi_i \rangle = 0, \quad l = 1, 2, 3. \tag{9}$$

The $\{U_{ij}\}$ and $\{\mu^m_i\}$ together constitute variational parameters that specify the mean-field "ansatz" for the Hamiltonian and the corresponding ground-state wavefunction. Variationally optimizing the parameters to obtain the lowest energy

ground state is equivalent to determining the parameters self-consistently.

It is crucial to realize that the ground state of the mean-field spinon Hamiltonian is not a valid spin wave function, since the on-site constraints are only enforced *on average*. The final wavefunction in terms of the physical spin degrees of freedom is constructed from the mean-field spinon state by Gutzwiller projection, i.e., $|\Psi_{\text{spin}}\rangle = P_G|\Psi_{\text{MFT}}\rangle$.

The spinor representation makes the $\mathsf{SU}(2)$ gauge redundancy of the mean-field Hamiltonian manifest. The Hamiltonian is invariant, trivially, under the site-dependent gauge transformation $\psi_i \mapsto W_i\psi_i, U_{ij} \mapsto W_iU_{ij}W_j^\dagger$ and $\mu_i^m \mapsto W_i\mu_i^mW_i^\dagger$, with $W_i \in \mathsf{SU}(2)$ since this leaves physical spin operator invariant [cf. (2)]. Therefore, the mean-field ansatzes parametrised by U_{ij}, μ_i^m and $W_iU_{ij}W_j^\dagger, W_i\mu_i^mW_i^\dagger$ share the same physical spin wavefunctions, i.e., after projection into the spin Hilbert space. This has significant consequences for what we require of symmetric mean-field ansatzes. Consider the action of a symmetry $g : U_{ij} \mapsto U_{g(i)g(j)}$. For a symmetric ansatz we no longer require $U_{g(i)g(j)} = U_{ij}$; instead, we only require that there exist transformations $G_g(n) \in \mathsf{SU}(2)$ for all sites n, such that $G_g(g(i))U_{g(i)g(j)}G_g^\dagger(g(j)) = U_{ij}$. The gauge redundancy then implies that the physical properties of the state represented by the ansatz have not changed. The physical transformations g together with the gauge transformation, $(G_g(i), g)$, which leaves the ansatz invariant, constitute the *projective symmetry group* (PSG). The PSG characterizes the symmetries of the ansatz, and serves to classify and characterize different mean-field spin liquid states.

The PSG also determines the low-energy description of fluctuations around the mean-field states. From the preceding discussion on the gauge structure it is clear that not all fluctuations of the mean-field parameters $\{U_{ij}\}$ are physical: the unphysical fluctuations between gauge inequivalent states must be described by gauge fields in the effective theory. The effective theories, then, are likely to be fermions coupled to gauge fields. The gauge structure of the low-energy theory is in general not given by the high-energy gauge group $\mathsf{SU}(2)$, but is instead determined by the "invariant gauge group" (IGG) [13]. The IGG is a subgroup of the PSG comprised of pure gauge transformations that leave the ansatz invariant, i.e., $\mathcal{G} = \{W_i|W_iU_{ij}W_j^\dagger = u_{ij}, W \in \mathsf{SU}(2)\}$. Given the central importance of the IGG, one usually labels QSLs by the IGG, leading to the terminology of "Z_2, $\mathsf{U}(1)$, or $\mathsf{SU}(2)$" QSLs. The PSGs, therefore, play a role for mean-field QSL phases akin to that of ordinary symmetry groups for broken-symmetry phases, distinguishing quantum disordered states with the same physical symmetries but different emergent properties.

This is a good place to flag one final complication: namely, that certain PSGs do not correspond to nonzero mean-field ansatzes. Therefore, simply tabulating the list of PSGs does not conclude the classification of QSLs; it is essential to investigate the physical constraints that each imposes on the mean-field ansatzes. Despite this complication, it is nevertheless useful to organize the investigation of symmetric spin liquid ground states on a given spatial lattice in terms of an enumeration of all PSGs, for a given set of physical symmetries (typically, the full lattice space group as well as time-reversal symmetry) and the IGG. This allows the construction of the corresponding mean-field ansatzes and spin liquid wavefunctions. In the balance of this paper, we implement such a program for the trillium lattice.

TABLE I. The labeling of the 12 translationally inequivalent nearest-neighboring links for a unit cell, indexed by ζ. Each link is specified by the unit-cell positions and sublattice indices of the two lattice sites making up the link. For a given label ζ, the head of the bond is labeled i and the end is labeled j. $\vec{u}_{i/j}$ is the position of the unit cell, whereas $s_{i/j}$ is the sublattice index.

ζ	$\vec{u}_j - \vec{u}_i$	(s_i, s_j)
1	(0,0,0)	(β, γ)
2	(0,0,1)	(β, γ)
3	(0,1,1)	(δ, α)
4	(0,1,0)	(δ, α)
5	(0,0,0)	(γ, δ)
6	(1,0,0)	(γ, δ)
7	(1,0,1)	(β, α)
8	(0,0,1)	(β, α)
9	(0,0,0)	(δ, β)
10	(0,1,0)	(δ, β)
11	(1,1,0)	(γ, α)
12	(1,0,0)	(γ, α)

III. PSGS OF THE TRILLIUM LATTICE

A. The trillium lattice

We begin by describing the trillium lattice and its spatial symmetries. These, along with time-reversal symmetry, constitute the physical symmetries that our QSL ground states (after projection to the correct Hilbert space) must respect, and are hence central to the PSG construction.

The trillium lattice, shown in Fig. 1, has a simple cubic Bravais lattice with four sublattices: α, β, γ, and δ. The positions of the sublattice sites relative to the unit cell center are given by

$$\begin{aligned} \vec{r}_\alpha^0 &= (\kappa, \kappa, \kappa), \quad \vec{r}_\beta^0 = \left(\tfrac{1}{2} + \kappa, \tfrac{1}{2} - \kappa, 1 - \kappa\right), \\ \vec{r}_\gamma^0 &= \left(1 - \kappa, \tfrac{1}{2} + \kappa, \tfrac{1}{2} - \kappa\right), \\ \vec{r}_\delta^0 &= \left(\tfrac{1}{2} - \kappa, 1 - \kappa, \tfrac{1}{2} + \kappa\right), \end{aligned} \tag{10}$$

where κ is a free parameter. As mentioned before, the nearest-neighbor bonds on the lattice form a network of corner sharing triangles, with each site participating in three triangles, which are the elementary frustrated motifs.

We denote the position of a unit cell i by the vector $\vec{u}_i = (x, y, z)$, where x, y, z are integers. A generic lattice site i is referred to by specifying its unit cell position and sublattice as $i \equiv (x, y, z; s)$; such a site lies at position $\vec{u}_i + \vec{r}_s^0$. Since the mean-field parameters $\{U_{ij}\}$ specifying the ansatz are associated with the links, it is convenient to uniquely label all links. We do so by exploiting lattice translation invariance: there are 12 links per unit cell, all of which are translationally inequivalent. We introduce the labels $\zeta = (1, 2 \ldots 12)$ for these links, and specify each of these links in Table I.

Trillium has space group $\mathsf{P2_13}$, with the symmetry generators $\{T_x, T_y, T_z, g_a, g_b, g_c\}$. Here, T_is are the three translational

generators. g_c is a threefold rotation about the (1,1,1) axis passing through the origin of an unit cell. g_a and g_b are the generators of the twofold nonsymmorphic screw rotations. g_a involves a π rotation about an axis in the (0,0,1) direction passing through the point $(1/4, 0, 0)$, followed by a translation by $1/2$ of the unit-cell distance along the rotation axis. g_b involves a π rotation about an axis in the direction (0,1,0) passing through the point $(0, 0, 1/4)$ followed by a translation of $1/2$ of the unit-cell distance along the rotation axis. It has been noted previously [28] that nonsymmorphic symmetries generally lead to strong constraints on possible PSGs, and a consequent reduction in their number.

The generators g_a, g_b, and g_c act on a lattice site $i \equiv (x, y, z, s)$ via

$$\begin{aligned}
g_a :&(x, y, z; \alpha) \mapsto (-x, -y-1, z; \delta),\\
&(x, y, z; \beta) \mapsto (-x-1, -y-1, z+1; \gamma),\\
&(x, y, z; \gamma) \mapsto (-x-1, -y-1, z; \beta),\\
&(x, y, z; \delta) \mapsto (-x, -y-1, z+1; \alpha),\\
g_b :&(x, y, z; \alpha) \mapsto (-x-1, y, -z; \gamma),\\
&(x, y, z; \beta) \mapsto (-x-1, y, -z-1; \delta),\\
&(x, y, z; \gamma) \mapsto (-x-1, y+1, -z; \alpha),\\
&(x, y, z; \delta) \mapsto (-x-1, y+1, -z-1; \beta),\\
g_c :&(x, y, z; \alpha) \mapsto (z, x, y; \alpha),\\
&(x, y, z; \beta) \mapsto (z, x, y; \gamma),\\
&(x, y, z; \gamma) \mapsto (z, x, y; \delta),\\
&(x, y, z; \delta) \mapsto (z, x, y; \beta).
\end{aligned} \tag{11}$$

The set of generators presented here is the one presented in standard sources of crystallographic data [67–69]. We note that this generating set is not "minimal"; only the threefold rotation g_a and one of the screws g_a and g_b suffice to generate the space group. The choice of the generating set in standard sources is usually made to highlight important subgroups of the space group (in the specific case of $\mathsf{P2_13}$, T_x, T_y, and T_z generate the translation group, while adding g_a and g_b generates $\mathsf{P2_12_12_1}$.

B. PSG classification on the trillium lattice

The PSG involves the group of transformations $(G_g(n), g)$ that leave the mean-field ansatz invariant. Here g is a physical symmetry transformation, and $G_g(n) \in \mathsf{SU(2)}$ is the associated site-dependent gauge transformation, with n denoting the physical site. $(G_g(n), g)$ acts on a mean-field parameter U_{ij} as

$$(G_g(n), g) : U_{ij} \mapsto G_g(i) U_{g^{-1}(i) g^{-1}(j)} G_g^\dagger(j). \tag{12}$$

It follows from consecutive action on the ansatz that the product of two PSG elements is given by the group compatibility condition

$$\big(G_{g_1}(n), g_1\big) \circ \big(G_{g_2}(n), g_2\big) = \big(G_{g_1}(n) G_{g_2}\big(g_1^{-1} n\big), g_1 g_2\big), \tag{13}$$

and the group inverse by

$$\big(G_{g_1}(n), g_1\big)^{-1} = \big[G_{g_1}^\dagger(g_1(n)), g_1^{-1}\big]. \tag{14}$$

Since the elements of the IGG $\mathcal{G}$ are pure gauge transformations that leave the ansatz invariant, it is clear that whenever $(G_g(i), g)$ is an element of the PSG, $(W G_g(i), g)$, for all $W \in \mathcal{G}$, is also an element of the PSG. If one considers a gauge-equivalent ansatz $W_i U_{ij} W_j^\dagger$, the PSG element $(G_g(i), g)$ changes to $(W_i G_g(i) W^\dagger_{g^{-1}(i)})$. PSGs related by such gauge transformations are equivalent; they are associated with gauge-equivalent ansatzes and represent the same QSL phase. Our task is to find all such equivalence classes; in other words, to single out one representative from each class by fixing the gauge freedom.

It is convenient to carry out this task purely "algebraically", i.e., by making no reference to the ansatz. To do this, we note that given a physical symmetry group and the IGG $\mathcal{G}$, the PSG can be viewed as a group equipped with a projection $\mathcal{P}$ to the physical symmetry group, such that $\mathcal{P} : (G_g(i), g) \mapsto g$. From the discussion in the previous paragraph, $\mathcal{P} : (W G_g(i), g) \mapsto g$ for $W \in \mathcal{G}$. As a corollary, $\mathcal{P}$ projects pure gauge transformations in the IGG back to the identity element, $\mathcal{P} : (W, e) \mapsto e$ for $W \in \mathcal{G}$.

The projection map between the PSG and the physical symmetry group implies that the gauge transformation $G_g(i)$ associated with the symmetry transformation g is constrained by the relations between symmetry group elements g. These constraints on G_g can be used to enumerate all gauge-inequivalent choices of G_g for all symmetry transformations g, and hence enumerate all PSGs.

To see this, one begins with the relations between the symmetry generators $\{T_x, T_y, T_z, g_a, g_b, g_c, \mathcal{T}\}$ that completely specify the group. Each such relation will lead to an equation constraining the associated PSG elements. The minimal set of such relations that specify the group is called the "presentation" of the group. Using the GAP programming language [70], which provides finite presentations of all space groups in terms of the standard [67–69] generating set, we obtain a finite presentation of the trillium space group,

$$g_c^3 = e, \tag{15a}$$
$$T_z^{-1} g_a^2 = e, \tag{15b}$$
$$T_y^{-1} g_b^2 = e, \tag{15c}$$
$$T_x^{-1} T_y^{-1} T_x T_y = e, \tag{15d}$$
$$T_y^{-1} T_z^{-1} T_y T_z = e, \tag{15e}$$
$$T_z^{-1} T_x^{-1} T_z T_x = e, \tag{15f}$$
$$g_a^{-1} T_x g_a T_x = e, \tag{15g}$$
$$g_a^{-1} T_y g_a T_y = e, \tag{15h}$$
$$g_a^{-1} T_z^{-1} g_a T_z = e, \tag{15i}$$
$$g_b^{-1} T_x g_b T_x = e, \tag{15j}$$
$$g_b^{-1} T_y^{-1} g_b T_y = e, \tag{15k}$$
$$g_b^{-1} T_z g_b T_z = e, \tag{15l}$$
$$g_c^{-1} T_y^{-1} g_c T_x = e, \tag{15m}$$
$$g_c^{-1} T_z^{-1} g_c T_y = e, \tag{15n}$$
$$g_c^{-1} T_x^{-1} g_c T_z = e, \tag{15o}$$

$$g_a^{-1} g_c^{-1} g_b^{-1} T_x^{-1} T_y g_a g_c = e, \tag{15p}$$

$$g_b^{-1} g_a^{-1} T_x T_y^{-1} T_z g_b g_a = e, \tag{15q}$$

$$g_c^{-1} g_b^{-1} T_x^{-1} T_y g_a g_b g_c g_b = e, \tag{15r}$$

where e denotes the identity of the symmetry group.

We focus further on QSLs on the trillium lattice that respect time-reversal symmetry (TRS). The TRS operator $\mathcal{T}$ acts on the mean-field ansatz by complex conjugating the mean-field parameters U_{ij} and μ_i. It is convenient to include a global gauge transformation $i\tau_2$ in the definition of $G_\mathcal{T}$, such that we have

$$\begin{aligned}(G_\mathcal{T}, \mathcal{T}) : U_{ij} &\mapsto G_\mathcal{T}(i) i\tau_2 U_{ij}^* (-i\tau_2) G_\mathcal{T}^\dagger(j) \\ &= -G_\mathcal{T}(i) U_{ij} G_\mathcal{T}^\dagger(j).\end{aligned} \tag{16}$$

Including TRS introduces the following additional relations, which express the fact that $\mathcal{T}$ commutes with generators in the space group:

$$\mathcal{T}^2 = e, \tag{17a}$$

$$\mathcal{T}^{-1} T_x^{-1} \mathcal{T} T_x = e, \tag{17b}$$

$$\mathcal{T}^{-1} T_y^{-1} \mathcal{T} T_y = e, \tag{17c}$$

$$\mathcal{T}^{-1} T_z^{-1} \mathcal{T} T_z = e, \tag{17d}$$

$$\mathcal{T}^{-1} g_a^{-1} \mathcal{T} g_a = e, \tag{17e}$$

$$\mathcal{T}^{-1} g_b^{-1} \mathcal{T} g_b = e, \tag{17f}$$

$$\mathcal{T}^{-1} g_c^{-1} \mathcal{T} g_c = e. \tag{17g}$$

Chiral spin liquids, which break TRS and some lattice symmetries individually while preserving their combinations, have also been discussed in the literature [26,71,72]. For chiral PSGs, one considers the symmetry group generated by $g\mathcal{T}^{\epsilon_g}$ instead of the usual symmetry group generated by $\{g\}$ [26,71]. $\epsilon_g = \{0, 1\}$ specifies whether the lattice symmetry g is preserved on its own ($\epsilon_g = 0$), or preserved only up to TRS ($\epsilon_g = 1$). The trillium SG relations given by Eqs. (15a)–(15r) impose the constraint $\epsilon_g = 0$ for all generators. This can be easily seen from the fact that for each generator g, there exists one SG relation that has only an odd number of appearances of that generator, which forces $\epsilon_g = 0$. One could still consider spin liquids that respect all lattice symmetries but not TRS. In all our PSG calculations, we first derive the PSG classification without TRS, and then impose TRS at the end. While this immediately gives us the PSGs without TRS, we do not consider mean-field ansatzes corresponding to such PSGs, restricting ourselves to the study of fully symmetric physical spin liquids. Ground states for classical spins on the trillium lattice [9] are also known to be nonchiral (which, for classical spin configurations, is equivalent to co-planarity).

The projective relation between the symmetry group elements and the corresponding PSG elements allows us to translate the above symmetry relations [Eqs. (15a)–(17g)] into constraint equations for the PSG elements. Consider a general symmetry group relation among a set of elements, $\prod_\nu g_\nu = e$. The product of the corresponding PSG elements is given by $(\tilde{G}, \prod_\nu g_\nu = e)$, where $\tilde{G}$ can be constructed from the matrices $G_{g_\nu}(i)$ using Eq. (13). Under the projection $\mathcal{P}$ to the symmetry group elements $(\tilde{G}, e) \mapsto e$); this immediately implies a constraint equation expressing that $\tilde{G}$ must be a member of the IGG, $\tilde{G} \in \mathcal{G}$.

The unknowns in these equations are of two kinds: first, the site-dependent gauge transformation matrices $\{G_x, G_y, G_z, G_a, G_b, G_c, G_\mathcal{T}\}$ accompanying each symmetry transformation in $\{T_x, T_y, T_z, g_a, g_b, g_z, \mathcal{T}\}$; and second, an element of the IGG $W \in \mathcal{G}$ corresponding to each symmetry group relation in Eqs. (15a)–(17g). Solving these equations, along with a choice of gauge described earlier, leads to the different inequivalent PSGs.

Explicit procedures for solving these equations in a fixed gauge are detailed for specific lattices in Ref. [13], as well as several later works classifying PSGs in different spatial lattices [26,28]. We have undertaken this procedure to enumerate and classify all symmetric spin liquids with the IGG set to both Z_2 and $\mathsf{U}(1)$. The calculations are tedious, and hence we have relegated their details to the Appendices A and B for conciseness. Each inequivalent PSG is uniquely specified by the expressions for site-dependent gauge transformations $\{G_x, G_y, G_z, G_a, G_b, G_c, G_\mathcal{T}\}$ that accompany the symmetry transformation. We now summarize our results by specifying these gauge transformations for all the PSGs that we identify.

When the IGG is fixed to Z_2, we find four inequivalent PSGs. Once the global gauge freedoms are fixed, the gauge transformation matrices associated with lattice translations are uniform, with no position or sublattice dependence for all PSGs, i.e., $G_x = G_y = G_z = 1$. The PSGs can be uniquely indexed by constraints on the gauge transformation matrices obtained from the PSG equations. First, the transformation corresponding to time-reversal $G_\mathcal{T}$ takes the values τ_0 or $i\tau_z$, though the PSGs corresponding to $G_\mathcal{T} = \tau_0$ do not lead to any nonzero mean-field ansatzes. Gauge transformation matrices associated with other symmetry generators are also unit-cell independent, although they retain a sublattice dependence. Second, the gauge transformation associated with the rotation g_c acting on sites of sublattice α, $G_c(\alpha) = \mathcal{A}$, takes the two values $\exp(ik(2\pi/3)\tau_z)$ for $k = \{0, 1\}$. All other gauge transformations can be specified in terms of these three, as detailed in Table II. The two possible values of $G_c(\alpha)$ and the two possible values of $G_\mathcal{T}$ lead to four inequivalent PSGs, out of which only two (corresponding to $G_\mathcal{T} = i\tau_z$) lead to nonzero mean-field ansatzes.

Next, we fix the IGG to $\mathsf{U}(1)$. As in the case of Z_2, the gauge transformations corresponding to the three translations are uniform, $G_x = G_y = G_z = 1$. The PSGs can again be indexed by the parameters specifying certain gauge transformations. The gauge transformation associated with the rotation g_c acting on sites of sublattice α, $G_c(\alpha) = \mathcal{A}$, takes the two values $\exp(ik(2\pi/3)\tau_z)$ for $k = \{0, 1\}$. On including time reversal, we find two possibilities for the associated gauge-transformation $G_\mathcal{T}$. First, $G_\mathcal{T}$ can be $i\tau_z$ uniformly, and this case does not lead to any physical spin-liquid ansatz with nonzero mean-field parameters, and so we do not consider these PSGs further. Second, $G_\mathcal{T}$ can acquire a space-dependent form depending on A, which leads to physical spin liquids. Following the second possibility, therefore, we have one $\mathsf{U}(1)$ spin liquid, as we will later show that only the $k = 0$ case leads to nearest-neighbor mean-field spin liquid states. We specify the PSGs by expressing all gauge transformations

TABLE II. The Z_2 PSG solutions for the trillium lattice with the symmetry group $\mathsf{P2}_1\mathsf{3} \times \mathsf{Z}_2^{\mathcal{T}}$. Here, $\mathcal{A} = \tau_0, e^{i\frac{2\pi}{3}\tau_z}$, and $\mathcal{E} = \tau_0, i\tau_z$. Thus in total we have four Z_2 PSG. We will, however, note that the $\mathcal{E} = \tau_0$ cases do not produce physical mean-field ansatzes. If TRS is not included, we have two PSG solutions.

	G_x	G_y	G_z	G_a	G_b	G_c	$G_{\mathcal{T}}$
$(\vec{u}, \alpha)$	τ_0	τ_0	τ_0	τ_0	$\mathcal{A}^\dagger$	$\mathcal{A}$	$\mathcal{E}$
$(\vec{u}, \beta)$	τ_0	τ_0	τ_0	$\mathcal{A}$	$\mathcal{A}^\dagger$	τ_0	$\mathcal{E}$
$(\vec{u}, \gamma)$	τ_0	τ_0	τ_0	$\mathcal{A}^\dagger$	$\mathcal{A}$	τ_0	$\mathcal{E}$
$(\vec{u}, \delta)$	τ_0	τ_0	τ_0	τ_0	$\mathcal{A}$	τ_0	$\mathcal{E}$

in terms of the parameters A in Table III. In the next section, we will construct mean-field ansatzes for spin liquids corresponding to these PSGs and proceed to investigate them.

IV. MEAN-FIELD SPIN LIQUID PHASES

In this section, we construct the mean-field QSL solutions to the Heisenberg Hamiltonian on the trillium lattice. For this purpose, we will consider only nearest-neighbor interactions and set $J = 8/3$ henceforth. The form of the ansatzes are constrained by the PSG. Concretely, a given PSG (G_g, g), $g \in \mathsf{P2}_1\mathsf{3} \times \mathsf{Z}_2^{\mathcal{T}}$ requires that

$$\begin{aligned} \forall g: \; & G_g^\dagger(g(i)) U_{g(i)g(j)} G_g(g(j)) = U_{ij}, \\ & G_g^\dagger(g(i)) \mu_{g(i)} G_g(g(i)) = \mu_i. \end{aligned} \tag{18}$$

The ansatz for each PSG is derived by systematically imposing Eq. (18) using the gauge transformations detailed in Tables II and III; the results of this procedure, detailed in Appendix C, are tabulated in Table IV. The labeling scheme in the table is such that, given a label $\mathsf{Z}_2 x$, we can read off the phases in our PSG solutions of Table II with $\mathcal{A} = \exp(ix\frac{2\pi}{3}\tau_z)$. There is only 1 $\mathsf{U}(1)$ QSL, which is labeled as such. The primed parameters, i.e., quantities like $U^{x'}$, are defined as follows:

$$\begin{aligned} \begin{bmatrix} U^{x'} \\ U^{y'} \end{bmatrix} &= \frac{1}{2}\begin{bmatrix} -1 & \sqrt{3} \\ -\sqrt{3} & -1 \end{bmatrix}\begin{bmatrix} U^x \\ U^y \end{bmatrix}, \\ \begin{bmatrix} U^{x''} \\ U^{y''} \end{bmatrix} &= \frac{1}{2}\begin{bmatrix} -1 & -\sqrt{3} \\ \sqrt{3} & -1 \end{bmatrix}\begin{bmatrix} U^x \\ U^y \end{bmatrix}. \end{aligned} \tag{19}$$

Concretely, this means we need to find $\{U_{ij}, \mu_i\}$ such that the following self-consistency equations and on-site constraints are satisfied:

$$\begin{aligned} \chi_{ij} &= \langle f_{i\uparrow}^\dagger f_{j\uparrow}\rangle + \langle f_{i\downarrow}^\dagger f_{j\downarrow}\rangle, \\ \eta_{ij} &= \langle f_{i\downarrow} f_{j\uparrow}\rangle - \langle f_{i\uparrow} f_{j\downarrow}\rangle, \\ 1 &= \langle f_{i\uparrow}^\dagger f_{i\uparrow}\rangle + \langle f_{i\downarrow}^\dagger f_{i\downarrow}\rangle, \\ 0 &= \langle f_{i\uparrow} f_{i\downarrow}\rangle. \end{aligned} \tag{20}$$

We can impose symmetry conditions on the mean-field solutions to reduce the number of parameters, and the PSG determines these symmetry conditions by requiring that Eq. (12) is respected. We discuss how the symmetry conditions constrain the mean-field ansatzes in detail in Appendices A and B, and the results are tabulated in Table IV. Once we obtain the form of the mean-field Hamiltonians, we assemble the Hamiltonian using our variational parameters, and solve the nonlinear equation set Eq. (20) using the NLSOLVE package [73] available in JULIA [74]. We set up our system with periodic boundary conditions (PBC), with $L = 99$ in the three directions.

The numerical values of mean-field parameters and the corresponding energies obtained from the self-consistent solutions are summarized in Table V. Note that the mean-field energies of the $\mathsf{Z}_2 0$ and $\mathsf{U}(1)$ state are the same, while $\mathsf{Z}_2 1$ has a higher energy. A comment on the close energies of the $\mathsf{Z}_2 0$ and $\mathsf{U}(1)$ states is in order. The ansatzes corresponding to these states are uniform, i.e., $U_{ij} = U^x\tau_x + U^y\tau_y$ $(\mu^i = \mu^x\tau_x + \mu^y\tau_y)$ for all links (sites) of the $\mathsf{Z}_2 0$ state while $U_{ij} = U^z\tau_z$ $(\mu_i = \mu^z\tau_z)$ uniformly on all links (sites) of the $\mathsf{U}(1)$ state. The saddle-point solutions for the mean-field parameters of the $\mathsf{Z}_2 0$ state have the property $|\mu^x/\mu^y| = |U^x/U^y|$. Thus we can use a global $\mathsf{SU}(2)$ transformation to change this ansatz—only at the saddle point—to the $\mathsf{U}(1)$ ansatz displayed in Table IV. Similar phenomenon has been noted in previous works such as [28]. Therefore, while the

TABLE III. The $\mathsf{U}(1)$ PSG solutions for the trillium lattice with the symmetry group $\mathsf{P2}_1\mathsf{3} \times \mathsf{Z}_2^{\mathcal{T}}$. When TRS is not included, the PSG solutions are characterized by A, where we have $A = 0, \frac{2\pi}{3}$. When TRS is included, there are two classes of PSG solutions. (1) $n_{\mathcal{T}} = 1$: in this class, no new constraint is introduced; (2) $n_{\mathcal{T}} = 0$: in this class, we have $G_{\mathcal{T}} = i\tau_z$ uniformly. Later we will see that only the case with $A = 0$ and $n_{\mathcal{T}} = 1$ leads to physical nearest-neighbor mean-field ansatz invariant under the PSG actions. Thus in total we have four $\mathsf{U}(1)$ PSG. If TRS is not included, we have two PSG solutions.

	G_x	G_y	G_z	G_a	G_b	G_c	$G_{\mathcal{T}}$ $(n_{\mathcal{T}} = 1)$	$G_{\mathcal{T}}$ $(n_{\mathcal{T}} = 0)$
$(\vec{u}, \alpha)$	τ_0	τ_0	τ_0	τ_0	$e^{-iA\tau_z}$	$e^{iA\tau_z}$	$i\tau_x e^{iA\tau_z}$	$i\tau_z$
$(\vec{u}, \beta)$	τ_0	τ_0	τ_0	$e^{iA\tau_z}$	$e^{-iA\tau_z}$	τ_0	$i\tau_x$	$i\tau_z$
$(\vec{u}, \gamma)$	τ_0	τ_0	τ_0	$e^{-iA\tau_z}$	$e^{iA\tau_z}$	τ_0	$i\tau_x e^{-iA\tau_z}$	$i\tau_z$
$(\vec{u}, \delta)$	τ_0	τ_0	τ_0	τ_0	$e^{iA\tau_z}$	τ_0	$i\tau_x e^{iA\tau_z}$	$i\tau_z$

TABLE IV. Forms of the nearest-neighbor mean-field ansatz corresponding to the various algebraic PSG solutions. The parameters denoted $U^{x'}$ etc., are related to U^x and U^y via Eq. (19).

QSL label	U_ζ	μ_s
$\mathsf{Z}_2 0$	$U_\zeta = U^x\tau_x + U^y\tau_y, \quad \zeta \in \{1,\ldots,12\}.$	$\mu_s = \mu^x\tau_x + \mu^y\tau_y, \quad s \in \{\alpha,\ldots,\delta\}.$
$\mathsf{Z}_2 1$	$U_\zeta = U^x\tau_x + U^y\tau_y, \quad \zeta \in \{1,2,3,4,5,6,9,10\},$ $U_\zeta = U^{x'}\tau_x + U^{y'}\tau_y, \quad \zeta \in \{11,12\},$ $U_\zeta = U^{x''}\tau_x + U^{y''}\tau_y, \quad \zeta \in \{7,8\}.$	$\mu_s = 0, \quad s \in \{\alpha,\ldots,\delta\}.$
$\mathsf{U}(1)$	$U_\zeta = U^z\tau_z, \quad \zeta \in \{1,\ldots,12\}.$	$\mu_s = \mu^z\tau_z, \quad s \in \{\alpha,\ldots,\delta\}.$

nearest-neighbor ansatzes for both QSLs are the same at the saddle point, the general ansatzes displayed in Table IV refer to different QSL states with different IGGs.

A. Relations between the QSLs

We can also infer connections between the three distinct QSLs. First, we note that the $\mathsf{U}(1)$ QSL is the parent state of the $\mathsf{Z}_2 0$ QSL. This can be seen by first performing a gauge transformation on $\mathsf{U}(1)$,

$$W(\alpha) = W(\beta) = W(\gamma) = W(\delta) = e^{-i\frac{\pi}{4}\tau_y}, \tag{21}$$

so that for this QSL we now have

$$\begin{aligned} U_\zeta &= U^z\tau_x, \quad \zeta \in \{1,\ldots,12\}, \\ \mu_s &= \mu^z\tau_x, \quad s \in \{\alpha,\ldots,\delta\}. \end{aligned} \tag{22}$$

From this, we see that introducing the perturbations $\Delta U_\zeta \sim \tau_y$ and $\Delta\mu_s \sim \tau_y$ breaks the $\mathsf{U}(1)$ symmetry down in a manner that results in the $\mathsf{Z}_2 0$ state. The $\mathsf{Z}_2 1$ QSL state cannot be obtained by perturbing around the $\mathsf{U}(1)$ QSL state.

B. Spinon spectra and the nodal star

Our mean-field ansatzes allow us to determine the structure of excitations of the mean-field ground state. We compute the eigenvalues of the mean-field Hamiltonian for different wavevectors to obtain the spinon dispersion spectra in the Brillouin zone.

Figure 2 shows the spinon band structures for the different mean-field QSL states. As explained earlier, the nearest-neighbour ansatzes for the $\mathsf{Z}_2 0$ and $\mathsf{U}(1)$ states are related by a global $\mathsf{SU}(2)$ at the saddle point, leading to identical band structures. To illustrate the structure of possible gapless modes, we plot the set of gapless points in the Brillouin zone (BZ) for the $\mathsf{U}(1)$ and $\mathsf{Z}_2 1$ states in Fig. 3. The collection of gapless points at the saddle point for the $\mathsf{Z}_2 0$ QSL is identical to that of the $\mathsf{U}(1)$ QSL.

We note that all the mean-field states we obtained are gapless at saddle point. The $\mathsf{U}(1)$ state possesses a spinon Fermi surface at the center of the BZ, with another sheet of spinon Fermi surface at the corners. The Z_2 mean-field states are also gapless. The $\mathsf{Z}_2 0$ state has similar spectrum to that of the $\mathsf{U}(1)$. We note that the gaplessness of the $\mathsf{Z}_2 0$ state seems to not be protected by symmetries and one might generically expect a gap to open up when our nearest-neighbor ansatzes are extended to include further neighbor terms.

The $\mathsf{Z}_2 1$ state hosts a spectrum with a "nodal star" of gapless points, with dispersionless bands running from the center of the BZ to its eight corners. This can be seen from Fig. 3. This nodal star is not a specific property of the short-range ansatz we use to display the bands in Fig. 3, rather it is robust to the addition of arbitrary links in the ansatz. In Appendix C we prove that the gapless nodal star is protected by projective symmetries of the $\mathsf{Z}_2 1$ phase. Such gapless nodal stars have received significant attention in the pyrochlore lattice [34,75], where two gapless bands along the nodal star were recently proven to be protected by projective symmetries [34]. Such lines were also observed in FCC structures in Ref. [30], where the whole mean-field Hamiltonian vanishes along the nodal star. Gapless nodal loops were observed in diamond lattice [32] where strong evidence of symmetry-protection was provided by showing that the gapless nodal loops persist despite longer range bond amplitudes in the ansatz. More generally, other features like quadratic band touching are also known to be protected by projective symmetries [76].

Our proof of the protected nodal star is algebraic and close in spirit to that of Ref. [34]. We look at the symmetries of the mean-field Hamiltonian directly in momentum space

$$H_{\mathrm{MFT}} = \sum_{\vec{k}} \psi^\dagger(\vec{k}) H_{\mathrm{MFT}}(\vec{k}) \psi(\vec{k}),$$

When the spinors [Eq. (6)] are arranged as $\psi(\vec{k}) = (\psi_1^\alpha(\vec{k}), \psi_1^\beta(\vec{k}), \psi_1^\gamma(\vec{k}), \psi_1^\delta(\vec{k}), \psi_2^\alpha(\vec{k}), \psi_2^\beta(\vec{k}), \psi_2^\gamma(\vec{k}), \psi_2^\delta(\vec{k}))$,

TABLE V. Numerical values of the mean-field parameters and their energetics for nearest-neighbor ansatzes. As explained in the main text, the nearest-neighbor ansatzes for the $\mathsf{Z}_2 0$ and $\mathsf{U}(1)$ QSLs are related by a global gauge transformation at the saddle point, and therefore have the same energy. The $\mathsf{Z}_2 1$ QSL state has a higher energy than this.

QSL label	Numerical values of the mean-field parameters	Energy density
$\mathsf{Z}_2 0$	$U^x = -0.161242, \quad U^y = -0.333897, \quad \mu^x = 0.115602, \quad \mu^y = 0.239386.$	–1.647184
$\mathsf{Z}_2 1$	$U^x = -0.110700, \quad U^y = 0.330299.$	–1.458114
$\mathsf{U}(1)$	$U^z = 0.370536, \quad \mu^z = -0.295063.$	–1.646913

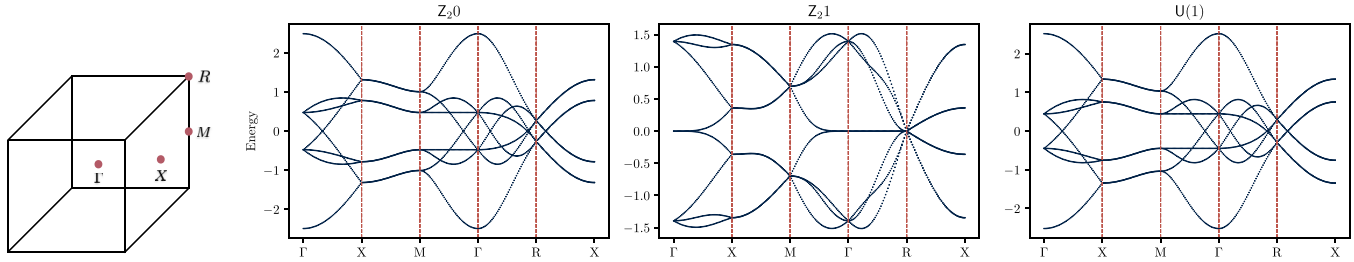


FIG. 2. (Left) The high-symmetry points of the Brillouin zone for the simple cubic lattice. (Right) Mean-field spinon band structures of the various quantum spin liquids along high symmetry lines in the Brillouin zone. Note that the saddle point (mean-field) parameters of the nearest-neighbor ansatz of the $\mathsf{Z}_2 0$ QSL looks identical to that of the $\mathsf{U}(1)$ QSL, as explained in Sec. IV.

time-reversal already implies that $H_{\mathrm{MFT}}(\vec{k})$ takes the form

$$H_{\mathrm{MFT}}(\vec{k}) = \begin{pmatrix} 0_{4\times4} & h_{4\times4}(\vec{k}) \\ h^{\dagger}_{4\times4}(\vec{k}) & 0_{4\times4} \end{pmatrix}. \tag{23}$$

This block off-diagonal Hermitian structure implies that the eigenvalues come in symmetric pairs of $\pm E(\vec{k})$ everywhere in the BZ. Next, we work out the most general form of $h_{4\times4}(\vec{k})$ allowed by the projective representations of the symmetries (G_a, g_a), (G_b, g_b), and (G_c, g_c). Restricting the general form of $h_{4\times4}(\vec{k})$ to the "nodal star" wavevectors $\vec{k} = (\pm k, \pm k, \pm k)$, we show, using elementary linear algebraic techniques, that it has a maximum rank of 3. This implies that H_{MFT} has a maximum rank of 6 along the nodal star, proving the existence of two gapless bands. The complete proof involves explicit expressions for the most general $h_{4\times4}(\vec{k})$ allowed by projective symmetries, and is fleshed out in Appendix C.

By computing the equilibrium state energy of the mean-field spinon models, we estimate the temperature dependence of the specific heat for the nodal star spin liquid state. Specifically, we see that for $\mathsf{Z}_2 0$, $C_v \sim T^{1.22}$, whereas for $\mathsf{Z}_2 1$, $C_v \sim T^{0.73}$. The numerical results are given in Fig. 4. The nearest-neighbor ansatz for the $\mathsf{Z}_2 0$ QSL is equivalent to the $\mathsf{U}(1)$ ansatz—which consequently exhibits the same specific heat scaling. However, we generally expect gauge field excitations in $\mathsf{U}(1)$ ansatzes at low energies to modify the results from the calculations of the noninteracting model.

C. Spin structure factors

In Fig. 5, we plot the static structure factor of $\mathsf{Z}_2 0$, $\mathsf{Z}_2 1$ and $\mathsf{U}(1)$ mean-field states in the k_y-k_z plane.

The definition of the static structure factor is

$$\mathfrak{S}^{s_i,s_j}(\vec{q}) \equiv \frac{1}{N}\sum_{\vec{R}} e^{-i\vec{q}\cdot(\vec{R}+\vec{d}^{0}_{ij})}\left\langle \vec{S}_{(0;s_i)} \cdot \vec{S}_{(\vec{R};s_j)} \right\rangle, \tag{24}$$

where s_i and s_j are the sublattice indices of site i and j, $\vec{R}$ is the distance between the two unit cells, and $\vec{d}^{0}_{ij}$ is the distance between the two sublattice sites within in the unit cell. And we compute the sum of all these components,

$$\mathfrak{S}(\vec{q}) \equiv \sum_{s_i,s_j} \mathfrak{S}^{s_i,s_j}(\vec{q}), \tag{25}$$

then plot the normalized results.

The structure factor plots indicate that we have obtained remarkable quantum spin liquid states, especially the $\mathsf{U}(1)$ QSLs, which are visibly featureless, implying a sharp departure from the ordered states. We also note that the $\mathsf{Z}_2 1$ state is the most featureful among the three.

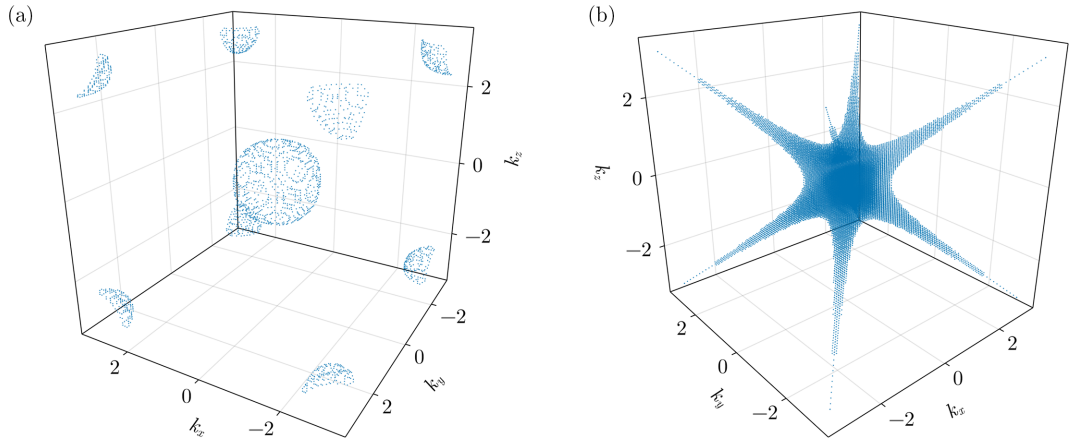


FIG. 3. In this figure, we plot the collection of gapless points for certain mean field QSL states. (a) $\mathsf{U}(1)$: this state features the two sheeted spinon fermi surfaces, with one located at the center of BZ, and another one at the corners; (b) $\mathsf{Z}_2 1$: this state has a star-shaped gapless manifold, and features a dispersion-less band along the diagonals of the BZ.

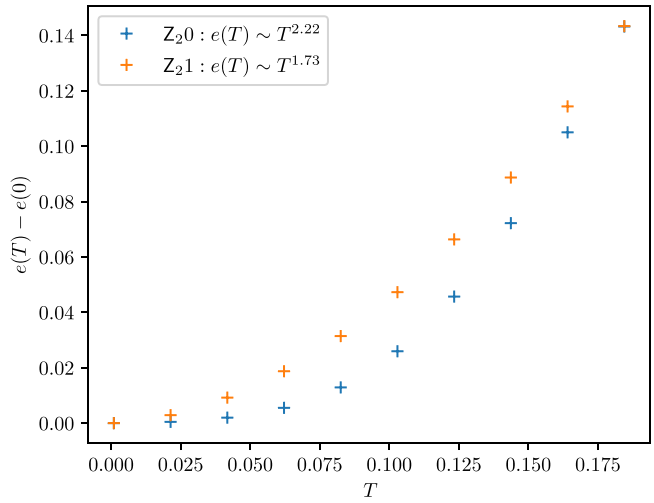


FIG. 4. Temperature dependence of the mean-field energies $e(T)$ for the Z_2 spin liquid ansatzes, which can be used to extract the respective specific heat scaling via $C_V(T) \sim \partial e/\partial T$. We note that the $Z_2 0$ and $Z_2 1$ spin liquids exhibit different scaling behaviors.

V. CONCLUSIONS AND OUTLOOK

In this work, we have computed the PSGs for the trillium lattice both with and without time reversal symmetry. In the former case, we implement the full construction of the nearest-neighbor mean-field (fermionic) parton Hamiltonian of the corresponding quantum spin liquid states. We find two distinct QSLs with a Z_2 gauge group, and a single example of a QSL with a $U(1)$ gauge group. We also obtained the corresponding mean-field spinon band structures and static structure factors, providing some basic thermodynamic and spectral information about these states. Our main results are reported in Tables II and III.

As noted in the Introduction, one of our principal motivations is the recent report of QSL-type behavior in $K_2Ni_2(SO_4)_3$; our work represents a stepping stone towards a parton mean-field analysis of this system, which hosts a double trillium lattice with spin-1 moments. The parton construction for higher-spin ($S > 1/2$) moments and corresponding QSL ansatzes have been considered previously in the literature [43,44]. The "high-energy gauge group" for fermionic theories of spin-1 and other integer spin models is no longer $SU(2)$, but the semidirect-product group $U(1) \rtimes Z_2$—which corresponds to gauge transformations $\tau_x^n \exp(i\theta\tau_z)$, $n \in (0, 1)$. The natural IGGs to consider now include $U(1) \rtimes Z_2$, $Z_2 \rtimes Z_2$, in addition to $U(1)$ and Z_2 [45]. The PSG classification for IGGs $U(1)$ and Z_2 goes through exactly as for spin-1/2. This can be seen from the fact that the solutions for the gauge transformations G_{g_v} listed in Tables II and III are all of the form $\tau_z^n \exp i\theta\tau_z$, $n \in (0, 1)$, and thus elements of the $U(1) \rtimes Z_2$ describing the high-energy gauge structure for integer-spin systems. However, the ansatzes are expected to have significant differences. In this case, Eq. (8) is now becomes

$$U_{ij} \equiv \begin{bmatrix} \chi_{ij}^\dagger & -\eta_{ij} \\ \eta_{ij}^\dagger & -\chi_{ij} \end{bmatrix}. \tag{26}$$

For spin-rotation invariant states, this implies a general form $U_{ij} = i\lambda_0\tau_0 + \lambda_z\tau_z + i\lambda_x\tau_x + i\lambda_y\tau_y$ with real coefficients λ_i. In contrast, for half-integer spin systems, Eq. (8) implies $U_{ij} = i\lambda_0\tau_0 + \lambda_z\tau_z + \lambda_x\tau_x + \lambda_y\tau_y$. Furthermore, the pairing terms have negative parity, $\eta_{ij} = -\eta_{ji}$ instead of $\eta_{ij} = \eta ji$. These differences are expected to change the qualitative properties of mean-field wave functions. Finally, we have a new IGG $Z_2 \rtimes Z_2$, which can lead to a new set of inequivalent ansatzes for the $S = 1$ problem. Accordingly, a natural next step in this program is to modify the PSG analysis to account for these differences, and perform variational Monte Carlo studies of the Gutzwiller projected mean-field QSL wavefunctions to compare with the available experimental data. These tasks are currently underway, and we hope to report on them in the near future.

ACKNOWLEDGMENTS

S.A.P. acknowledges useful conversations with Yasir Iqbal, and the hospitality of the Max Planck Institute for Complex Systems (MPI-PKS) Dresden, where part of this work

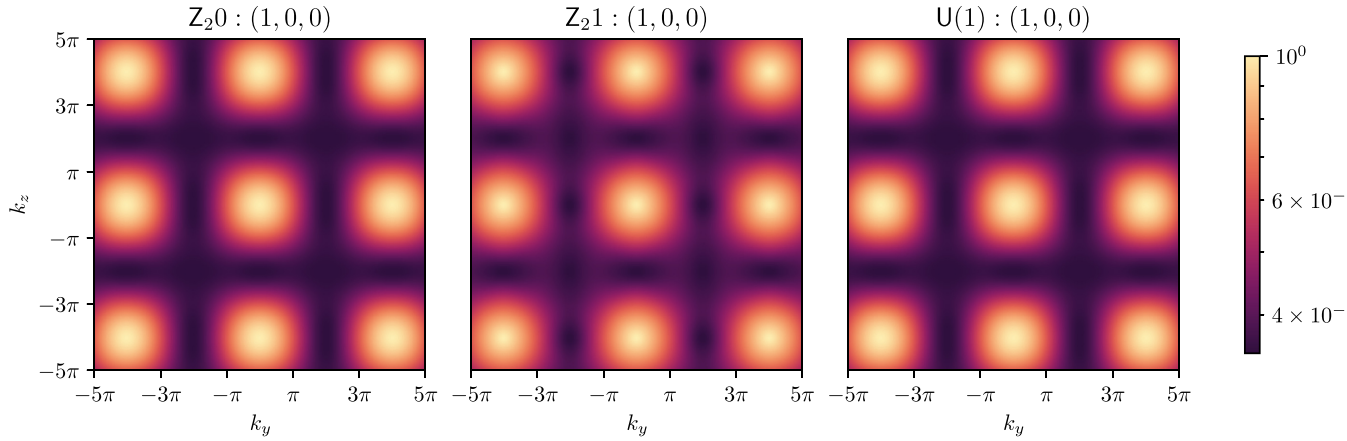


FIG. 5. Static structure factors for $Z_2 0$, $Z_2 1$, and $U(1)$ mean-field states, plotted in the k_y-k_z plane with $k_x = 0$. We note that the $U(1)$ QSL exhibits remarkably broadened static structure factors, whereas those of the $Z_2 1$ QSL are the most featureful. The seemingly fourfold rotation symmetry in the k_y-k_z plane results from the two screw symmetries on the lattice.

was completed. S.B. acknowledges useful discussions with Atanu Maity. This work was supported by the European Research Council under the European Union Horizon 2020 Research and Innovation Programme, Starting Grant (Agreement No. 804213-TMCS), a Buckee Scholarship at Merton College (M.L.), the Deutsche Forschungsgemeinschaft via Grant No. AS120/16-1, Project No. 493886309 (S.B.) and the Gutzwiller Fellowship of the MPI-PKS (S.A.P.).

APPENDIX A: IGG = $\mathbf{Z}_2$

One can translate the SG relations to the PSG relations,

$$G_c\big(g_c^3(i)\big)G_c\big(g_c^2(i)\big)G_c(g_c(i)) = \eta_c, \tag{A1a}$$

$$G_z^\dagger\big(g_a^2(i)\big)G_a\big(g_a^2(i)\big)G_a(g_a(i)) = \eta_a, \tag{A1b}$$

$$G_y^\dagger\big(g_b^2(i)\big)G_b\big(g_b^2(i)\big)G_b(g_b(i)) = \eta_b, \tag{A1c}$$

$$G_x^\dagger\big(T_y^{-1}T_xT_y(i)\big)G_y^\dagger(T_xT_y(i))G_x(T_xT_y(i))G_y(T_y(i)) = \eta_{xy}, \tag{A1d}$$

$$G_y^\dagger\big(T_z^{-1}T_yT_z(i)\big)G_z^\dagger(T_yT_z(i))G_y(T_yT_z(i))G_z(T_z(i)) = \eta_{yz}, \tag{A1e}$$

$$G_z^\dagger(T_x^{-1}T_zT_x(i))G_x^\dagger(T_zT_x(i))G_z(T_zT_x(i))G_x(T_x(i)) = \eta_{zx}, \tag{A1f}$$

$$G_a^\dagger(T_xg_aT_x(i))G_x(T_xg_aT_x(i))G_a(g_aT_x(i))G_x(T_x(i)) = \eta_{ax}, \tag{A1g}$$

$$G_a^\dagger(T_yg_aT_y(i))G_y(T_yg_aT_y(i))G_a(g_aT_y(i))G_y(T_y(i)) = \eta_{ay}, \tag{A1h}$$

$$G_a^\dagger\big(T_z^{-1}g_aT_z(i)\big)G_z^\dagger(g_aT_z(i))G_a(g_aT_z(i))G_z(T_z(i)) = \eta_{az}, \tag{A1i}$$

$$G_b^\dagger(T_xg_bT_x(i))G_x(T_xg_bT_x(i))G_b(g_bT_x(i))G_x(T_x(i)) = \eta_{bx}, \tag{A1j}$$

$$G_b^\dagger\big(T_y^{-1}g_bT_y(i)\big)G_y^\dagger(g_bT_y(i))G_b(g_bT_y(i))G_y(T_y(i)) = \eta_{by}, \tag{A1k}$$

$$G_b^\dagger(T_zg_bT_z(i))G_z(T_zg_bT_z(i))G_b(g_bT_z(i))G_z(T_z(i)) = \eta_{bz}, \tag{A1l}$$

$$G_c^\dagger\big(T_y^{-1}g_cT_x(i)\big)G_y^\dagger(g_cT_x(i))G_c(g_cT_x(i))G_x(T_x(i)) = \eta_{cyx}, \tag{A1m}$$

$$G_c^\dagger\big(T_z^{-1}g_cT_y(i)\big)G_z^\dagger(g_cT_y(i))G_c(g_cT_y(i))G_y(T_y(i)) = \eta_{czy}, \tag{A1n}$$

$$G_c^\dagger\big(T_x^{-1}g_cT_z(i)\big)G_x^\dagger(g_cT_z(i))G_c(g_cT_z(i))G_z(T_z(i)) = \eta_{cxz}, \tag{A1o}$$

$$\begin{aligned}&G_a^\dagger\big(g_c^{-1}g_b^{-1}T_x^{-1}T_yg_ag_c(i)\big)G_c^\dagger\big(g_b^{-1}T_x^{-1}T_yg_ag_c(i)\big)\\&\times G_b^\dagger\big(T_x^{-1}T_yg_ag_c(i)\big)G_x^\dagger(T_yg_ag_c(i))\\&\times G_y(T_yg_ag_c(i))G_a(g_ag_c(i))G_c(g_c(i)) = \eta_{acb},\end{aligned} \tag{A1p}$$

$$\begin{aligned}&G_b^\dagger\big(g_a^{-1}T_xT_y^{-1}T_zg_bg_a(i)\big)G_a^\dagger\big(T_xT_y^{-1}T_zg_bg_a(i)\big)\\&\times G_x\big(T_xT_y^{-1}T_zg_bg_a(i)\big)G_y^\dagger\big(T_zg_bg_a(i)\big)\\&\times G_z\big(T_zg_bg_a(i)\big)G_b(g_bg_a(i))G_a(g_a(i)) = \eta_{ab},\end{aligned} \tag{A1q}$$

$$\begin{aligned}&G_c^\dagger\big(g_b^{-1}T_x^{-1}T_yg_ag_bg_cg_b(i)\big)G_b^\dagger\big(T_x^{-1}T_yg_ag_bg_cg_b(i)\big)\\&\times G_x^\dagger\big(T_yg_ag_bg_cg_b(i)\big)G_y\big(T_yg_ag_bg_cg_b(i)\big)G_a(g_ag_bg_cg_b(i))\\&\times G_b(g_bg_cg_b(i))G_c(g_cg_b(i))G_b(g_b(i)) = \eta_{cba}.\end{aligned} \tag{A1r}$$

The Gs in the above relations are SU(2) matrices, and are associated with the SU(2) gauge symmetry, which transforms the G in the following way:

$$G_g(i) \mapsto W(i)G_g(i)W^\dagger(g^{-1}(i)), \quad W \in \mathsf{SU}(2). \tag{A2}$$

This equation can be understood as follows: under gauge transformation, we have

$$U_{ij} \mapsto \tilde{U}_{ij} \equiv W(i)U_{ij}W^\dagger(j), \tag{A3}$$

and the requirement for the gauge transformed PSG is

$$\tilde{G}_g(i)\tilde{U}_{g^{-1}(i)g^{-1}(j)}\tilde{G}_g^\dagger(j) = \tilde{U}_{ij}. \tag{A4}$$

From the above relations we derived the gauge transformation of Gs.

Aside from the gauge symmetry, we note that we can replace a generic element G with $\mathfrak{g}G$, where $\mathfrak{g} \in \mathrm{IGG} = \{\tau_0, -\tau_0\}$. Wisely making use of this fact is going to help us reduce the number of phases on the right-hand side (RHS) of the PSG equations.

By performing

$$\begin{aligned}&G_x \mapsto \eta_{cyx}G_x, \quad G_z \mapsto \eta_{czy}G_z,\\&G_a \mapsto \eta_{acb}\eta_{cba}G_a, \quad G_b \mapsto \eta_{acb}\eta_{cyx}G_b,\\&G_c \mapsto \eta_c G_c,\end{aligned} \tag{A5}$$

we eliminate the phases on the RHS of Eqs. (A1a), (A1m), (A1n), (A1p), and (A1r).

1. Solving for the translational elements

Let us start by considering the following equations Eqs. (A1d)–(A1f) that arise because of the commutation of translational generators. Canonically, this gives us the following expressions of G_x, G_y, G_z:

$$\begin{aligned}&G_x(x, y, z; s) = \tau_0,\ G_y(x, y, z; s) = \eta_{xy}^x\tau_0,\\&G_z(x, y, z; s) = \eta_{zx}^x\eta_{yz}^y\tau_0.\end{aligned} \tag{A6}$$

2. Solving for G_c

Using the IGG $\mathbf{Z}_2$ gauge symmetry, we had eliminated the phases on the RHS of Eqs. (A1m) and (A1n). To solve for G_c, one then plug the canonical expressions of the translational PSG elements into Eqs. (A1m)–(A1o). One arrives at the following expressions:

$$G_c^\dagger\big(T_y^{-1}(i)\big)\eta_{xy}^{-x}G_c(i) = \tau_0, \tag{A7a}$$

$$G_c^\dagger\big(T_z^{-1}(i)\big)\eta_{zx}^{-x}\eta_{yz}^{-y}G_c(i)G_y\big(g_c^{-1}(i)\big) = \tau_0, \tag{A7b}$$

$$G_c^\dagger\big(T_x^{-1}(i)\big)G_c(i)G_z\big(g_c^{-1}(i)\big) = \eta_{cxz}. \tag{A7c}$$

Further simplifying the expressions, one arrives at

$$G_c(x,y,z) = \eta^x_{xy} G_c(x,y-1,z), \tag{A8a}$$
$$G_c(x,y,z) = \eta^x_{zx}\eta^y_{yz}\eta^{-y}_{xy} G_c(x,y,z-1), \tag{A8b}$$
$$G_c(x,y,z) = \eta^{-y}_{zx}\eta^{-z}_{yz}\eta_{cxz} G_c(x-1,y,z). \tag{A8c}$$

The above expressions are valid for all sublattice indices, and we have suppressed the s indices. One then assumes that the following form is valid for G_c: $G_c \equiv f_c(x,y,z;s)\mathfrak{M}_c(s)$. Because of the mentioned reason, we have $f_c(x,y,z;s) = f_c(x,y,z)$. Then the separation of variables allows one to arrive at

$$f_c(x,y,z) = \eta^x_{xy} f_c(x,y-1,z), \tag{A9a}$$
$$f_c(x,y,z) = \eta^x_{zx}\eta^y_{yz}\eta^{-y}_{xy} f_c(x,y,z-1), \tag{A9b}$$
$$f_c(x,y,z) = \eta^{-y}_{zx}\eta^{-z}_{yz}\eta_{cxz} f_c(x-1,y,z). \tag{A9c}$$

For f_c to be a path-independent function, there are certain constraints that the phases have to satisfy. For example, one considers two paths to arrive at $f_c(x+1,y+1,z)$: (1) $f_c(x,y,z) \mapsto f_c(x+1,y,z) \mapsto f_c(x+1,y+1,z)$ and (2) $f_c(x,y,z) \mapsto f_c(x,y+1,z) \mapsto f_c(x+1,y+1,z)$. One then compares the phases resulting from the two paths, and enforces them to be identical. Such a process produces the relevant constraints on the phases. We check the path independence on the xy, yz and zx planes respectively, and arrive at the following constraint:

$$\eta_{xy} = \eta^{-1}_{zx}; \quad \eta_{yz} = \eta_{xy}; \quad \eta_{zx} = \eta^{-1}_{yz}. \tag{A10}$$

It follows then $\eta_{xy} = \eta_{yz} = \eta_{zx} = \eta_1$. The previous equations on f_c become

$$f_c(x,y,z) = \eta^x_1 f_c(x,y-1,z), \tag{A11a}$$
$$f_c(x,y,z) = \eta^x_1 f_c(x,y,z-1), \tag{A11b}$$
$$f_c(x,y,z) = \eta_1^{-(y+z)}\eta_{cxz} f_c(x-1,y,z). \tag{A11c}$$

Therefore, at this point we claim that $G_c = \eta_1^{xy+xz}\eta^x_{cxz}\mathfrak{M}_c(s)$.

Let us take a look at Eq. (A1a). One can eliminate the phase on the RHS by making use of the IGG gauge symmetry. Plugging the above expression into Eq. (A1a), we arrive at

$$\mathfrak{M}^3_c(\alpha) = \tau_0, \tag{A12a}$$
$$\mathfrak{M}_c(\delta)\mathfrak{M}_c(\gamma)\mathfrak{M}_c(\beta) = \tau_0, \tag{A12b}$$
$$\eta_{cxz} = 1. \tag{A12c}$$

It is useful to make a summary before we close this subsection,

(1) $\eta_c = \eta_{cyx} = \eta_{czy} = \eta_{cxz} = 1$;
(2) $\eta_{xy} = \eta_{yz} = \eta_{zx} = \eta_1$;
(3) $G_c = \eta_1^{xy+xz}\mathfrak{M}_c(s)$, for which the following relations are satisfied:

$$\mathfrak{M}^3_c(\alpha) = \tau_0; \tag{A13}$$

$$\mathfrak{M}_c(\delta)\mathfrak{M}_c(\gamma)\mathfrak{M}_c(\beta) = \tau_0; \tag{A14}$$

3. Solving for G_a

To solve for G_a, one plugs the simplified expressions of the translational PSG elements into Eqs. (A1g)–(A1i). One arrives at the following expressions:

$$G^\dagger_a(T_x(i))G_a(i) = \eta_{ax}, \tag{A15a}$$
$$G^\dagger_a(T_y(i))G_y(T_y(i))G_a(i)G_y\big(g_a^{-1}(i)\big) = \eta_{ay}, \tag{A15b}$$
$$G^\dagger_a\big(T_z^{-1}(i)\big)G^\dagger_z(i)G_a(i)G_z\big(g_a^{-1}(i)\big) = \eta_{az}. \tag{A15c}$$

One makes the usual ansatz $G_a(i) \equiv f_a(x,y,z;s)\mathfrak{M}_a(s)$, only this time one does not have $f_a(x,y,z;s) = f_a(x,y,z)$, for the evaluation of $G_{y/z}(g_a^{-1}(i))$ is not s-independent.

We have, for $s = \alpha/\delta$, the following conditions for f_a:

$$\eta^{-1}_{ax} f_a(x,y,z;\alpha/\delta) = f_a(x+1,y,z;\alpha/\delta), \tag{A16a}$$
$$\eta^{-1}_{ay} f_a(x,y,z;\alpha/\delta) = f_a(x,y+1,z;\alpha/\delta), \tag{A16b}$$
$$\eta_{az}\eta_1 f_a(x,y,z;\alpha/\delta) = f_a(x,y,z+1;\alpha/\delta); \tag{A16c}$$

and for $s = \beta/\gamma$, the following conditions for f_a:

$$\eta^{-1}_{ax} f_a(x,y,z;\beta/\gamma) = f_a(x+1,y,z;\beta/\gamma), \tag{A17a}$$
$$\eta^{-1}_{ay}\eta_1^{-1} f_a(x,y,z;\beta/\gamma) = f_a(x,y+1,z;\beta/\gamma), \tag{A17b}$$
$$\eta_{az} f_a(x,y,z;\beta/\gamma) = f_a(x,y,z+1;\beta/\gamma). \tag{A17c}$$

Note that this time we do not have to check the path independence of f_a, as the phases appearing in the above equations are constants. We then arrive at the following expressions:

$$f_a(x,y,z;\alpha/\delta) = \eta^{-x}_{ax}\eta^{-y}_{ay}\eta^z_{az}\eta_1^z,$$
$$f_a(x,y,z;\beta/\gamma) = \eta^{-x}_{ax}\eta^{-y}_{ay}\eta_1^{-y}\eta^z_{az}, \tag{A18}$$

from which we write

$$G_a(x,y,z;\alpha/\delta) = \eta^{-x}_{ax}\eta^{-y}_{ay}\eta^z_{az}\eta_1^z\mathfrak{M}_a(\alpha/\delta),$$
$$G_a(x,y,z;\beta/\gamma) = \eta^{-x}_{ax}\eta^{-y}_{ay}\eta_1^{-y}\eta^z_{az}\mathfrak{M}_a(\beta/\gamma). \tag{A19}$$

In plugging these expressions into Eq. (A1b), we first consider $i \equiv (x,y,z;\alpha)$. The condition we arrive at is

$$G^\dagger_z(-x,-y-1,z;\delta)G_a(-x,-y-1,z;\delta)G_a(x,y,z;\alpha) = \eta_a, \tag{A20}$$

which further simplifies to

$$\eta_1^{x+y+1}\eta_{ay}\mathfrak{M}_a(\delta)\mathfrak{M}_a(\alpha) = \eta_a. \tag{A21}$$

The above equation dictates that $\eta_1 = 1$. Consequently, one has

$$\mathfrak{M}_a(\delta)\mathfrak{M}_a(\alpha) = \eta_a\eta^{-1}_{ay}. \tag{A22}$$

We then consider other sublattice sites, and they give us

$$G_a(-x-1,-y-1,z+1;\gamma)G_a(x,y,z;\beta) = \eta_a, \tag{A23a}$$
$$G_a(-x-1,-y-1,z;\beta)G_a(x,y,z;\gamma) = \eta_a, \tag{A23b}$$
$$G_a(-x,-y-1,z+1;\alpha)G_a(x,y,z;\delta) = \eta_a. \tag{A23c}$$

Plugging the explicit forms into the above equations, and we arrive at

$$\mathfrak{M}_a(\gamma)\mathfrak{M}_a(\beta) = \eta_a\eta^{-1}_{ax}\eta^{-1}_{ay}\eta^{-1}_{az}, \tag{A24a}$$
$$\mathfrak{M}_a(\beta)\mathfrak{M}_a(\gamma) = \eta_a\eta^{-1}_{ax}\eta^{-1}_{ay}, \tag{A24b}$$
$$\mathfrak{M}_a(\alpha)\mathfrak{M}_a(\delta) = \eta_a\eta^{-1}_{ay}\eta^{-1}_{az}. \tag{A24c}$$

It is useful to make a summary again before we close this subsection:

(1) $\eta_{xy} = \eta_{yz} = \eta_{zx} = \eta_1 = 1$, and as a result $G_x = G_y = G_z = \tau_0$;

(2) We have $G_a(x, y, z; s) = \eta_{ax}^{-x}\eta_{ay}^{-y}\eta_{az}^{z}\mathfrak{M}_a(s)$; for which the following relations are satisfied:

$$\mathfrak{M}_a(\delta)\mathfrak{M}_a(\alpha) = \eta_a\eta_{ay}^{-1}, \tag{A25a}$$

$$\mathfrak{M}_a(\gamma)\mathfrak{M}_a(\beta) = \eta_a\eta_{ax}^{-1}\eta_{ay}^{-1}\eta_{az}^{-1}, \tag{A25b}$$

$$\mathfrak{M}_a(\beta)\mathfrak{M}_a(\gamma) = \eta_a\eta_{ax}^{-1}\eta_{ay}^{-1}, \tag{A25c}$$

$$\mathfrak{M}_a(\alpha)\mathfrak{M}_a(\delta) = \eta_a\eta_{ay}^{-1}\eta_{az}^{-1}. \tag{A25d}$$

4. Solving for G_b

Now we attack Eqs. (A1j)–(A1l). Since G_x, G_y, and G_z are trivial now, the equations are reduced to the following form:

$$G_b^\dagger(T_x(i))G_b(i) = \eta_{bx}, \tag{A26a}$$

$$G_b^\dagger\big(T_y^{-1}(i)\big)G_b(i) = \eta_{by}, \tag{A26b}$$

$$G_b^\dagger(T_z(i))G_b(i) = \eta_{bz}. \tag{A26c}$$

We make the ansatz $G_b \equiv f_b(x, y, z)\mathfrak{M}_b(s)$, where the separation of variables is possible because the above conditions are s-independent. One can quickly arrive at the condition that $G_b = \eta_{bx}^{-x}\eta_{by}^{y}\eta_{bz}^{-z}\mathfrak{M}_b(s)$.

Plugging the expression into Eq. (A1c), one ends up with

$$G_b(g_b(i))G_b(i) = \eta_b. \tag{A27}$$

Considering the individual sublattice sites respectively, one arrives at

$$\mathfrak{M}_b(\gamma)\mathfrak{M}_b(\alpha) = \eta_b\eta_{bx}^{-1}, \tag{A28a}$$

$$\mathfrak{M}_b(\delta)\mathfrak{M}_b(\beta) = \eta_b\eta_{bx}^{-1}\eta_{bz}^{-1}, \tag{A28b}$$

$$\mathfrak{M}_b(\alpha)\mathfrak{M}_b(\gamma) = \eta_b\eta_{bx}^{-1}\eta_{by}^{-1}, \tag{A28c}$$

$$\mathfrak{M}_b(\beta)\mathfrak{M}_b(\delta) = \eta_b\eta_{bx}^{-1}\eta_{by}^{-1}\eta_{bz}^{-1}. \tag{A28d}$$

A quick summary:

We have $G_b(x, y, z; s) = \eta_{bx}^{-x}\eta_{by}^{y}\eta_{bz}^{-z}\mathfrak{M}_b(s)$; for which the following relations are satisfied:

$$\mathfrak{M}_b(\gamma)\mathfrak{M}_b(\alpha) = \eta_b\eta_{bx}^{-1}, \tag{A29a}$$

$$\mathfrak{M}_b(\delta)\mathfrak{M}_b(\beta) = \eta_b\eta_{bx}^{-1}\eta_{bz}^{-1}, \tag{A29b}$$

$$\mathfrak{M}_b(\alpha)\mathfrak{M}_b(\gamma) = \eta_b\eta_{bx}^{-1}\eta_{by}^{-1}, \tag{A29c}$$

$$\mathfrak{M}_b(\beta)\mathfrak{M}_b(\delta) = \eta_b\eta_{bx}^{-1}\eta_{by}^{-1}\eta_{bz}^{-1}. \tag{A29d}$$

5. Solving Eqs. (A1p)–(A1r)

To attack the remaining three equations, note that we can use the IGG gauge symmetry of G_a and G_b to eliminate η_{acb} and η_{cba}. The equations are reduced to

$$G_a^\dagger\big(g_c^{-1}g_b^{-1}(i)\big)G_c^\dagger\big(g_b^{-1}(i)\big)G_b^\dagger(i) \times G_a\big(T_y^{-1}T_x(i)\big)G_c\big(g_a^{-1}T_y^{-1}T_x(i)\big) = \tau_0, \tag{A30a}$$

$$G_b^\dagger\big(g_a^{-1}(i)\big)G_a^\dagger(i)G_b\big(T_z^{-1}T_yT_x^{-1}(i)\big) \times G_a\big(g_b^{-1}T_z^{-1}T_yT_x^{-1}(i)\big) = \eta_{ab}\tau_0, \tag{A30b}$$

$$G_c^\dagger\big(g_b^{-1}T_x^{-1}T_y(i)\big)G_b^\dagger\big(T_x^{-1}T_y(i)\big)G_a(i) \times G_b\big(g_a^{-1}(i)\big)G_c\big(g_b^{-1}g_a^{-1}(i)\big)G_b\big(g_c^{-1}g_b^{-1}g_a^{-1}(i)\big) = \tau_0. \tag{A30c}$$

We consider first $i = (x, y, z; \alpha)$. Plugging this into Eq. (A30a) gives us the following:

$$G_a^\dagger(y-1, -z, -x-1; \beta)\mathfrak{M}_c(\gamma)G_b^\dagger(x, y, z; \alpha) \times G_a(x+1, y-1, z; \alpha)\mathfrak{M}_c(\delta) = \tau_0. \tag{A31}$$

Recalling $G_a = \eta_{ax}^{-x}\eta_{ay}^{-y}\eta_{az}^{z}\mathfrak{M}_a(s)$ and $G_b = \eta_{bx}^{-x}\eta_{by}^{y}\eta_{bz}^{-z}\mathfrak{M}_b(s)$, the left-hand side (LHS) of the above expression is evaluated as

$$\begin{aligned}&\eta_{ax}^{y-1}\eta_{ay}^{-z}\eta_{az}^{x+1}\mathfrak{M}_a^\dagger(\beta)\mathfrak{M}_c^\dagger(\gamma) \times \eta_{bx}^{x}\eta_{by}^{-y}\eta_{bz}^{z}\mathfrak{M}_b^\dagger(\alpha)\eta_{ax}^{-x-1}\eta_{ay}^{-y+1}\eta_{az}^{z}\mathfrak{M}_a(\alpha)\mathfrak{M}_c(\delta)\\ &= \big(\eta_{az}\eta_{bx}\eta_{ax}^{-1}\big)^x\big(\eta_{ax}\eta_{ay}^{-1}\eta_{by}^{-1}\big)^y\big(\eta_{az}\eta_{bz}\eta_{ay}^{-1}\big)^z\eta_{az}\eta_{ay} \times \mathfrak{M}_a^\dagger(\beta)\mathfrak{M}_c^\dagger(\gamma)\mathfrak{M}_b^\dagger(\alpha)\mathfrak{M}_a(\alpha)\mathfrak{M}_c(\delta).\end{aligned} \tag{A32}$$

Since the RHS of the previous expression is unit cell independent, we would have the following equations:

$$\eta_{az}\eta_{bx} = \eta_{ax}, \quad \eta_{by}\eta_{ay} = \eta_{ax}, \quad \eta_{az}\eta_{bz} = \eta_{ay}. \tag{A33}$$

Naming $\eta_2 \equiv \eta_{ax}$, $\eta_3 \equiv \eta_{ay}$ and $\eta_4 \equiv \eta_{az}$, we would have $\eta_{bx} = \eta_2\eta_4^{-1}$, $\eta_{by} = \eta_2\eta_3^{-1}$, and $\eta_{bz} = \eta_3\eta_4^{-1}$. Also, we now have $G_a = \eta_2^{-x}\eta_3^{-y}\eta_4^{z}\mathfrak{M}_a(s)$ and $G_b = \eta_2^{-x+y}\eta_3^{-y-z}\eta_4^{x+z}\mathfrak{M}_b(s)$. The previous constraint becomes

$$\mathfrak{M}_a^\dagger(\beta)\mathfrak{M}_c^\dagger(\gamma)\mathfrak{M}_b^\dagger(\alpha)\mathfrak{M}_a(\alpha)\mathfrak{M}_c(\delta) = \eta_3^{-1}\eta_4^{-1}. \tag{A34}$$

What happens now for Eq. (A30c)? Plugging $i = (x, y, z; \alpha)$ into the equation gives us

$$\mathfrak{M}_c^\dagger(\gamma)G_b^\dagger(x-1, y+1, z; \alpha) \times G_a(x, y, z; \alpha)G_b(-x, -y-1, z-1; \delta) \times \mathfrak{M}_c(\beta)G_b(-y-1, -z, x-1; \delta) = \tau_0. \tag{A35}$$

Evaluating the LHS of the above equation gives us

$$\begin{aligned}&\eta_2^{x-y}\eta_3^{y+z+1}\eta_4^{-x-z+1}\eta_2^{-x}\eta_3^{-y}\eta_4^{-z}\eta_2^{x-y-1} \times \eta_3^{y-z}\eta_4^{-x+z-1}\eta_2^{y+1-z}\eta_3^{z-x+1}\eta_4^{-y+x} \times \mathfrak{M}_c^\dagger(\gamma)\mathfrak{M}_b^\dagger(\alpha)\mathfrak{M}_a(\alpha)\mathfrak{M}_b(\delta)\mathfrak{M}_c(\beta)\mathfrak{M}_b(\delta)\\ &= \big(\eta_2^{-1}\eta_3^{-1}\eta_4\big)^x\big(\eta_3^{-1}\eta_4^{-1}\eta_2\big)^y\big(\eta_4\eta_2^{-1}\eta_3\big)^z \times \mathfrak{M}_c^\dagger(\gamma)\mathfrak{M}_b^\dagger(\alpha)\mathfrak{M}_a(\alpha)\mathfrak{M}_b(\delta)\mathfrak{M}_c(\beta)\mathfrak{M}_b(\delta).\end{aligned} \tag{A36}$$

Again, the unit cell independence gives us an extra condition $\eta_2 = \eta_3\eta_4$. The original equation becomes

$$\mathfrak{M}_c^\dagger(\gamma)\mathfrak{M}_b^\dagger(\alpha)\mathfrak{M}_a(\alpha)\mathfrak{M}_b(\delta)\mathfrak{M}_c(\beta)\mathfrak{M}_b(\delta) = \tau_0. \tag{A37}$$

No further conditions on the phases can be derived from the three equations. We are in the position to write $G_a = \eta_3^{-x-y}\eta_4^{-x+z}\mathfrak{M}_a(s)$ and $G_b = \eta_3^{-x-z}\eta_4^{y+z}\mathfrak{M}_b(s)$. Iterating scenarios with different s for $i \equiv (x, y, z; s)$, we arrive at the

following constraints:

$$\mathfrak{M}_a^\dagger(\beta)\mathfrak{M}_c^\dagger(\gamma)\mathfrak{M}_b^\dagger(\alpha)\mathfrak{M}_a(\alpha)\mathfrak{M}_c(\delta) = \eta_3^{-1}\eta_4^{-1}, \tag{A38a}$$
$$\mathfrak{M}_a^\dagger(\gamma)\mathfrak{M}_c^\dagger(\delta)\mathfrak{M}_b^\dagger(\beta)\mathfrak{M}_a(\beta)\mathfrak{M}_c(\gamma) = \eta_4, \tag{A38b}$$
$$\mathfrak{M}_a^\dagger(\alpha)\mathfrak{M}_c^\dagger(\alpha)\mathfrak{M}_b^\dagger(\gamma)\mathfrak{M}_a(\gamma)\mathfrak{M}_c(\beta) = \tau_0, \tag{A38c}$$
$$\mathfrak{M}_a^\dagger(\delta)\mathfrak{M}_c^\dagger(\beta)\mathfrak{M}_b^\dagger(\delta)\mathfrak{M}_a(\delta)\mathfrak{M}_c(\alpha) = \eta_3, \tag{A38d}$$
$$\mathfrak{M}_b^\dagger(\delta)\mathfrak{M}_a^\dagger(\alpha)\mathfrak{M}_b(\alpha)\mathfrak{M}_a(\gamma) = \eta_{ab}\eta_3\eta_4, \tag{A38e}$$
$$\mathfrak{M}_b^\dagger(\gamma)\mathfrak{M}_a^\dagger(\beta)\mathfrak{M}_b(\beta)\mathfrak{M}_a(\delta) = \eta_{ab}\eta_3\eta_4^{-1}, \tag{A38f}$$
$$\mathfrak{M}_b^\dagger(\beta)\mathfrak{M}_a^\dagger(\gamma)\mathfrak{M}_b(\gamma)\mathfrak{M}_a(\alpha) = \eta_{ab}\eta_3\eta_4^{-1}, \tag{A38g}$$
$$\mathfrak{M}_b^\dagger(\alpha)\mathfrak{M}_a^\dagger(\delta)\mathfrak{M}_b(\delta)\mathfrak{M}_a(\beta) = \eta_{ab}\eta_3\eta_4^{-1}, \tag{A38h}$$
$$\mathfrak{M}_c^\dagger(\gamma)\mathfrak{M}_b^\dagger(\alpha)\mathfrak{M}_a(\alpha)\mathfrak{M}_b(\delta)\mathfrak{M}_c(\beta)\mathfrak{M}_b(\delta) = \tau_0, \tag{A38i}$$
$$\mathfrak{M}_c^\dagger(\delta)\mathfrak{M}_b^\dagger(\beta)\mathfrak{M}_a(\beta)\mathfrak{M}_b(\gamma)\mathfrak{M}_c(\alpha)\mathfrak{M}_b(\alpha) = \eta_3^{-1}, \tag{A38j}$$
$$\mathfrak{M}_c^\dagger(\alpha)\mathfrak{M}_b^\dagger(\gamma)\mathfrak{M}_a(\gamma)\mathfrak{M}_b(\beta)\mathfrak{M}_c(\delta)\mathfrak{M}_b(\gamma) = \eta_3\eta_4, \tag{A38k}$$
$$\mathfrak{M}_c^\dagger(\beta)\mathfrak{M}_b^\dagger(\delta)\mathfrak{M}_a(\delta)\mathfrak{M}_b(\alpha)\mathfrak{M}_c(\gamma)\mathfrak{M}_b(\beta) = \eta_4. \tag{A38l}$$

6. Solving for the $\mathfrak{M}$s

We start by performing some SU(2) gauge transformations, described in Eq. (A2). Let us consider a sublattice-dependent gauge transformation $W(i) \equiv W(s)$. Had we started at an arbitrary gauge, we could always make the following gauge transformation:

$$W(\alpha) = \mathfrak{M}_a^\dagger(\alpha), \quad W(\beta) = \mathfrak{M}_c(\gamma),$$
$$W(\gamma) = \mathfrak{M}_c(\delta), \quad W(\delta) = \tau_0, \tag{A39}$$

so that

$$g.t.: \quad \mathfrak{M}_c(\delta) \mapsto W(\delta)\mathfrak{M}_c(\delta)W^\dagger(\gamma) = \tau_0, \tag{A40a}$$
$$\mathfrak{M}_c(\gamma) \mapsto W(\gamma)\mathfrak{M}_c(\gamma)W^\dagger(\beta) = \tau_0, \tag{A40b}$$
$$\mathfrak{M}_a(\alpha) \mapsto W(\alpha)\mathfrak{M}_a(\alpha)W^\dagger(\delta) = \tau_0. \tag{A40c}$$

Now we make use of Eq. (A14), and arrive at $\mathfrak{M}_c(\beta) = \mathfrak{M}_c(\gamma) = \mathfrak{M}_c(\delta) = \tau_0$. It should be noted that we are silent on $\mathfrak{M}_c(\alpha)$. Indeed, it is not possible to use gauge symmetry alone to trivialise $\mathfrak{M}_c(\alpha)$. However, as we shall see, other equations will bring enough restrictions on the form of $\mathfrak{M}_c(\alpha)$.

Before we take a step further, let us note that taking traces over Eqs. (A25a) and (A25d) dictates that $\eta_4 = 1$. After the simplification, we have

$$\mathfrak{M}_c^3(\alpha) = \tau_0, \tag{A41a}$$
$$\mathfrak{M}_a(\delta)\mathfrak{M}_a(\alpha) = \eta_a\eta_3^{-1}, \tag{A41b}$$
$$\mathfrak{M}_a(\gamma)\mathfrak{M}_a(\beta) = \eta_a, \tag{A41c}$$
$$\mathfrak{M}_a(\beta)\mathfrak{M}_a(\gamma) = \eta_a, \tag{A41d}$$
$$\mathfrak{M}_a(\alpha)\mathfrak{M}_a(\delta) = \eta_a\eta_3^{-1}, \tag{A41e}$$
$$\mathfrak{M}_b(\gamma)\mathfrak{M}_b(\alpha) = \eta_b\eta_3^{-1}, \tag{A41f}$$
$$\mathfrak{M}_b(\delta)\mathfrak{M}_b(\beta) = \eta_b, \tag{A41g}$$
$$\mathfrak{M}_b(\alpha)\mathfrak{M}_b(\gamma) = \eta_b\eta_3^{-1}, \tag{A41h}$$
$$\mathfrak{M}_b(\beta)\mathfrak{M}_b(\delta) = \eta_b, \tag{A41i}$$
$$\mathfrak{M}_a^\dagger(\beta)\mathfrak{M}_b^\dagger(\alpha)\mathfrak{M}_a(\alpha) = \eta_3^{-1}, \tag{A41j}$$
$$\mathfrak{M}_a^\dagger(\gamma)\mathfrak{M}_b^\dagger(\beta)\mathfrak{M}_a(\beta) = \tau_0, \tag{A41k}$$
$$\mathfrak{M}_a^\dagger(\alpha)\mathfrak{M}_c^\dagger(\alpha)\mathfrak{M}_b^\dagger(\gamma)\mathfrak{M}_a(\gamma) = \tau_0, \tag{A41l}$$
$$\mathfrak{M}_a^\dagger(\delta)\mathfrak{M}_b^\dagger(\delta)\mathfrak{M}_a(\delta)\mathfrak{M}_c(\alpha) = \eta_3, \tag{A41m}$$
$$\mathfrak{M}_b^\dagger(\delta)\mathfrak{M}_a^\dagger(\alpha)\mathfrak{M}_b(\alpha)\mathfrak{M}_a(\gamma) = \eta_{ab}\eta_3, \tag{A41n}$$
$$\mathfrak{M}_b^\dagger(\gamma)\mathfrak{M}_a^\dagger(\beta)\mathfrak{M}_b(\beta)\mathfrak{M}_a(\delta) = \eta_{ab}\eta_3, \tag{A41o}$$
$$\mathfrak{M}_b^\dagger(\beta)\mathfrak{M}_a^\dagger(\gamma)\mathfrak{M}_b(\gamma)\mathfrak{M}_a(\alpha) = \eta_{ab}\eta_3, \tag{A41p}$$
$$\mathfrak{M}_b^\dagger(\alpha)\mathfrak{M}_a^\dagger(\delta)\mathfrak{M}_b(\delta)\mathfrak{M}_a(\beta) = \eta_{ab}\eta_3, \tag{A41q}$$
$$\mathfrak{M}_b^\dagger(\alpha)\mathfrak{M}_a(\alpha)\mathfrak{M}_b(\delta)\mathfrak{M}_b(\delta) = \tau_0, \tag{A41r}$$
$$\mathfrak{M}_b^\dagger(\beta)\mathfrak{M}_a(\beta)\mathfrak{M}_b(\gamma)\mathfrak{M}_c(\alpha)\mathfrak{M}_b(\alpha) = \eta_3^{-1}, \tag{A41s}$$
$$\mathfrak{M}_c^\dagger(\alpha)\mathfrak{M}_b^\dagger(\gamma)\mathfrak{M}_a(\gamma)\mathfrak{M}_b(\beta)\mathfrak{M}_b(\gamma) = \eta_3, \tag{A41t}$$
$$\mathfrak{M}_b^\dagger(\delta)\mathfrak{M}_a(\delta)\mathfrak{M}_b(\alpha)\mathfrak{M}_b(\beta) = \tau_0. \tag{A41u}$$

Let us first look at Eq. (A41s), which can be rewritten as

$$\mathfrak{M}_b(\alpha)\mathfrak{M}_b^\dagger(\beta)\mathfrak{M}_a(\beta)\mathfrak{M}_b(\gamma)\mathfrak{M}_c(\alpha) = \eta_3^{-1}.$$

The above expression, when combined with Eqs. (A41t) and (A41d), gives us

$$\mathfrak{M}_b(\alpha)\mathfrak{M}_b(\gamma) = \eta_a^{-1}, \tag{A42}$$

that, when combined with Eq. (A41h), gives us

$$\eta_a^{-1} = \eta_b\eta_3^{-1}. \tag{A43}$$

Now we look at Eq. (A41o), which can be rewritten as

$$\mathfrak{M}_a(\delta)\mathfrak{M}_b^\dagger(\gamma)\mathfrak{M}_a^\dagger(\beta)\mathfrak{M}_b(\beta) = \eta_{ab}\eta_3.$$

The above expression, when combined with Eqs. (A41p) and (A41d), gives us

$$\mathfrak{M}_a(\delta)\mathfrak{M}_a(\alpha) = \eta_a, \tag{A44}$$

that, when combined with Eq. (A41b), gives us

$$\eta_3 = 1. \tag{A45}$$

Looking at Eqs. (A41q) and (A41r), with the help of Eq. (A41b), we reach

$$\mathfrak{M}_a(\beta) = \eta_{ab}\eta_a\mathfrak{M}_b(\delta). \tag{A46}$$

Similarly, Eqs. (A41n) and (A41u), with the help of Eq. (A41b), give us

$$\mathfrak{M}_a(\gamma) = \eta_{ab}\eta_a\mathfrak{M}_b(\beta). \tag{A47}$$

Consider now Eqs. (A41t) and (A41l). The coupled equations can be manoeuvred to give us

$$\mathfrak{M}_a(\alpha)\mathfrak{M}_b(\beta)\mathfrak{M}_b(\gamma) = \tau_0. \tag{A48}$$

The above equation, when paired with Eq. (A41j), gives us (note that $\eta_a = \eta_b$ now)

$$\mathfrak{M}_b(\beta)\mathfrak{M}_a(\beta) = \eta_a^{-1}, \tag{A49}$$

which can be coupled with Eq. (A41i) and (A46) to give us

$$\eta_{ab} = \eta_a. \tag{A50}$$

At this point, there is only one phase left in the problem: $\eta_a = \eta_b = \eta_{ab}$. Let us lois not s independent.ok at Eq. (A41k), which gives us

$$\mathfrak{M}_b^3(\beta) = \eta_a^{-1}, \tag{A51}$$

which then implies that

$$\mathfrak{M}_b^3(\delta) = \tau_0. \tag{A52}$$

We note that, at this point, there are four independent SU(2) matrices, denoted as follows:

$$\mathcal{A} \equiv \mathfrak{M}_c(\alpha), \quad \mathcal{B} \equiv \mathfrak{M}_b(\delta), \quad \mathcal{C} \equiv \mathfrak{M}_a(\alpha), \quad \mathcal{D} \equiv \mathfrak{M}_b(\alpha). \tag{A53}$$

More completely, the $\mathfrak{M}_a$s and $\mathfrak{M}_b$s are represented as follows:

$$\begin{aligned} \mathfrak{M}_a(\alpha) &= \mathcal{C}, \\ \mathfrak{M}_a(\beta) &= \mathcal{B}, \\ \mathfrak{M}_a(\gamma) &= \eta_a \mathcal{B}^\dagger, \\ \mathfrak{M}_a(\delta) &= \eta_a \mathcal{C}^\dagger; \end{aligned} \tag{A54}$$

and

$$\begin{aligned} \mathfrak{M}_b(\alpha) &= \mathcal{D}, \\ \mathfrak{M}_b(\beta) &= \eta_a \mathcal{B}^\dagger, \\ \mathfrak{M}_b(\gamma) &= \eta_a \mathcal{D}^\dagger, \\ \mathfrak{M}_b(\delta) &= \mathcal{B}. \end{aligned} \tag{A55}$$

There are, in fact, only five independent constraints for these matrices,

$$\mathcal{A}^3 = \tau_0, \tag{A56a}$$
$$\mathcal{B}^3 = \tau_0, \tag{A56b}$$
$$\mathcal{A} = \mathcal{C}\mathcal{B}\mathcal{C}^\dagger, \tag{A56c}$$
$$\mathcal{A} = \mathcal{D}\mathcal{B}\mathcal{D}^\dagger, \tag{A56d}$$
$$\mathcal{A} = \mathcal{D}\mathcal{B}^\dagger\mathcal{C}^\dagger. \tag{A56e}$$

However, note that $\mathcal{C} = \tau_0$ from Eq. (A40c), we immediately have

$$\mathcal{A} = \mathcal{B}, \quad \mathcal{D} = \mathcal{A}^\dagger. \tag{A57}$$

In summary:

(1) $G_x = G_y = G_z = \tau_0$;

(2) $G_{a/b/c}(x, y, z; s) = \mathfrak{M}_{a/b/c}(s)$, where the $\mathfrak{M}$s have the following forms:

$$\begin{aligned} &\mathfrak{M}_a(\alpha) = \tau_0, \quad \mathfrak{M}_a(\beta) = \mathcal{A}, \\ &\mathfrak{M}_a(\gamma) = \eta_a \mathcal{A}^\dagger, \quad \mathfrak{M}_a(\delta) = \eta_a \tau_0; \\ &\mathfrak{M}_b(\alpha) = \mathcal{A}^\dagger, \quad \mathfrak{M}_b(\beta) = \eta_a \mathcal{A}^\dagger, \\ &\mathfrak{M}_b(\gamma) = \eta_a \mathcal{A}, \quad \mathfrak{M}_b(\delta) = \mathcal{A}; \\ &\mathfrak{M}_c(\alpha) = \mathcal{A}, \quad \mathfrak{M}_c(\beta) = \tau_0, \\ &\mathfrak{M}_c(\gamma) = \tau_0, \quad \mathfrak{M}_c(\delta) = \tau_0. \end{aligned} \tag{A58}$$

Since we have $\eta_a = \pm 1$, and $\mathcal{A} = \tau_0, e^{i\frac{2\pi}{3}\tau_z}, e^{i\frac{4\pi}{3}\tau_z}$, corresponding to apparently six solutions. However, let us note that a further gauge transformation $W(x, y, z; s) \equiv \eta_a^{(x+y+z)}$ leads us to

(1) $G_x = G_y = G_z = \eta_a \tau_0$;

(2) $G_{a/b/c}(x, y, z; s) = \mathfrak{M}_{a/b/c}(s)$, where the $\mathfrak{M}$s have the following forms:

$$\begin{aligned} &\mathfrak{M}_a(\alpha) = \tau_0, \quad \mathfrak{M}_a(\beta) = \mathcal{A}, \\ &\mathfrak{M}_a(\gamma) = \mathcal{A}^\dagger, \quad \mathfrak{M}_a(\delta) = \tau_0; \\ &\mathfrak{M}_b(\alpha) = \mathcal{A}^\dagger, \quad \mathfrak{M}_b(\beta) = \mathcal{A}^\dagger, \\ &\mathfrak{M}_b(\gamma) = \mathcal{A}, \quad \mathfrak{M}_b(\delta) = \mathcal{A}; \\ &\mathfrak{M}_c(\alpha) = \mathcal{A}, \quad \mathfrak{M}_c(\beta) = \tau_0, \\ &\mathfrak{M}_c(\gamma) = \tau_0, \quad \mathfrak{M}_c(\delta) = \tau_0. \end{aligned} \tag{A59}$$

Because of the fact that η_a now becomes global signs that are elements of the IGG, we conclude that $\eta_a = \pm 1$ PSGs are equivalent. We also remark that a gauge transformation $W(x, y, z; s) \equiv i\tau_x$ maps the PSG solutions in which $\mathcal{A} = e^{i\frac{2\pi}{3}\tau_z}$ to that in which $\mathcal{A} = e^{i\frac{4\pi}{3}\tau_z}$.

In conclusion, we have

(1) $G_x = G_y = G_z = \tau_0$;

(2) $G_{a/b/c}(x, y, z; s) = \mathfrak{M}_{a/b/c}(s)$, where the $\mathfrak{M}$s have the following forms:

$$\begin{aligned} &\mathfrak{M}_a(\alpha) = \tau_0, \quad \mathfrak{M}_a(\beta) = \mathcal{A}, \\ &\mathfrak{M}_a(\gamma) = \mathcal{A}^\dagger, \quad \mathfrak{M}_a(\delta) = \tau_0; \\ &\mathfrak{M}_b(\alpha) = \mathcal{A}^\dagger, \quad \mathfrak{M}_b(\beta) = \mathcal{A}^\dagger, \\ &\mathfrak{M}_b(\gamma) = \mathcal{A}, \quad \mathfrak{M}_b(\delta) = \mathcal{A}; \\ &\mathfrak{M}_c(\alpha) = \mathcal{A}, \quad \mathfrak{M}_c(\beta) = \tau_0, \\ &\mathfrak{M}_c(\gamma) = \tau_0, \quad \mathfrak{M}_c(\delta) = \tau_0, \end{aligned} \tag{A60}$$

where $\mathcal{A} = \tau_0, e^{i\frac{2\pi}{3}\tau_z}$, corresponding to two solutions.

7. Adding time-reversal symmetry

Having arrived at the PSG solutions given the space group for the trillium lattice, we are at a position to add time-reversal symmetry (TRS) to the story. The extra relations are translated into the corresponding PSG equations,

$$G_\mathcal{T}(i)G_\mathcal{T}(i) = \eta_\mathcal{T}, \tag{A61a}$$
$$G_\mathcal{T}^\dagger\big(T_x^{-1}(i)\big)G_x^\dagger(i)G_\mathcal{T}(i)G_x(i) = \eta_{x\mathcal{T}}, \tag{A61b}$$
$$G_\mathcal{T}^\dagger\big(T_y^{-1}(i)\big)G_y^\dagger(i)G_\mathcal{T}(i)G_y(i) = \eta_{y\mathcal{T}}, \tag{A61c}$$
$$G_\mathcal{T}^\dagger\big(T_z^{-1}(i)\big)G_z^\dagger(i)G_\mathcal{T}(i)G_z(i) = \eta_{z\mathcal{T}}, \tag{A61d}$$
$$G_\mathcal{T}^\dagger\big(g_a^{-1}(i)\big)G_a^\dagger(i)G_\mathcal{T}(i)G_a(i) = \eta_{a\mathcal{T}}, \tag{A61e}$$
$$G_\mathcal{T}^\dagger\big(g_b^{-1}(i)\big)G_b^\dagger(i)G_\mathcal{T}(i)G_b(i) = \eta_{b\mathcal{T}}, \tag{A61f}$$
$$G_\mathcal{T}^\dagger\big(g_c^{-1}(i)\big)G_c^\dagger(i)G_\mathcal{T}(i)G_c(i) = \eta_{c\mathcal{T}}. \tag{A61g}$$

We make the ansatz that $G_\mathcal{T} \equiv f(x, y, z; s)\mathfrak{M}_\mathcal{T}(s)$, and Eqs. (A61b)–(A61d) immediately tell us that

$$G_\mathcal{T}(i) = \eta_{x\mathcal{T}}^x \eta_{y\mathcal{T}}^y \eta_{z\mathcal{T}}^z \mathfrak{M}_\mathcal{T}(s). \tag{A62}$$

The above form, when plugged into Eq. (A61a), gives us the following constraint:

$$\mathfrak{M}_\mathcal{T}^2(s) = \eta_\mathcal{T}. \tag{A63}$$

We now discuss about the consequences of Eqs. (A61e)–(A61g).

a. Solving Eq. (A61g)

First, we consider $i \equiv (x, y, z; \beta)$, since in this case $G_c(i) = \tau_0$. It is straightforward to reach the following constraint on the phases:

$$\eta_{x\mathcal{T}} = \eta_{y\mathcal{T}} = \eta_{z\mathcal{T}} \equiv \eta_5. \tag{A64}$$

Also the following constraints for $\mathfrak{M}_\mathcal{T}(s)$ arise if we iterate the sublattice indices,

$$\mathfrak{M}_\mathcal{T}^\dagger(\delta)\mathfrak{M}_\mathcal{T}(\beta) = \eta_{c\mathcal{T}}, \tag{A65a}$$

$$\mathfrak{M}_\mathcal{T}^\dagger(\beta)\mathfrak{M}_\mathcal{T}(\gamma) = \eta_{c\mathcal{T}}, \tag{A65b}$$

$$\mathfrak{M}_\mathcal{T}^\dagger(\gamma)\mathfrak{M}_\mathcal{T}(\delta) = \eta_{c\mathcal{T}}, \tag{A65c}$$

$$\mathfrak{M}_\mathcal{T}^\dagger(\alpha)\mathfrak{M}_c^\dagger(\alpha)\mathfrak{M}_\mathcal{T}(\alpha)\mathfrak{M}_c(\alpha) = \eta_{c\mathcal{T}}. \tag{A65d}$$

From Eqs. (A65a) and (A65b), we can reach $\mathfrak{M}_\mathcal{T}^\dagger(\delta)\mathfrak{M}_\mathcal{T}(\gamma) = \tau_0$. This statement, when coupled with Eq. (A65c) gives us $\eta_{c\mathcal{T}} = 1$.

A quick summary:

(1) $\eta_{x\mathcal{T}} = \eta_{y\mathcal{T}} = \eta_{z\mathcal{T}} \equiv \eta_5$, $\eta_{c\mathcal{T}} = 1$;

(2) We have $G_\mathcal{T}(x, y, z; s) = \eta_5^{x+y+z}\mathfrak{M}_\mathcal{T}(s)$; for which the following relations are satisfied:

$$\mathfrak{M}_\mathcal{T}^\dagger(\alpha)\mathfrak{M}_c^\dagger(\alpha)\mathfrak{M}_\mathcal{T}(\alpha)\mathfrak{M}_c(\alpha) = \tau_0, \tag{A66}$$

$$\mathfrak{M}_\mathcal{T}(\beta) = \mathfrak{M}_\mathcal{T}(\gamma) = \mathfrak{M}_\mathcal{T}(\delta). \tag{A67}$$

b. Solving Eqs. (A61e) and (A61f)

Iterating the sublattice indices, we arrive at the following constraints:

$$\mathfrak{M}_\mathcal{T}^\dagger(\delta)\mathfrak{M}_a^\dagger(\alpha)\mathfrak{M}_\mathcal{T}(\alpha)\mathfrak{M}_a(\alpha) = \eta_{a\mathcal{T}}, \tag{A68a}$$

$$\mathfrak{M}_\mathcal{T}^\dagger(\gamma)\mathfrak{M}_a^\dagger(\beta)\mathfrak{M}_\mathcal{T}(\beta)\mathfrak{M}_a(\beta) = \eta_{a\mathcal{T}}, \tag{A68b}$$

$$\mathfrak{M}_\mathcal{T}^\dagger(\beta)\mathfrak{M}_a^\dagger(\gamma)\mathfrak{M}_\mathcal{T}(\gamma)\mathfrak{M}_a(\gamma) = \eta_{a\mathcal{T}}\eta_5, \tag{A68c}$$

$$\mathfrak{M}_\mathcal{T}^\dagger(\alpha)\mathfrak{M}_a^\dagger(\delta)\mathfrak{M}_\mathcal{T}(\delta)\mathfrak{M}_a(\delta) = \eta_{a\mathcal{T}}\eta_5, \tag{A68d}$$

$$\mathfrak{M}_\mathcal{T}^\dagger(\gamma)\mathfrak{M}_b^\dagger(\alpha)\mathfrak{M}_\mathcal{T}(\alpha)\mathfrak{M}_b(\alpha) = \eta_{b\mathcal{T}}, \tag{A68e}$$

$$\mathfrak{M}_\mathcal{T}^\dagger(\delta)\mathfrak{M}_b^\dagger(\beta)\mathfrak{M}_\mathcal{T}(\beta)\mathfrak{M}_b(\beta) = \eta_{b\mathcal{T}}\eta_5, \tag{A68f}$$

$$\mathfrak{M}_\mathcal{T}^\dagger(\alpha)\mathfrak{M}_b^\dagger(\gamma)\mathfrak{M}_\mathcal{T}(\gamma)\mathfrak{M}_b(\gamma) = \eta_{b\mathcal{T}}\eta_5, \tag{A68g}$$

$$\mathfrak{M}_\mathcal{T}^\dagger(\beta)\mathfrak{M}_b^\dagger(\delta)\mathfrak{M}_\mathcal{T}(\delta)\mathfrak{M}_b(\delta) = \eta_{b\mathcal{T}}. \tag{A68h}$$

c. Collection of constraints

We further specify that $\mathfrak{M}_\mathcal{T}(\alpha) \equiv \mathcal{E}$ and $\mathfrak{M}_\mathcal{T}(\beta) = \mathfrak{M}_\mathcal{T}(\gamma) = \mathfrak{M}_\mathcal{T}(\delta) \equiv \mathcal{F}$. We note that Eqs. (A68b) and (A68c) immediately imply that $\eta_5 = 1$ since $\mathfrak{M}_a(\gamma) = \eta_a\mathfrak{M}_a^\dagger(\beta)$. Furthermore, comparing Eqs. (A68b) and (A68h) gives us $\eta_{a\mathcal{T}} = \eta_{b\mathcal{T}} \equiv \eta_6$, since $\mathfrak{M}_a(\beta) = \mathfrak{M}_b(\delta)$.

In the end, we reach the following five independent constraints:

$$\mathcal{E}^2 = \eta_\mathcal{T}, \tag{A69a}$$

$$\mathcal{F}^2 = \eta_\mathcal{T}, \tag{A69b}$$

$$\mathcal{E}^\dagger\mathcal{A}^\dagger\mathcal{E}\mathcal{A} = \tau_0, \tag{A69c}$$

$$\mathcal{F}^\dagger\mathcal{B}^\dagger\mathcal{F}\mathcal{B} = \eta_6, \tag{A69d}$$

$$\mathcal{C}^\dagger\mathcal{E}^\dagger\mathcal{C}\mathcal{F} = \eta_6. \tag{A69e}$$

Since $\mathcal{C} = \tau_0$, and $\mathcal{A} = \mathcal{B}$, we can determine that $\eta_6 = 1$ and $\mathcal{E} = \mathcal{F}$. Also, when $\eta_\mathcal{T} = 1$, we have $\mathcal{E} = \mathcal{F} = \tau_0$; when $\eta_\mathcal{T} = -1$, we have $\mathcal{E} = \mathcal{F} = i\tau_z$. Since without TRS, we had two solutions, now we have four solutions, as collected in Table II.

APPENDIX B: IGG = U(1)

In this Appendix, our target is to find the PSG solutions with U(1) IGG. The PSG relations listed in Appendix A still hold, only with the signs on the RHS being replaced as $\eta_\mathfrak{g} \equiv \exp[i\phi_\mathfrak{g}]$.

To proceed, we mention a fact which is a blessing for us. In [13], Wen proved that for PSG solutions with U(1) IGG, the Gs always have the following canonical forms:

$$G_g(i) \equiv (i\tau_x)^{n_g} e^{i\theta_g(i)\tau_z}, \quad n_g = 0 \text{ or } 1, \tag{B1}$$

where $\theta_g \in [0, 2\pi)$. Another thing we would like to mention before moving on is that, in this Appendix θ always stands for *a function* that depends on position i, whereas ϕ always stands for *a constant phase*.

Let us first look at Eq. (A1b), which can be rewritten as

$$G_a(g_a(i))G_a(i) = G_z(g_a(i))e^{i\phi_a\tau_z}. \tag{B2}$$

The above equation already dictates that $n_z = 0$. Why? This is straightforward to see if $n_a = 0$. Now supposing $n_a = 1$, we would have

$$\text{LHS}_{B2} = e^{i(-\theta_a(g_a(i))+\theta_a(i))\tau_z}, \tag{B3}$$

which also implies that $n_z = 0$ on the RHS_{B2}. Similarly, due to Eqs. (A1a) and (A1c), we can conclude that $n_y = n_c = 0$.

There is a valuable lesson from the above operation. Given a PSG equation $G_\mathfrak{g}G_\mathfrak{h}^\dagger \cdots = e^{i\phi_1\tau_z}$, we demand that $(n_\mathfrak{g} - n_\mathfrak{h} \ldots) = 0 \bmod 2$. Using the above lesson, we see from Eq. (A1q) that $n_x = 0$. And Eq. (A1p) tells us that $n_b = 0$, whereas Eq. (A1r) implies that $n_a = 0$. This is remarkable, for $n_x = n_y = n_z = n_a = n_b = n_c = 0$! What was for us originally a set of coupled SU(2) matrix equations now reduces to a set of coupled U(1) matrix equations, which are equations of compact U(1) phases.

1. Solving for the translational elements and the simplification

Before we take a step further, let us rewrite the remaining PSG equations in terms of θs,

$$\theta_c\big(g_c^2(i)\big) + \theta_c(g_c(i)) + \theta_c(i) = \phi_c, \tag{B4a}$$

$$-\theta_z(g_a(i)) + \theta_a(g_a(i)) + \theta_a(i) = \phi_a, \tag{B4b}$$

$$-\theta_y(g_b(i)) + \theta_b(g_b(i)) + \theta_b(i) = \phi_b, \tag{B4c}$$

$$-\theta_a(T_x(i)) + \theta_x(T_x(i)) + \theta_a(i) + \theta_x\big(g_a^{-1}(i)\big) = \phi_{ax}, \tag{B4d}$$

$$-\theta_a(T_y(i)) + \theta_y(T_y(i)) + \theta_a(i) + \theta_y\big(g_a^{-1}(i)\big) = \phi_{ay}, \tag{B4e}$$

$$-\theta_a\big(T_z^{-1}(i)\big) - \theta_z(i) + \theta_a(i) + \theta_z\big(g_a^{-1}(i)\big) = \phi_{az}, \tag{B4f}$$

$$-\theta_b(T_x(i)) + \theta_x(T_x(i)) + \theta_b(i) + \theta_x\big(g_b^{-1}(i)\big) = \phi_{bx}, \tag{B4g}$$

$$-\theta_b\big(T_y^{-1}(i)\big) - \theta_y(i) + \theta_b(i) + \theta_y\big(g_b^{-1}(i)\big) = \phi_{by}, \tag{B4h}$$

$$-\theta_b(T_z(i)) + \theta_z(T_z(i)) + \theta_b(i) + \theta_z\left(g_b^{-1}(i)\right) = \phi_{bz}, \quad \text{(B4i)}$$

$$-\theta_c\left(T_y^{-1}(i)\right) - \theta_y(i) + \theta_c(i) + \theta_x\left(g_c^{-1}(i)\right) = \phi_{cyx}, \quad \text{(B4j)}$$

$$-\theta_c\left(T_z^{-1}(i)\right) - \theta_z(i) + \theta_c(i) + \theta_y\left(g_c^{-1}(i)\right) = \phi_{czy}, \quad \text{(B4k)}$$

$$-\theta_c\left(T_x^{-1}(i)\right) - \theta_x(i) + \theta_c(i) + \theta_z\left(g_c^{-1}(i)\right) = \phi_{cxz}, \quad \text{(B4l)}$$

$$\begin{aligned}&-\theta_a\left(g_c^{-1}g_b^{-1}T_x^{-1}T_y g_a g_c(i)\right) - \theta_c\left(g_b^{-1}T_x^{-1}T_y g_a g_c(i)\right)\\ &-\theta_b\left(T_x^{-1}T_y g_a g_c(i)\right) - \theta_x(T_y g_a g_c(i))\\ &+\theta_y(T_y g_a g_c(i)) + \theta_a(g_a g_c(i)) + \theta_c(g_c(i)) = \phi_{acb},\end{aligned} \quad \text{(B4m)}$$

$$\begin{aligned}&-\theta_b\left(g_a^{-1}T_x T_y^{-1}T_z g_b g_a(i)\right) - \theta_a\left(T_x T_y^{-1}T_z g_b g_a(i)\right)\\ &+\theta_x\left(T_x T_y^{-1}T_z g_b g_a(i)\right) - \theta_y(T_z g_b g_a(i))\\ &+\theta_z(T_z g_b g_a(i)) + \theta_b(g_b g_a(i)) + \theta_a(g_a(i)) = \phi_{ab},\end{aligned} \quad \text{(B4n)}$$

$$\begin{aligned}&-\theta_c\left(g_b^{-1}T_x^{-1}T_y g_a g_b g_c g_b(i)\right) - \theta_b\left(T_x^{-1}T_y g_a g_b g_c g_b(i)\right)\\ &-\theta_x(T_y g_a g_b g_c g_b(i)) + \theta_y(T_y g_a g_b g_c g_b(i))\\ &+\theta_a(g_a g_b g_c g_b(i)) + \theta_b(g_b g_c g_b(i))\\ &+\theta_c(g_c g_b(i)) + \theta_b(g_b(i)) = \phi_{cba}.\end{aligned} \quad \text{(B4o)}$$

These θs and ϕs in the above equations are compact $\mathsf{U}(1)$ phase factors, and an equation $\theta = \phi$ means $\theta = \phi \bmod 2\pi$. The θs are associated with the $\mathsf{SU}(2)$ gauge symmetry like before, specifically the $\mathsf{U}(1)$ subgroup of $\mathsf{SU}(2)$ transforms the θ in the following way:

$$\theta_U(i) \mapsto \theta_U(i) + \varphi(i) - \varphi(U^{-1}(i)), \quad \varphi \in [0, 2\pi); \quad \text{(B5)}$$

note that since we do not want to spoil the choice of τ_z, we consider only the $\mathsf{U}(1)$ subgroup of $\mathsf{SU}(2)$.

Similar to the Z_2 case, we eliminate the phases on the RHS of Eqs. (B4a), (B4j), (B4k), (B4m), and (B4o).

2. Solving for the translational elements

Let us start by considering the equations that arise because of the commutation of translational generators. Canonically, this gives us the following expressions of G_x, G_y, G_z after a gauge fixing

$$\begin{aligned}&G_x(x, y, z; s) = \tau_0, \quad G_y(x, y, z; s) = e^{ix\phi_{xy}\tau_z},\\ &G_z(x, y, z; s) = e^{i(x\phi_{zx} + y\phi_{yz})\tau_z}.\end{aligned} \quad \text{(B6)}$$

In other words, we have the following representation:

$$\begin{aligned}&\theta_x(x, y, z; s) = 0, \quad \theta_y(x, y, z; s) = x\phi_{xy},\\ &\theta_z(x, y, z; s) = x\phi_{zx} + y\phi_{yz}.\end{aligned} \quad \text{(B7)}$$

3. Solving for θ_c

Using the IGG gauge symmetry, one can eliminate the phases on the RHS of Eqs. (B4j)–(B4l), as each of θ_x, θ_y and θ_z appears only once in these equations. To solve for θ_c, one then plug the canonical expressions of the translational PSG elements into Eqs. (B4j)–(B4l). We make an ansatz analogous to the one we made in the Z_2 case: $\theta(i) \equiv f(x, y, z; s) + \mathfrak{m}(s)$. We realize that the equations under attention are valid for all sublattice indices, therefore we have $f_c(x, y, z; s) \equiv f_c(x, y, z)$, and

$$f_c(x, y, z) = f_c(x, y - 1, z) + x\phi_{xy}, \quad \text{(B8a)}$$

$$f_c(x, y, z) = f_c(x, y, z - 1) + x\phi_{zx} + y\phi_{yz} - y\phi_{xy}, \quad \text{(B8b)}$$

$$f_c(x, y, z) = f_c(x - 1, y, z) - y\phi_{zx} - z\phi_{yz} + \phi_{cxz}. \quad \text{(B8c)}$$

Checking the path-independency of f_c, we arrive at the following constraint:

$$\phi_{xy} = \phi_{yz} = -\phi_{zx} \equiv \phi_1. \quad \text{(B9)}$$

Eventually we arrive at the conclusion that $f_c(x, y, z) = (xy - xz)\phi_1$.

Let us look at Eq. (B4a). We had eliminated the phase on the RHS by making use of the IGG gauge symmetry. Plugging the above expression into Eq. (B4a), we arrive at

$$3\mathfrak{m}_c(\alpha) = 0, \quad \text{(B10a)}$$

$$\mathfrak{m}_c(\beta) + \mathfrak{m}_c(\gamma) + \mathfrak{m}_c(\delta) = 0, \quad \text{(B10b)}$$

$$\phi_{cxz} = 0. \quad \text{(B10c)}$$

Before moving on, we make a brief summary:

$$\begin{aligned}&\theta_x(i) = 0, \quad \theta_y(i) = x\phi_1, \quad \theta_z(i) = (y - x)\phi_1,\\ &\theta_c(i) = (xy - xz)\phi_1 + \mathfrak{m}_c(s).\end{aligned} \quad \text{(B11)}$$

4. Solving for θ_a

To solve for θ_a, one plugs the simplified expressions of the translational PSG elements into Eqs. (B4d)–(B4f). One arrives at the following expressions:

$$\theta_a(T_x(i)) = \theta_a(i) - \phi_{ax}, \quad \text{(B12a)}$$

$$\theta_a(T_y(i)) = \theta_a(i) + \theta_y(T_y(i)) + \theta_y\left(g_a^{-1}(i)\right) - \phi_{ay}, \quad \text{(B12b)}$$

$$\theta_a(i) = \theta_a\left(T_z^{-1}(i)\right) + \phi_{az} + \theta_z(i) - \theta_z\left(g_a^{-1}(i)\right). \quad \text{(B12c)}$$

One makes the usual ansatz $\theta_a \equiv f_a(x, y, z; s) + \mathfrak{m}_a(s)$, only this time one does not have $f_a(x, y, z; s) = f_a(x, y, z)$, for the evaluation of $\theta_{y/z}(g_a^{-1}(i))$ is not s-independent.

We have, for $s = \alpha/\delta$, the following conditions for f_a:

$$f_a(x + 1, y, z; \alpha/\delta) = f_a(x, y, z; \alpha/\delta) - \phi_{ax}, \quad \text{(B13a)}$$

$$f_a(x, y + 1, z; \alpha/\delta) = f_a(x, y, z; \alpha/\delta) - \phi_{ay}, \quad \text{(B13b)}$$

$$\begin{aligned}f_a(x, y, z; \alpha/\delta) = {}& f_a(x, y, z - 1; \alpha/\delta)\\ &+\phi_{az} + (2y - 2x + 1)\phi_1;\end{aligned} \quad \text{(B13c)}$$

and for $s = \beta/\gamma$, the following conditions for f_a:

$$f_a(x + 1, y, z; \beta/\gamma) = f_a(x, y, z; \beta/\gamma) - \phi_{ax}, \quad \text{(B14a)}$$

$$f_a(x, y + 1, z; \beta/\gamma) = f_a(x, y, z; \beta/\gamma) - \phi_{ay} - \phi_1, \quad \text{(B14b)}$$

$$\begin{aligned}f_a(x, y, z; \beta/\gamma) = {}& f_a(x, y, z - 1; \beta/\gamma) + \phi_{az}\\ &+(2y - 2x)\phi_1.\end{aligned} \quad \text{(B14c)}$$

Checking the path-independency of f_a, we arrive at the following constraint:

$$2\phi_1 = 0 \Rightarrow \phi_1 = 0 \quad \text{or} \quad \pi. \quad \text{(B15)}$$

After the path-independency is guaranteed, we arrive at the following expressions:

$$f_a(x,y,z;\alpha/\delta) = -x\phi_{ax} - y\phi_{ay} + z(\phi_{az}+\phi_1), \quad \text{(B16a)}$$

$$f_a(x,y,z;\beta/\gamma) = -x\phi_{ax} - y(\phi_{ay}+\phi_1) + z\phi_{az}. \quad \text{(B16b)}$$

Plugging the forms of $\theta_a \equiv f_a(x,y,z;s) + \mathfrak{m}_a(s)$ into Eq. (B4b), further constraints can be derived. Specifically, we iterate the sublattice index. Let us consider $i \equiv (x,y,z;\alpha)$, we have

$$\begin{aligned} &-\theta_z(-x,-y-1,z;\delta) + \theta_a(-x,-y-1,z;\delta) \\ &\quad + \theta_a(x,y,z;\alpha) = \phi_a, \end{aligned} \quad \text{(B17)}$$

which gives us

$$\begin{aligned} \phi_a =& -(-y-1+x)\phi_1 + (x\phi_{ax} + (y+1)\phi_{ay} \\ &+ z(\phi_{az}+\phi_1)) + (-x\phi_{ax} - y\phi_{ay} \\ &+ z(\phi_{az}+\phi_1)) + \mathfrak{m}_a(\alpha) + \mathfrak{m}_a(\delta) \\ =& -(-y-1+x)\phi_1 + \phi_{ay} + 2z\phi_{az} + \mathfrak{m}_a(\alpha) + \mathfrak{m}_a(\delta). \end{aligned} \quad \text{(B18)}$$

The implication from the above equation is that

$$\phi_1 = 0, \quad 2\phi_{az} = 0; \quad \mathfrak{m}_a(\alpha) + \mathfrak{m}_a(\delta) = \phi_a - \phi_{ay}. \quad \text{(B19)}$$

For $i \equiv (x,y,z;\beta)$, we have

$$\theta_a(-x-1,-y-1,z+1;\gamma) + \theta_a(x,y,z;\beta) = \phi_a, \quad \text{(B20)}$$

which gives us

$$\begin{aligned} \phi_a &= ((x+1)\phi_{ax} + (y+1)\phi_{ay} + (z+1)\phi_{az}) \\ &\quad + (-x\phi_{ax} - y\phi_{ay} + z\phi_{az}) + \mathfrak{m}_a(\beta) + \mathfrak{m}_a(\gamma) \\ &= \phi_{ax} + \phi_{ay} + \phi_{az} + \mathfrak{m}_a(\beta) + \mathfrak{m}_a(\gamma). \end{aligned} \quad \text{(B21)}$$

For $i \equiv (x,y,z;\gamma)$, we have

$$\theta_a(-x-1,-y-1,z;\beta) + \theta_a(x,y,z;\gamma) = \phi_a, \quad \text{(B22)}$$

which gives us

$$\begin{aligned} \phi_a &= ((x+1)\phi_{ax} + (y+1)\phi_{ay} + z\phi_{az}) \\ &\quad + (-x\phi_{ax} - y\phi_{ay} + z\phi_{az}) + \mathfrak{m}_a(\beta) + \mathfrak{m}_a(\gamma) \\ &= \phi_{ax} + \phi_{ay} + \mathfrak{m}_a(\beta) + \mathfrak{m}_a(\gamma). \end{aligned} \quad \text{(B23)}$$

Combining with the equation for $i \equiv (x,y,z;\beta)$, we have

$$\phi_{az} = 0; \quad \mathfrak{m}_a(\beta) + \mathfrak{m}_a(\gamma) = \phi_a - \phi_{ay} - \phi_{ax}. \quad \text{(B24)}$$

Lastly, the case for $i \equiv (x,y,z;\delta)$ does not give us new relations.

Before moving on, we make a brief summary:

$$\theta_{x/y/z}(i) = 0, \quad \theta_a(i) = -x\phi_{ax} - y\phi_{ay} + \mathfrak{m}_a(s). \quad \text{(B25)}$$

5. Solving for θ_b

To solve for θ_b, one plugs the simplified expressions of the translational PSG elements into Eq. (B4g)–(B4i). One arrives at the following expressions:

$$\begin{aligned} \theta_b(T_x(i)) &= \theta_b(i) - \phi_{bx}, \\ \theta_b(i) &= \theta_b\big(T_y^{-1}(i)\big) + \phi_{by}, \\ \theta_b(T_z(i)) &= \theta_b(i) - \phi_{bz}. \end{aligned} \quad \text{(B26)}$$

One makes the usual ansatz $\theta_b \equiv f_b(x,y,z;s) + \mathfrak{m}_b(s)$, we arrive at

$$f_b(x,y,z;s) = -x\phi_{bx} + y\phi_{by} - z\phi_{bz}. \quad \text{(B27)}$$

Plugging the forms of $\theta_b \equiv f_b(x,y,z;s) + \mathfrak{m}_b(s)$ into Eq. (B4c), further constraints can be derived. Specifically, we iterate the sublattice index. Let us consider $i \equiv (x,y,z;\alpha)$, we have

$$\theta_b(-x-1,y,-z;\gamma) + \theta_b(x,y,z;\alpha) = \phi_b, \quad \text{(B28)}$$

which gives us

$$\begin{aligned} \phi_b &= ((x+1)\phi_{bx} + y\phi_{by} + z\phi_{bz}) \\ &\quad + (-x\phi_{bx} + y\phi_{by} - z\phi_{bz}) + \mathfrak{m}_b(\alpha) + \mathfrak{m}_b(\gamma) \\ &= \phi_{bx} + 2y\phi_{by} + \mathfrak{m}_b(\alpha) + \mathfrak{m}_b(\gamma). \end{aligned} \quad \text{(B29)}$$

The implication from the above equation is that

$$2\phi_{by} = 0; \quad \mathfrak{m}_b(\alpha) + \mathfrak{m}_b(\gamma) = \phi_b - \phi_{bx}. \quad \text{(B30)}$$

For $i \equiv (x,y,z;\beta)$, we have

$$\theta_b(-x-1,y,-z-1;\delta) + \theta_b(x,y,z;\beta) = \phi_b, \quad \text{(B31)}$$

which gives us

$$\begin{aligned} \phi_b &= ((x+1)\phi_{bx} + y\phi_{by} + (z+1)\phi_{bz}) \\ &\quad + (-x\phi_{bx} + y\phi_{by} - z\phi_{bz}) + \mathfrak{m}_b(\beta) + \mathfrak{m}_b(\delta) \\ &= \phi_{bx} + \phi_{bz} + \mathfrak{m}_b(\beta) + \mathfrak{m}_b(\delta). \end{aligned} \quad \text{(B32)}$$

For $i \equiv (x,y,z;\gamma)$, we have

$$\theta_b(-x-1,y+1,-z;\alpha) + \theta_b(x,y,z;\gamma) = \phi_b, \quad \text{(B33)}$$

which gives us

$$\begin{aligned} \phi_b &= ((x+1)\phi_{bx} + (y+1)\phi_{by} + z\phi_{bz}) \\ &\quad + (-x\phi_{bx} + y\phi_{by} - z\phi_{bz}) + \mathfrak{m}_b(\alpha) + \mathfrak{m}_b(\gamma) \\ &= \phi_{bx} + \phi_{by} + \mathfrak{m}_b(\alpha) + \mathfrak{m}_b(\gamma). \end{aligned} \quad \text{(B34)}$$

Combining with the equation for $i \equiv (x,y,z;\alpha)$, we have

$$\phi_{by} = 0; \quad \mathfrak{m}_b(\alpha) + \mathfrak{m}_b(\gamma) = \phi_b - \phi_{bx}. \quad \text{(B35)}$$

Lastly, the case for $i \equiv (x,y,z;\delta)$ gives us the same relation from the case for $i \equiv (x,y,z;\beta)$, which is

$$\mathfrak{m}_b(\beta) + \mathfrak{m}_b(\delta) = \phi_b - \phi_{bx} - \phi_{bz}. \quad \text{(B36)}$$

Before moving on, we make a brief summary:

$$\theta_b(i) = -x\phi_{bx} - z\phi_{bz} + \mathfrak{m}_b(s). \quad \text{(B37)}$$

6. Solving Eq. (B4m)

Equation (B4m) is then reduced to

$$\begin{aligned} &-\theta_a\big(g_c^{-1}g_b^{-1}T_x^{-1}T_y(i)\big) - \theta_c\big(g_b^{-1}T_x^{-1}T_y(i)\big) \\ &\quad - \theta_b\big(T_x^{-1}T_y(i)\big) + \theta_a(i) + \theta_c\big(g_a^{-1}(i)\big) = 0. \end{aligned} \quad \text{(B38)}$$

For $i \equiv (x,y,z;\alpha)$, the above equation is

$$\begin{aligned} 0 =& -\theta_a(y,-z,-x;\beta) - \theta_c(-x,y,-z;\gamma) \\ &- \theta_b(x-1,y+1,z;\alpha) \\ &+ \theta_a(x,y,z;\alpha) + \theta_c(-x,-y-1,z-1;\delta) \\ =& x(\phi_{bx} - \phi_{ax}) + y(\phi_{ax} - \phi_{ay}) + z(\phi_{bz} - \phi_{ay}) - \phi_{bx} \\ &- \mathfrak{m}_a(\beta) - \mathfrak{m}_c(\gamma) - \mathfrak{m}_b(\alpha) + \mathfrak{m}_a(\alpha) + \mathfrak{m}_c(\delta). \end{aligned} \quad \text{(B39)}$$

We can conclude from the above equation that $\phi_2 \equiv \phi_{ax} = \phi_{ay} = \phi_{bx} = \phi_{bz}$. Thus, we have $f_a(x, y, z) = -(x + y)\phi_2$ and $f_b(x, y, z) = -(x + z)\phi_2$.

For $i \equiv (x, y, z; \beta)$, the above equation is

$$\begin{aligned} 0 &= -\theta_a(y, -z-1, -x; \gamma) - \theta_c(-x, y, -z-1; \delta) \\ &\quad - \theta_b(x-1, y+1, z; \beta) + \theta_a(x, y, z; \beta) \\ &\quad + \theta_c(-x-1, -y-1, z; \gamma) \\ &= -2\phi_2 - \mathfrak{m}_a(\gamma) - \mathfrak{m}_c(\delta) - \mathfrak{m}_b(\beta) + \mathfrak{m}_a(\beta) + \mathfrak{m}_c(\gamma). \end{aligned} \tag{B40}$$

For $i \equiv (x, y, z; \gamma)$, the above equation is

$$\begin{aligned} 0 &= -\theta_a(y+1, -z, -x; \alpha) - \theta_c(-x, y+1, -z; \alpha) \\ &\quad - \theta_b(x-1, y+1, z; \gamma) + \theta_a(x, y, z; \gamma) \\ &\quad + \theta_c(-x-1, -y-1, z-1; \beta) \\ &= -\mathfrak{m}_a(\alpha) - \mathfrak{m}_c(\alpha) - \mathfrak{m}_b(\gamma) + \mathfrak{m}_a(\gamma) + \mathfrak{m}_c(\beta). \end{aligned} \tag{B41}$$

For $i \equiv (x, y, z; \delta)$, the above equation is

$$\begin{aligned} 0 &= -\theta_a(y+1, -z-1, -x; \delta) - \theta_c(-x, y+1, -z-1; \beta) \\ &\quad - \theta_b(x-1, y+1, z; \delta) + \theta_a(x, y, z; \delta) \\ &\quad + \theta_c(-x, -y-1, z; \alpha) \\ &= -\phi_2 - \mathfrak{m}_a(\delta) - \mathfrak{m}_c(\beta) - \mathfrak{m}_b(\delta) + \mathfrak{m}_a(\delta) + \mathfrak{m}_c(\alpha). \end{aligned} \tag{B42}$$

7. Solving Eq. (B4n)

The equation is reduced to

$$\begin{aligned} &- \theta_b\big(g_a^{-1} T_x T_y^{-1} T_z(i)\big) - \theta_a\big(T_x T_y^{-1} T_z(i)\big) \\ &\quad + \theta_b(i) + \theta_a\big(g_b^{-1}(i)\big) = \phi_{ab}. \end{aligned} \tag{B43}$$

For $i \equiv (x, y, z; \alpha)$, the above equation is

$$\begin{aligned} \phi_{ab} &= -\theta_b(-x-1, -y, z; \delta) - \theta_a(x+1, y-1, z+1; \alpha) \\ &\quad + \theta_b(x, y, z; \alpha) + \theta_a(-x-1, y-1, -z; \gamma) \\ &= \phi_2 - \mathfrak{m}_b(\delta) - \mathfrak{m}_a(\alpha) + \mathfrak{m}_b(\alpha) + \mathfrak{m}_a(\gamma). \end{aligned} \tag{B44}$$

For $i \equiv (x, y, z; \beta)$, the above equation is

$$\begin{aligned} \phi_{ab} &= -\theta_b(-x-2, -y, z+1; \gamma) - \theta_a(x+1, y-1, z+1; \beta) \\ &\quad + \theta_b(x, y, z; \beta) + \theta_a(-x-1, y-1, -z-1; \delta) \\ &= \phi_2 - \mathfrak{m}_b(\gamma) - \mathfrak{m}_a(\beta) + \mathfrak{m}_b(\beta) + \mathfrak{m}_a(\delta). \end{aligned} \tag{B45}$$

For $i \equiv (x, y, z; \gamma)$, the above equation is

$$\begin{aligned} \phi_{ab} &= -\theta_b(-x-2, -y, z; \beta) - \theta_a(x+1, y-1, z+1; \gamma) \\ &\quad + \theta_b(x, y, z; \gamma) + \theta_a(-x-1, y, -z; \alpha) \\ &= -\phi_2 - \mathfrak{m}_b(\beta) - \mathfrak{m}_a(\gamma) + \mathfrak{m}_b(\gamma) + \mathfrak{m}_a(\alpha). \end{aligned} \tag{B46}$$

For $i \equiv (x, y, z; \delta)$, the above equation is

$$\begin{aligned} \phi_{ab} &= -\theta_b(-x-1, -y, z+1; \alpha) - \theta_a(x+1, y-1, z+1; \delta) \\ &\quad + \theta_b(x, y, z; \delta) + \theta_a(-x-1, y, -z-1; \beta) \\ &= \phi_2 - \mathfrak{m}_b(\alpha) - \mathfrak{m}_a(\delta) + \mathfrak{m}_b(\delta) + \mathfrak{m}_a(\beta). \end{aligned} \tag{B47}$$

8. Solving Eq. (B4o)

Equation (B4o) is then reduced to

$$\begin{aligned} &- \theta_c\big(g_b^{-1} T_x^{-1} T_y(i)\big) - \theta_b\big(T_x^{-1} T_y(i)\big) + \theta_a(i) \\ &\quad + \theta_b\big(g_a^{-1}(i)\big) + \theta_c\big(g_b^{-1} g_a^{-1}(i)\big) + \theta_b\big(g_c^{-1} g_b^{-1} g_a^{-1}(i)\big) = 0. \end{aligned} \tag{B48}$$

For $i \equiv (x, y, z; \alpha)$, the above equation is

$$\begin{aligned} 0 &= -\theta_c(-x, y, -z; \gamma) - \theta_b(x-1, y+1, z; \alpha) \\ &\quad + \theta_a(x, y, z; \alpha) + \theta_b(-x, -y-1, z-1; \delta) \\ &\quad + \theta_c(x-1, -y-1, -z; \beta) + \theta_b(-y-1, -z, x-1; \delta) \\ &= 2\phi_2 - \mathfrak{m}_c(\gamma) - \mathfrak{m}_b(\alpha) + \mathfrak{m}_a(\alpha) \\ &\quad + \mathfrak{m}_b(\delta) + \mathfrak{m}_c(\beta) + \mathfrak{m}_b(\delta). \end{aligned} \tag{B49}$$

For $i \equiv (x, y, z; \beta)$, the above equation is

$$\begin{aligned} 0 &= -\theta_c(-x, y, -z-1; \delta) - \theta_b(x-1, y+1, z; \beta) \\ &\quad + \theta_a(x, y, z; \beta) + \theta_b(-x-1, -y-1, z; \gamma) \\ &\quad + \theta_c(x, -y-1, -z; \alpha) + \theta_b(-y-1, -z, x; \alpha) \\ &= \phi_2 - \mathfrak{m}_c(\delta) - \mathfrak{m}_b(\beta) + \mathfrak{m}_a(\beta) \\ &\quad + \mathfrak{m}_b(\gamma) + \mathfrak{m}_c(\alpha) + \mathfrak{m}_b(\alpha). \end{aligned} \tag{B50}$$

For $i \equiv (x, y, z; \gamma)$, the above equation is

$$\begin{aligned} 0 &= -\theta_c(-x, y+1, -z; \alpha) - \theta_b(x-1, y+1, z; \gamma) \\ &\quad + \theta_a(x, y, z; \gamma) + \theta_b(-x-1, -y-1, z-1; \beta) \\ &\quad + \theta_c(x, -y-2, -z; \delta) + \theta_b(-y-2, -z, x; \gamma) \\ &= 3\phi_2 - \mathfrak{m}_c(\alpha) - \mathfrak{m}_b(\gamma) + \mathfrak{m}_a(\gamma) \\ &\quad + \mathfrak{m}_b(\beta) + \mathfrak{m}_c(\delta) + \mathfrak{m}_b(\gamma). \end{aligned} \tag{B51}$$

For $i \equiv (x, y, z; \delta)$, the above equation is

$$\begin{aligned} 0 &= -\theta_c(-x, y+1, -z-1; \beta) - \theta_b(x-1, y+1, z; \delta) \\ &\quad \theta_a(x, y, z; \delta) + \theta_b(-x, -y-1, z; \alpha) \\ &\quad + \theta_c(x-1, -y-2, -z; \gamma) + \theta_b(-y-2, -z, x-1; \beta) \\ &= 2\phi_2 - \mathfrak{m}_c(\beta) - \mathfrak{m}_b(\delta) + \mathfrak{m}_a(\delta) \\ &\quad + \mathfrak{m}_b(\alpha) + \mathfrak{m}_c(\gamma) + \mathfrak{m}_b(\beta). \end{aligned} \tag{B52}$$

9. Collected equations for ms

In this subsection, we summarize the coupled equations to solve for ms. Before doing so, we note that we can use the SU(2) gauge symmetry to fix certain ms. Recall that the action of the gauge transformation is

$$g.t. : \theta_U(i) \mapsto w(i) + \theta_U(i) - w(U^{-1}(i)). \tag{B53}$$

We start off in a generic gauge where all ms are nontrivial. We first perform the gauge transformation $w(\beta) = -\mathfrak{m}_c(\beta)$ and $w(\gamma) = +\mathfrak{m}_c(\delta)$. The consequence is that $\mathfrak{m}_c(\beta) = \mathfrak{m}_c(\delta) = 0$. And because $\mathfrak{m}_c(\beta) + \mathfrak{m}_c(\gamma) + \mathfrak{m}_c(\delta) = 0$ from one of our constraints, we have $\mathfrak{m}_c(\gamma) = 0$. We then perform the gauge transformation $w(\alpha) = -\mathfrak{m}_a(\alpha)$, such that $\mathfrak{m}_a(\alpha) = 0$. And because $\mathfrak{m}_a(\alpha) + \mathfrak{m}_a(\delta) = \phi_a - \phi_2$ from one of our constraints, we have $\mathfrak{m}_a(\delta) = \phi_a - \phi_2$.

The remaining equations after the reductions are

$$3\mathfrak{m}_c(\alpha) = 0, \tag{B54a}$$
$$\mathfrak{m}_a(\beta) + \mathfrak{m}_a(\gamma) = \phi_a - 2\phi_2, \tag{B54b}$$
$$\mathfrak{m}_b(\alpha) + \mathfrak{m}_b(\gamma) = \phi_b - \phi_2, \tag{B54c}$$
$$\mathfrak{m}_b(\beta) + \mathfrak{m}_b(\delta) = \phi_b - 2\phi_2, \tag{B54d}$$
$$-\mathfrak{m}_a(\beta) - \mathfrak{m}_b(\alpha) = \phi_2, \tag{B54e}$$
$$-\mathfrak{m}_a(\gamma) - \mathfrak{m}_b(\beta) + \mathfrak{m}_a(\beta) = 2\phi_2, \tag{B54f}$$
$$-\mathfrak{m}_c(\alpha) - \mathfrak{m}_b(\gamma) + \mathfrak{m}_a(\gamma) = 0, \tag{B54g}$$
$$-\mathfrak{m}_b(\delta) + \mathfrak{m}_c(\alpha) = \phi_2, \tag{B54h}$$
$$-\mathfrak{m}_b(\delta) + \mathfrak{m}_b(\alpha) + \mathfrak{m}_a(\gamma) = \phi_{ab} - \phi_2, \tag{B54i}$$
$$-\mathfrak{m}_b(\gamma) - \mathfrak{m}_a(\beta) + \mathfrak{m}_b(\beta) = \phi_{ab} - \phi_a, \tag{B54j}$$
$$-\mathfrak{m}_b(\beta) - \mathfrak{m}_a(\gamma) + \mathfrak{m}_b(\gamma) = \phi_{ab} + \phi_2, \tag{B54k}$$
$$-\mathfrak{m}_b(\alpha) + \mathfrak{m}_b(\delta) + \mathfrak{m}_a(\beta) = \phi_{ab} + \phi_a - 2\phi_2, \tag{B54l}$$
$$-\mathfrak{m}_b(\alpha) + \mathfrak{m}_b(\delta) + \mathfrak{m}_b(\delta) = -2\phi_2, \tag{B54m}$$
$$-\mathfrak{m}_b(\beta) + \mathfrak{m}_a(\beta) + \mathfrak{m}_b(\gamma) + \mathfrak{m}_c(\alpha) + \mathfrak{m}_b(\alpha) = -\phi_2, \tag{B54n}$$
$$-\mathfrak{m}_c(\alpha) - \mathfrak{m}_b(\gamma) + \mathfrak{m}_a(\gamma) + \mathfrak{m}_b(\beta) + \mathfrak{m}_b(\gamma) = -3\phi_2, \tag{B54o}$$
$$-\mathfrak{m}_b(\delta) + \mathfrak{m}_b(\alpha) + \mathfrak{m}_b(\beta) = -\phi_a - \phi_2. \tag{B54p}$$

We now set $A \equiv \mathfrak{m}_c(\alpha)$, $B \equiv \mathfrak{m}_a(\beta)$, $C \equiv \mathfrak{m}_b(\alpha)$, and $D \equiv \mathfrak{m}_b(\beta)$. Equation (B54e) tells us that $-B - C = \phi_2$. Also, Eq. (B54f) tells us that $D = 2B - \phi_a$. Thus all the $\mathfrak{m}$s can be represented using A and B, as deduced from Eq. (B54a)–(B54f),

$$\begin{aligned}
\mathfrak{m}_a(\alpha) &= 0,\\
\mathfrak{m}_a(\beta) &= B,\\
\mathfrak{m}_a(\gamma) &= \phi_a - 2\phi_2 - B,\\
\mathfrak{m}_a(\delta) &= \phi_a - \phi_2,\\
\mathfrak{m}_b(\alpha) &= -\phi_2 - B,\\
\mathfrak{m}_b(\beta) &= 2B - \phi_a,\\
\mathfrak{m}_b(\gamma) &= \phi_b + B,\\
\mathfrak{m}_b(\delta) &= \phi_b - 2\phi_2 + \phi_a - 2B,\\
\mathfrak{m}_c(\alpha) &= A,\\
\mathfrak{m}_c(\beta) &= 0,\\
\mathfrak{m}_c(\gamma) &= 0,\\
\mathfrak{m}_c(\delta) &= 0.
\end{aligned} \tag{B55}$$

Equation (B54g) tells us that

$$A + 2B = \phi_a - \phi_b - 2\phi_2, \tag{B56}$$

whereas Eq. (B54h) tells us that

$$A + 2B = \phi_a + \phi_b - \phi_2. \tag{B57}$$

From which we can see that $\phi_2 = -2\phi_b$. Now if we look at Eq. (B54i), we have $\phi_{ab} = -\phi_b$. In fact, Eqs. (B54j)–(B54l) do not tell us more than this. Equation (B54m) tells us that $3B = 4\phi_b + 2\phi_a$, Eq. (B54n) tells us that $A - B = -\phi_a - \phi_b$, Eq. (B54o) tells us that $A - B = -2\phi_b$ and finally Eq. (B54p) tells us that $3B = \phi_a + \phi_b - 2\phi_2$. The above relations allow us to assert that

$$\phi_3 \equiv -\phi_{ab} = \phi_a = \phi_b, \quad \phi_2 = -2\phi_3, \quad B = A + 2\phi_3, \tag{B58}$$

and

$$\begin{aligned}
\mathfrak{m}_a(\alpha) &= 0,\\
\mathfrak{m}_a(\beta) &= A + 2\phi_3,\\
\mathfrak{m}_a(\gamma) &= 3\phi_3 - A,\\
\mathfrak{m}_a(\delta) &= 3\phi_3,\\
\mathfrak{m}_b(\alpha) &= -A,\\
\mathfrak{m}_b(\beta) &= -A + 3\phi_3,\\
\mathfrak{m}_b(\gamma) &= 3\phi_3 + A,\\
\mathfrak{m}_b(\delta) &= 2\phi_3 + A,\\
\mathfrak{m}_c(\alpha) &= A,\\
\mathfrak{m}_c(\beta) &= 0,\\
\mathfrak{m}_c(\gamma) &= 0,\\
\mathfrak{m}_c(\delta) &= 0.
\end{aligned} \tag{B59}$$

We also have

$$f_a(i) = 2(x + y)\phi_3, \quad f_b(i) = 2(x + z)\phi_3. \tag{B60}$$

Similar to the Z_2 case, we now consider a further gauge transformation,

$$\begin{aligned}
w(x, y, z; \alpha) &= +2\phi_3 - \phi_3(x + y + z),\\
w(x, y, z; \beta/\gamma/\delta) &= -\phi_3(x + y + z),
\end{aligned} \tag{B61}$$

we see that

(1) $G_x = G_y = G_z = e^{-i\phi_3\tau_z}$;

(2) $G_{a/b/c}(x, y, z; s) = e^{i\mathfrak{m}_{a/b/c}(s)\tau_z}$, where the $\mathfrak{m}$s have the following forms:

$$\begin{aligned}
&\mathfrak{m}_a(\alpha) = 0, \quad \mathfrak{m}_a(\beta) = A, \quad \mathfrak{m}_a(\gamma) = -A, \quad \mathfrak{m}_a(\delta) = 0;\\
&\mathfrak{m}_b(\alpha) = -A, \quad \mathfrak{m}_b(\beta) = -A, \quad \mathfrak{m}_b(\gamma) = A, \quad \mathfrak{m}_b(\delta) = A;\\
&\mathfrak{m}_c(\alpha) = A, \quad \mathfrak{m}_c(\beta) = 0, \quad \mathfrak{m}_c(\gamma) = 0, \quad \mathfrak{m}_c(\delta) = 0.
\end{aligned} \tag{B62}$$

Because of the fact that ϕ_3 now becomes global signs that are elements of the IGG, we conclude that ϕ_3 is redundant. We also remark that a gauge transformation $W(x, y, z; s) \equiv i\tau_x$ maps the PSG solutions in which $\mathcal{A} = e^{i\frac{2\pi}{3}\tau_z}$ to that in which $\mathcal{A} = e^{i\frac{4\pi}{3}\tau_z}$.

In conclusion, we have

(1) $G_x = G_y = G_z = \tau_0$;

(2) $G_{a/b/c}(x, y, z; s) = e^{i\mathfrak{m}_{a/b/c}(s)\tau_z}$, where the $\mathfrak{m}$s have the following forms:

$$\begin{aligned}
&\mathfrak{m}_a(\alpha) = 0, \quad \mathfrak{m}_a(\beta) = A, \quad \mathfrak{m}_a(\gamma) = -A, \quad \mathfrak{m}_a(\delta) = 0;\\
&\mathfrak{m}_b(\alpha) = -A, \quad \mathfrak{m}_b(\beta) = -A, \quad \mathfrak{m}_b(\gamma) = A, \quad \mathfrak{m}_b(\delta) = A;\\
&\mathfrak{m}_c(\alpha) = A, \quad \mathfrak{m}_c(\beta) = 0, \quad \mathfrak{m}_c(\gamma) = 0, \quad \mathfrak{m}_c(\delta) = 0,
\end{aligned} \tag{B63}$$

where $\mathcal{A} = \tau_0, e^{i\frac{2\pi}{3}\tau_z}$.

10. Adding time-reversal symmetry

We firstly write the algebraic relations,

$$G_{\mathcal{T}}(i)G_{\mathcal{T}}(i) = e^{i\phi_{\mathcal{T}}\tau_z}, \tag{B64a}$$
$$G_{\mathcal{T}}^{\dagger}\big(T_x^{-1}(i)\big)G_x^{\dagger}(i)G_{\mathcal{T}}(i)G_x(i) = e^{i\phi_{x\mathcal{T}}\tau_z}, \tag{B64b}$$
$$G_{\mathcal{T}}^{\dagger}\big(T_y^{-1}(i)\big)G_y^{\dagger}(i)G_{\mathcal{T}}(i)G_y(i) = e^{i\phi_{y\mathcal{T}}\tau_z}, \tag{B64c}$$
$$G_{\mathcal{T}}^{\dagger}\big(T_z^{-1}(i)\big)G_z^{\dagger}(i)G_{\mathcal{T}}(i)G_z(i) = e^{i\phi_{z\mathcal{T}}\tau_z}, \tag{B64d}$$
$$G_{\mathcal{T}}^{\dagger}\big(g_a^{-1}(i)\big)G_a^{\dagger}(i)G_{\mathcal{T}}(i)G_a(i) = e^{i\phi_{a\mathcal{T}}\tau_z}, \tag{B64e}$$
$$G_{\mathcal{T}}^{\dagger}\big(g_b^{-1}(i)\big)G_b^{\dagger}(i)G_{\mathcal{T}}(i)G_b(i) = e^{i\phi_{b\mathcal{T}}\tau_z}, \tag{B64f}$$
$$G_{\mathcal{T}}^{\dagger}\big(g_c^{-1}(i)\big)G_c^{\dagger}(i)G_{\mathcal{T}}(i)G_c(i) = e^{i\phi_{c\mathcal{T}}\tau_z}. \tag{B64g}$$

As usual, the canonical form of $G_{\mathcal{T}}(i) = (i\tau_x)^{n_{\mathcal{T}}}e^{i\theta_{\mathcal{T}}(i)\tau_z}$. When $n_{\mathcal{T}} = 0$, we can show that $G_{\mathcal{T}} = i\tau_z$ uniformly much like the case for Z_2. Since the derivation is very similar to the Z_2 case, it is not included here. This group of PSG solutions does not produce mean-field $\mathsf{U}(1)$ spin liquids if we consider the constraint imposed by TRS. For the rest of the Appendix, let us focus on the case when $n_{\mathcal{T}} = 1$.

Let us first look at Eq. (B64a), we straightforwardly conclude that $\phi_{\mathcal{T}} = \pi$. We denote $\theta_{\mathcal{T}} \equiv f_{\mathcal{T}}(x, y, z; s) + \mathfrak{m}_{\mathcal{T}}(s)$. Then, Eqs. (B64b)–(B64d) tell us that

$$f_{\mathcal{T}}(x, y, z; s) = x\phi_{x\mathcal{T}} + y\phi_{y\mathcal{T}} + z\phi_{z\mathcal{T}}. \tag{B65}$$

We would like to plug the above results into Eq. (B64g). We arrive at the following constraint:

$$-\theta_{\mathcal{T}}\big(g_c^{-1}(i)\big) + 2\theta_c(i) + \theta_{\mathcal{T}}(i) = \phi_{c\mathcal{T}}. \tag{B66}$$

For the case with $i = (x, y, z; \alpha)$, we have

$$\begin{aligned}\phi_{c\mathcal{T}} &= -\theta_{\mathcal{T}}(y, z, x; \alpha) + 2A + \theta_{\mathcal{T}}(x, y, z; \alpha)\\ &= x(\phi_{x\mathcal{T}} - \phi_{y\mathcal{T}}) + y(\phi_{y\mathcal{T}} - \phi_{z\mathcal{T}})\\ &\quad + z(\phi_{z\mathcal{T}} - \phi_{x\mathcal{T}}) + 2A,\end{aligned} \tag{B67}$$

we arrive at $\phi_4 \equiv \phi_{x\mathcal{T}} = \phi_{y\mathcal{T}} = \phi_{z\mathcal{T}}$, and $\phi_{c\mathcal{T}} = -A$, where we used $3A = 0$.

For the case with $i = (x, y, z; \beta)$, we have

$$\begin{aligned}\phi_{c\mathcal{T}} &= -\theta_{\mathcal{T}}(y, z, x; \delta) + \theta_{\mathcal{T}}(x, y, z; \beta)\\ &= -\mathfrak{m}_{\mathcal{T}}(\delta) + \mathfrak{m}_{\mathcal{T}}(\beta).\end{aligned} \tag{B68}$$

For the case with $i = (x, y, z; \gamma)$, we have

$$\begin{aligned}\phi_{c\mathcal{T}} &= -\theta_{\mathcal{T}}(y, z, x; \beta) + \theta_{\mathcal{T}}(x, y, z; \gamma)\\ &= -\mathfrak{m}_{\mathcal{T}}(\beta) + \mathfrak{m}_{\mathcal{T}}(\gamma).\end{aligned} \tag{B69}$$

For the case with $i = (x, y, z; \delta)$, we have

$$\begin{aligned}\phi_{c\mathcal{T}} &= -\theta_{\mathcal{T}}(y, z, x; \gamma) + \theta_{\mathcal{T}}(x, y, z; \delta)\\ &= -\mathfrak{m}_{\mathcal{T}}(\gamma) + \mathfrak{m}_{\mathcal{T}}(\delta).\end{aligned} \tag{B70}$$

Thus, if we denote $\mathfrak{m}_{\mathcal{T}}(\beta) \equiv E$, we have $\mathfrak{m}_{\mathcal{T}}(\gamma) = E - A$ and $\mathfrak{m}_{\mathcal{T}}(\delta) = E + A$.

We now look at Eq. (B64e). Similar to the case before,

$$-\theta_{\mathcal{T}}\big(g_a^{-1}(i)\big) + 2\theta_a(i) + \theta_{\mathcal{T}}(i) = \phi_{a\mathcal{T}}. \tag{B71}$$

For the case with $i = (x, y, z; \alpha)$, we have

$$\begin{aligned}\phi_{a\mathcal{T}} &= -\theta_{\mathcal{T}}(-x, -y - 1, z - 1; \delta)\\ &\quad + 2\mathfrak{m}_a(\alpha) + \theta_{\mathcal{T}}(x, y, z; \alpha)\\ &= -(-x - y - 1 + z - 1)\phi_4 - \mathfrak{m}_{\mathcal{T}}(\delta)\\ &\quad + (x + y + z)\phi_4 + \mathfrak{m}_{\mathcal{T}}(\alpha)\\ &= x(2\phi_4) + y(2\phi_4)\\ &\quad + 2\phi_4 + \mathfrak{m}_{\mathcal{T}}(\alpha) - \mathfrak{m}_{\mathcal{T}}(\delta),\end{aligned} \tag{B72}$$

from which we have

$$2\phi_4 = 0, \quad \mathfrak{m}_{\mathcal{T}}(\alpha) - \mathfrak{m}_{\mathcal{T}}(\delta) = \phi_{a\mathcal{T}}. \tag{B73}$$

For the case with $i = (x, y, z; \beta)$, we have

$$\begin{aligned}\phi_{a\mathcal{T}} &= -\theta_{\mathcal{T}}(-x - 1, -y - 1, z; \gamma)\\ &\quad + 2\mathfrak{m}_a(\beta) + \theta_{\mathcal{T}}(x, y, z; \beta)\\ &= \mathfrak{m}_{\mathcal{T}}(\beta) - \mathfrak{m}_{\mathcal{T}}(\gamma) + 2A\\ &= 0.\end{aligned} \tag{B74}$$

For the case with $i = (x, y, z; \gamma)$, we have

$$\begin{aligned}\phi_{a\mathcal{T}} &= -\theta_{\mathcal{T}}(-x - 1, -y - 1, z - 1; \beta)\\ &\quad + 2\mathfrak{m}_a(\gamma) + \theta_{\mathcal{T}}(x, y, z; \gamma)\\ &= 3\phi_4 + \mathfrak{m}_{\mathcal{T}}(\gamma) - \mathfrak{m}_{\mathcal{T}}(\beta) - 2A\\ &= 3\phi_4.\end{aligned} \tag{B75}$$

Note that this relation combined with the one before, gives us $\phi_4 = 0$.

For the case with $i = (x, y, z; \delta)$, we have

$$\begin{aligned}\phi_{a\mathcal{T}} &= -\theta_{\mathcal{T}}(-x, -y - 1, z; \alpha)\\ &\quad + 2\mathfrak{m}_a(\delta) + \theta_{\mathcal{T}}(x, y, z; \delta)\\ &= \phi_4 + \mathfrak{m}_{\mathcal{T}}(\delta) - \mathfrak{m}_{\mathcal{T}}(\alpha).\end{aligned} \tag{B76}$$

Combining the above constraints, we arrive at a set of relations summarized here,

$$\begin{aligned}\phi_{a\mathcal{T}} = \phi_4 = 0\\ \mathfrak{m}_{\mathcal{T}}(\alpha) = \mathfrak{m}_{\mathcal{T}}(\delta),\\ \mathfrak{m}_{\mathcal{T}}(\beta) = \mathfrak{m}_{\mathcal{T}}(\gamma) + A.\end{aligned} \tag{B77}$$

Let us now look at Eq. (B64f),

$$-\theta_{\mathcal{T}}\big(g_b^{-1}(i)\big) + 2\theta_b(i) + \theta_{\mathcal{T}}(i) = \phi_{b\mathcal{T}}. \tag{B78}$$

For the case with $i = (x, y, z; \alpha)$, we have

$$\begin{aligned}\phi_{b\mathcal{T}} &= -\theta_{\mathcal{T}}(-x - 1, y - 1, -z; \gamma)\\ &\quad + 2\mathfrak{m}_b(\alpha) + \theta_{\mathcal{T}}(x, y, z; \alpha)\\ &= -2A + \mathfrak{m}_{\mathcal{T}}(\alpha) - \mathfrak{m}_{\mathcal{T}}(\gamma).\end{aligned} \tag{B79}$$

For the case with $i = (x, y, z; \beta)$, we have

$$\begin{aligned}\phi_{b\mathcal{T}} &= -\theta_{\mathcal{T}}(-x - 1, y - 1, -z - 1; \delta)\\ &\quad + 2\mathfrak{m}_b(\beta) + \theta_{\mathcal{T}}(x, y, z; \beta)\\ &= -2A + \mathfrak{m}_{\mathcal{T}}(\beta) - \mathfrak{m}_{\mathcal{T}}(\delta).\end{aligned} \tag{B80}$$

For the case with $i = (x, y, z; \gamma)$, we have

$$\begin{aligned}\phi_{b\mathcal{T}} &= -\theta_{\mathcal{T}}(-x-1, y, -z; \alpha) \\ &\quad + 2\mathfrak{m}_b(\gamma) + \theta_{\mathcal{T}}(x, y, z; \gamma) \\ &= 2A + \mathfrak{m}_{\mathcal{T}}(\gamma) - \mathfrak{m}_{\mathcal{T}}(\alpha). \end{aligned} \tag{B81}$$

For the case with $i = (x, y, z; \delta)$, we have

$$\begin{aligned}\phi_{b\mathcal{T}} &= -\theta_{\mathcal{T}}(-x-1, y, -z-1; \beta) \\ &\quad + 2\mathfrak{m}_b(\delta) + \theta_{\mathcal{T}}(x, y, z; \delta) \\ &= 2A + \mathfrak{m}_{\mathcal{T}}(\delta) - \mathfrak{m}_{\mathcal{T}}(\beta). \end{aligned} \tag{B82}$$

Combining the above constraints, we arrive at $\phi_{b\mathcal{T}} = 0$ and no new relations.

We can then summarize:

$$\begin{aligned}\mathfrak{m}_{\mathcal{T}}(\alpha) &= E + A, \\ \mathfrak{m}_{\mathcal{T}}(\beta) &= E, \\ \mathfrak{m}_{\mathcal{T}}(\gamma) &= E - A, \\ \mathfrak{m}_{\mathcal{T}}(\delta) &= E + A. \end{aligned} \tag{B83}$$

In the above, E is a free $\mathsf{U}(1)$ phase. However, note that we did not make use of the IGG gauge degrees of freedom associated with TRS. Recalling that $G_{\mathcal{T}} \sim G_{\mathcal{T}} W_{\mathcal{T}}$, where $W_{\mathcal{T}} \in \mathsf{U}(1)$. We choose $W_{\mathcal{T}} \equiv \exp(-iE)$, thus eliminating the free phase in our solutions. We collect the $\mathsf{U}(1)$ PSG solutions into Table III. Thus, we have

$$\begin{aligned}G_{\mathcal{T}}(\vec{r}, \alpha) &= i\tau_x e^{iA\tau_z}, \\ G_{\mathcal{T}}(\vec{r}, \beta) &= i\tau_x, \\ G_{\mathcal{T}}(\vec{r}, \gamma) &= i\tau_x e^{-iA\tau_z}, \\ G_{\mathcal{T}}(\vec{r}, \delta) &= i\tau_x e^{iA\tau_z}. \end{aligned} \tag{B84}$$

APPENDIX C: MEAN-FIELD ANSATZES FOR THE PSG SOLUTIONS

Our PSG classification obtains a set of gauge-inequivalent transformations G_g for all $g \in \mathsf{P}2_13 \times \mathsf{Z}_2$. In this Appendix, we derive the constraints imposed on the mean-field parameters U_{ij} and μ_i by requiring that an element of the PSG leaves the ansatz invariant. We repeat this condition for convenience,

$$\begin{aligned}&\forall g : G_g^\dagger(g(i)) U_{g(i)g(j)} G_g(g(j)) = U_{ij}, \\ &\quad G_g^\dagger(g(i)) \mu_{g(i)} G_g(g(i)) = \mu_i. \end{aligned} \tag{18}$$

1. Z_2

Here, we specify the ansatzes for the PSGs corresponding to the IGG being Z_2. As derived in Appendix A and displayed in Table II in the main text, the four Z_2 PSGs can be indexed by, $\mathcal{A} = \exp(i2\pi n/3)$ for $i = 0, 1$, and $\mathcal{E} = \tau_0$ or $\mathcal{E} = i\tau_z$, in terms of which all gauge transformations are listed in Table II.

We note that if $G_{\mathcal{T}} = \tau_0$ then the invariance of the ansatz under time-reversal requires $U_{ij} = -U_{ij}$ and $\mu_i = -\mu_i$, leading to no nonzero mean-field ansatzes.

For $G_{\mathcal{T}} = i\tau_z$, the invariance under TRS requires the following form for all links and sites:

$$U_{ij} = U_{ij}^x \tau_x + U_{ij}^y \tau_y \tag{C1}$$

$$\mu_i = \mu_i^x \tau_x + \mu_i^y \tau_y. \tag{C2}$$

Finally, since $G_x = G_y = G_z = \tau_0$ in our solutions, we must require U_{ij} and μ_{ij} to be translationally invariant. We then encode the dependence of the parameters U_{ij} on the link (ij) by determining U for each of the unique links in Table I, and determining the functions U_i^x, U_i^y, where $i \in \{1, 2 \cdots 12\}$ specifies the link in Table I. The on-site parameters are described as $\mu_\alpha, \mu_\beta, \mu_\gamma$, and μ_δ, where the subscripts denote the sublattice dependence.

Imposing the invariance of the ansatz under the action of (G_c, g_c), we get the following relations between four groups of links that are closed under the application of g_c,

$$\begin{aligned}U_1 &= U_5 = U_9, \\ U_2 &= U_6 = U_{10}, \\ U_3 &= \mathcal{A}^2 U_7 = \mathcal{A} U_{11}, \\ U_4 &= \mathcal{A}^2 U_8 = \mathcal{A} U_{12}. \end{aligned} \tag{C3}$$

The relations between different groups of links are obtained by the invariance under (G_b, g_b) and (G_a, g_a). The action of (G_a, g_a) gives us

$$\begin{aligned}U_1 &= U_2, \\ U_3 &= U_4, \\ U_5 &= \mathcal{A} U_7, \\ U_6 &= \mathcal{A} U_8, \\ U_9 &= \mathcal{A}^2 U_{12}, \\ U_{10} &= \mathcal{A}^2 U_{11}. \end{aligned} \tag{C4}$$

Similarly, the invariance of all links under (G_b, g_b) give us the conditions

$$\begin{aligned}U_1 &= U_3, \\ U_2 &= U_4, \\ U_5 &= \mathcal{A} U_8, \\ U_6 &= \mathcal{A} U_7, \\ U_9 &= U_{10}, \\ U_{11} &= U_{12}. \end{aligned} \tag{C5}$$

Combining the conditions in Eqs. (C3)–(C5) we find that the U_{ij} for all links can be specified in terms of only two parameters U^x and U^y,

$$\begin{aligned}&U_1 = U^x \tau_x + U^y \tau_y, \\ &U_2 = U_1, \quad U_3 = U_1, \quad U_4 = U_1, \\ &U_5 = U_1, \quad U_6 = U_1, \quad U_7 = \mathcal{A} U_1, \\ &U_8 = \mathcal{A} U_1, \quad U_9 = U_1, \quad U_{10} = U_1, \\ &U_{11} = \mathcal{A} U_1, \quad U_{12} = \mathcal{A} U_1. \end{aligned} \tag{C6}$$

Similarly, demanding the invariance of μ_i under (G_c, g_c) gives us $\mu_\gamma = \mu_\delta = \mu_\beta$, and $\mu_\alpha = \mathcal{A}\mu_\alpha$. Under (G_a, g_a), we

have $\mu_\alpha = \mu_\delta$ and $\mu_\beta = \mathcal{A}\mu_\gamma$. This already implies that when $\mathcal{A} \neq 1$, $\mu = 0$ on all sites. When $\mathcal{A} = 1$, site-independent on-site terms of the form $\mu^x\tau_x + \mu^y\tau_y$ are allowed in the ansatz.

2. PSG-protected gapless nodal star in $Z_2$1 spin liquid

In this Appendix, we prove that the mean-field Hamiltonian $H_{\mathrm{MFT}}(\vec{k})$ [Eqs. (7) and (23)] for the $Z_2$1 QSL has two zero-energy eigenvalues for $\vec{k} = (\pm k, \pm k, \pm k)$. To this end, we first work out the most general PSG-allowed $H_{\mathrm{MFT}}(\vec{k})$ for the $Z_2$1 QSL. The rest of the discussion assumes the translation invariance of the ansatzes, which is true for all our QSLs. First, we use the basis $(\psi_1^\alpha, \psi_2^\alpha, \cdots \psi_1^\delta \psi_2^\delta)$ to express the $H_{\mathrm{MFT}}(\vec{k})$ in terms of 2×2 blocks as

$$H_{\mathrm{MFT}}(\vec{k}) = \begin{pmatrix} h_{\alpha,\alpha}(\vec{k}) & h_{\alpha,\beta}(\vec{k}) & h_{\alpha,\gamma}(\vec{k}) & h_{\alpha,\gamma}(\vec{k}) \\ h_{\beta,\alpha}(\vec{k}) & h_{\beta,\beta}(\vec{k}) & h_{\beta,\gamma}(\vec{k}) & h_{\beta,\gamma}(\vec{k}) \\ h_{\gamma,\alpha}(\vec{k}) & h_{\gamma,\beta}(\vec{k}) & h_{\gamma,\gamma}(\vec{k}) & h_{\gamma,\gamma}(\vec{k}) \\ h_{\delta,\alpha}(\vec{k}) & h_{\delta,\beta}(\vec{k}) & h_{\delta,\gamma}(\vec{k}) & h_{\delta,\gamma}(\vec{k}) \end{pmatrix}. \tag{C7}$$

As just demonstrated in the previous section, when $\mathcal{A} \neq 1$ and $G_{\mathcal{T}} = i\tau_z$, we have $h_{\alpha,\alpha} = h_{\beta,\beta} = h_{\gamma,\gamma} = h_{\delta,\delta} = 0$ for all $\vec{k}$. The block matrices have the form $U_x\tau^x + U_y\tau^y$ [Eq. (C2)] in real space, leading to

$$h_{\alpha,\beta}(\vec{r}, \vec{r}') = \begin{pmatrix} 0 & U_{\alpha,\beta}(\vec{r} - \vec{r}') \\ U^*_{\alpha,\beta}(\vec{r} - \vec{r}') & 0 \end{pmatrix} \tag{C8}$$

for a complex amplitude $U(\vec{r})$. The Fourier-transformed equivalent is given by

$$h_{\alpha,\beta}(\vec{k}) = \frac{1}{N}\sum_{\vec{r},\vec{r}'} h_{\alpha,\beta}(\vec{r}, \vec{r}')e^{i\vec{k}.(\vec{r}-\vec{r}')} \tag{C9}$$

$$= \begin{pmatrix} 0 & U_{\alpha,\beta}(\vec{k}) \\ U^*_{\alpha,\beta}(-\vec{k}) & 0 \end{pmatrix}. \tag{C10}$$

Foreseeing repeated appearances of the off-diagonal form in Eq. (C10), we introduce the shorthand $M[u(k)]$, defined by

$$M[u(\vec{k})] = \begin{pmatrix} 0 & u(\vec{k}) \\ u^*(-\vec{k}) & 0 \end{pmatrix}. \tag{C11}$$

Also note that from Eq. (4) we know that $h_{\alpha,\beta}(\vec{r}, \vec{r}') = h_{\beta,\alpha}(\vec{r}', \vec{r})$. So we have from Eq. (C10),

$$h_{\alpha,\beta}(\vec{k}) = h_{\alpha,\beta}(-\vec{k}) \tag{C12}$$

The action of symmetries on the block matrices in k-space can be worked from their real-space equivalents, given by Eq. (12). To show this explicitly for a general symmetry transformation g, we assume the unit-cell independence of gauge transformations that has been shown for all our QSLs. To simplify cumbersome expressions, we introduce the shorthand $\bar{\alpha}$ and $g_\alpha(\vec{r})$ to denote the sublattice index and unit-cell position of the operation $g(\vec{r}; \alpha)$. We have, from Eq. (18),

$$\begin{aligned}
(G_g, g)\colon \left(h_{\alpha,\beta}(\vec{k}) = \frac{1}{N}\sum_{\vec{r},\vec{r}'} h_{\alpha,\beta}(\vec{r}, \vec{r}')e^{i\vec{k}.(\vec{r}-\vec{r}')}\right) \\
= \frac{1}{N}\sum_{\vec{r},\vec{r}'} G_g^\dagger(\bar{\alpha})h_{\bar{\alpha}\bar{\beta}}(g_\alpha(\vec{r}), g_\beta(\vec{r}'))G_g(\bar{\beta})e^{i\vec{k}.(\vec{r}-\vec{r}')} \\
= \frac{1}{N}\sum_{\vec{r},\vec{r}'} G_g^\dagger(\bar{\alpha})h_{\bar{\alpha}\bar{\beta}}(\vec{r}, \vec{r}')G_g(\bar{\beta})e^{i\vec{k}.(g_{\bar{\alpha}}^{-1}\vec{r} - g_{\bar{\beta}}^{-1}(\vec{r}'))} \\
= \frac{1}{N}\sum_{\vec{r},\vec{r}'} G_g^\dagger(\bar{\alpha})h_{\bar{\alpha}\bar{\beta}}(\vec{r}, \vec{r}')G_g(\bar{\beta})e^{i\vec{k}'.(\vec{r}-\vec{r}')+\phi_g(\alpha,\beta)} \\
= G_g^\dagger(\bar{\alpha})h_{\bar{\alpha},\bar{\beta}}(\vec{k}')G_g(\bar{\beta})e^{i\phi_g(\alpha,\beta)} \\
\Rightarrow (G_g, g)\colon h_{\alpha,\beta}(\vec{k}) \mapsto G_g^\dagger(\bar{\alpha})h_{\bar{\alpha},\bar{\beta}}(\vec{k}')G_g(\bar{\beta})e^{i\phi_g(\alpha,\beta)}.
\end{aligned} \tag{C13}$$

From the third line to the fourth, we have used the fact that one can always write $\vec{k}.(g_{\bar{\alpha}}^{-1}\vec{r} - g_{\bar{\beta}}^{-1}(\vec{r}'))$ as $\vec{k}'.(\vec{r} - \vec{r}') + \phi_g(\alpha, \beta)$ for some $\vec{k}'$ and a constant $\phi_g(\alpha, \beta)$ independent of $\vec{r} - \vec{r}'$—this is always true for symmetry operations that are linearly represented on the lattice sites.

Now, let us consider the symmetry transformation $g = g_b.g_a$ acting on $h_{\alpha,\beta}$. Using Eq. (C13), followed by Eq. (C12), we find

$$\begin{aligned}
h_{\alpha,\beta}(k_x, k_y, k_z) &= h_{\beta,\alpha}(k_x, -k_y, -k_z)e^{ik_x} \\
&= h_{\alpha,\beta}(-k_x, k_y, k_z)e^{ik_x}.
\end{aligned} \tag{C14}$$

Equation (C14) can only be satisfied if the real-space amplitudes $u(\vec{r}, \vec{r}')$ in Eq. (C8) satisfy

$$U_{\alpha,\beta}(\vec{r}) = u(y, z)(\delta_{x,1} + \delta_{x,0}), \tag{C15}$$

where δ is the Kronecker delta not to be confused with the sublattice index, and $u(y, z)$ is any complex function of the coordinates y and z. This form implies that

$$\begin{aligned}
h_{\alpha,\beta} &= M[u(k_y, k_z)\zeta(k_x)], \\
\zeta(k_x) &= (1 + \exp(ik_x)).
\end{aligned} \tag{C16}$$

The function $u(k_x, k_y)$ is the Fourier transform of $u(y, z)$ defined in Eq. (C15). All other block matrices in Eq. (C7) can be expressed in terms of $u(k_x, k_y)$ by applying symmetry transformations to $h_{\alpha,\beta}$. Applying g_c to $h_{\alpha,\beta}$ using Eq. (C13) gives us

$$\begin{aligned}
h_{\alpha,\gamma} &= \mathcal{A}M[u(k_z, k_x)\zeta(k_y)], \\
h_{\alpha,\delta} &= \mathcal{A}^2M[u(k_x, k_y)\zeta(k_z)], \quad \text{where} \\
\mathcal{A} &= \exp(i(2\pi/3)\tau^z).
\end{aligned}$$

We note that

$$\mathcal{A}^nM[u] = M[\omega^n u], \quad \text{where } \omega = 2\pi/3. \tag{C17}$$

This gives us

$$\begin{aligned}
h_{\alpha,\gamma} &= M[\omega u(k_z, k_x)\zeta(k_y)], \\
h_{\alpha,\delta} &= M[\omega^2 u(k_x, k_y)\zeta(k_z)], \quad \text{where} \\
\omega &= \exp(i2\pi/3).
\end{aligned} \tag{C18}$$

Applying g_b to $h_{\gamma,\delta}$ gives us

$$h_{\gamma,\delta} = M[\omega^2 u(k_y, -k_z)\zeta(-k_x)\exp(ik_x)]. \tag{C19}$$

Finally, applying g_c and g_c^2 to $h_{\gamma,\delta}$ gives us

$$\begin{aligned} h_{\beta,\gamma} &= M[\omega^2 u(k_x, -k_y)\zeta(-k_z)\exp(ik_y)], \\ h_{\delta,\beta} &= M[\omega^2 u(k_z, -k_x)\zeta(-k_y)\exp(ik_x)]. \end{aligned} \tag{C20}$$

$$h(\vec{k}) = \begin{pmatrix} 0 & \zeta(k_x)u(k_y, k_z) \\ \zeta(-k_x)u(-k_y, -k_z) & 0 \\ \omega\zeta(-k_y)u(-k_z, -k_x) & \omega^2 e^{-ik_y}\zeta(k_z)u(-k_x, k_y) \\ \omega^2\zeta(-k_z)u(-k_x, -k_y) & \omega^2 e^{ik_x}\zeta(-k_y)u(k_z, -k_x) \end{pmatrix}$$

Now, we proceed to show that $h(\vec{k})$ has a maximum rank of 3 on the points $(\pm k, \pm k, \pm k)$. First consider $\vec{k} = (k, k, k)$. With the further shorthands

$$\begin{aligned} &u = u(k, k), \quad v = u(-k, -k), \quad \rho = u(k, -k), \\ &\lambda = u(-k, k), \quad \zeta = \zeta(k), \quad r = e^{ik}, \end{aligned} \tag{C23}$$

we have

$$h(k, k, k) = \begin{pmatrix} 0 & \zeta u & \zeta u\omega & \zeta u\omega^2 \\ \zeta^* v & 0 & \zeta\rho\omega^2 & \zeta^*\lambda\omega^2 \\ \zeta^* v\omega & \zeta^*\lambda\omega^2 & 0 & \zeta\rho\omega^2 \\ \zeta^* v\omega^2 & \zeta\rho\omega^2 & \zeta^*\lambda\omega^2 & 0 \end{pmatrix}$$

$h(k, k, k)$ can now be brought to the row-echelon form by the sequence of elementary row-transformations given by

$$\begin{aligned} &R_2 \leftrightarrow R_1, \quad R_3 \to \omega^2 R_3 - R_1, \quad R_4 \to \omega R_4 - R_1, \\ &R_3 \to u\omega^2\zeta R_3 - \lambda\zeta^* R_2, \quad R_4 \to R_4 u - R_2\rho, \\ &R_4 = -u\omega^2(\zeta\rho(\omega^2+1) - \zeta^*\lambda\omega^2)R_4 \\ &\qquad + u\zeta\omega(\zeta^*\lambda + \zeta\rho)R_3, \end{aligned}$$

in conjunction with the using the identities $\omega^3 = 1$, $\zeta r* = \zeta^*$ and $rr^* = 1$. The result of the row transformations is

$$\begin{pmatrix} \zeta^* v & 0 & \zeta^*\rho r\omega^2 & \zeta\lambda r^*\omega^2 \\ 0 & \zeta u & \zeta u\omega & \zeta u\omega^2 \\ 0 & 0 & \zeta u(\omega^2+1)(\zeta^*\lambda + \zeta\rho) & \zeta u(\zeta^*\lambda + \zeta\rho) \\ 0 & 0 & 0 & 0 \end{pmatrix}.$$

The appearance of the 0 in the last diagonal element establishes that the maximum rank of $h(k, k, k)$ can be 3.

The analysis need not be repeated for the H_{MFT} at other gapless points like $(-k, k, k)$, $(k, -k, k)$ etc. All of $h(\pm k, \pm k, \pm k)$ are related to $h(k, k, k)$ by elementary "rank-preserving" row and column transformations. $h(-k, k, k)$ can be obtained from $h(k, k, k)$ by the transformations

$$\begin{aligned} &R_1 \leftrightarrow R_2, R_3 \leftrightarrow R_4, \\ &C_1 \leftrightarrow C_2, C_3 \leftrightarrow C_4, \\ &R_4 \to r^* C_4, C_4 \to rC_4, \end{aligned} \tag{C24}$$

Equations (C16) and (C18)–(C20), along with Eq. (C12) specify the most general form of all block matrices appearing in $H_{\mathrm{MFT}}(\vec{k})$ in Eq. (C7) that is allowed by projective symmetries of the $\mathsf{Z}_2 1$ state.

Now, we express $H_{\mathrm{MFT}}(\vec{k})$ in the basis $(\psi_1^\alpha, \cdots \psi_1^\delta, \psi_2^\alpha, \cdots \psi_2^\delta)$ to have

$$H_{\mathrm{MFT}}(\vec{k}) = \begin{pmatrix} 0 & h(\vec{k}) \\ h^\dagger(\vec{k}) & 0 \end{pmatrix}. \tag{C21}$$

The matrix the most general $h(\vec{k})$ allowed by the PSG is given by

$$\begin{pmatrix} \omega\zeta(k_y)u(k_z, k_x) & \omega^2\zeta(k_z)u(k_x, k_y) \\ \omega^2 e^{ik_y}\zeta(-k_z)u(k_x, -k_y) & \omega^2 e^{-ik_x}\zeta(k_y)u(-k_z, k_x) \\ 0 & \omega^2 e^{ik_z}\zeta(-k_x)u(k_y, -k_z) \\ \omega^2 e^{-ik_z}\zeta(k_x)u(-k_y, k_z) & 0 \end{pmatrix}. \tag{C22}$$

followed by two re-identifications: $u \leftrightarrow v$, which have been considered independent complex numbers in the proof; and $\omega \leftrightarrow \omega^2$ that survive the important properties $\omega^3 = 1$ and $1 + \omega + \omega^2 = 0$. $h(k, -k, k)$ can be obtained in turn from $h(-k, k, k)$ by the transformations

$$R_2 \to R_3, \quad R_3 \to R_4, \quad R_4 \to R_2, \tag{C25}$$

$$C_2 \to C_3, \quad C_3 \to C_4, \quad C_4 \to C_2, \tag{C26}$$

$$R_1 \to \omega R_1, \quad C_1 \to \omega C_1. \tag{C27}$$

$h(k, k, -k)$ can be obtained from $h(-k, k, k)$ by the transformations

$$R_2 \to R_4, \quad R_4 \to R_3, \quad R_3 \to R_2, \tag{C28}$$

$$C_2 \to C_4, \quad C_4 \to C_3, \quad C_3 \to C_2, \tag{C29}$$

$$R_1 \to \omega^2 R_1, \quad C_1 \to \omega^2 C_1. \tag{C30}$$

This completes the proof that $h(\pm k, \pm k, \pm k)$ has a maximum rank of 3, and consequently, $H_{\mathrm{MFT}}(\pm k, \pm k, \pm k)$ has two gapless bands that are protected by projective symmetries against the addition of arbitrarily long-ranged terms in the mean-field ansatz.

3. U(1)

The $\mathsf{U}(1)$ spin liquid mean-field ansatz has the following form:

$$U_{ij} = iU_{ij}^0\tau_0 + U_{ij}^z\tau_z, \tag{C31}$$

dictated by the fact that the ansatz is invariant under the $\mathsf{U}(1)$ IGG gauge transformation. We would like to investigate how the PSG solutions we obtained constrain the nearest-neighbor mean-field ansatz by subjecting them to the following test:

$$\forall g \in \mathsf{P}2_1 3 \times \mathsf{Z}_2^{\mathcal{T}} : \hat{G}_g \hat{g}(U_{ij}) = U_{ij}. \tag{C32}$$

Among the PSGs we have, we first study the class in which $A = 0$. After enumerating all the conditions imposed by the PSG, we arrive at the following nearest-neighbor mean-field

ansatz in the class where $A = 0$,

$$U_i = \lambda\tau_z, \quad \text{where } i \in \{1, \ldots, 12\}. \tag{C33}$$

Next, we would like to argue that, when $A \neq 0$, there would be no nearest-neighbor mean-field ansatz. We write $U_{1/3} \equiv i\mathfrak{U}_{1/3}\exp[i\varphi_{1/3}\tau_z]$. The TRS conditions on these two bonds give

$$2\varphi_1 + 2A = \pi, \quad \varphi_3 = \pi/2. \tag{C34}$$

However, the condition $\hat{G}_b\hat{g}_b(U_1) = U_1$ gives us

$$\varphi_3 + A + 4\phi_3 = \varphi_1. \tag{C35}$$

Multiplying the above equation by 2 and combining with the two previous relations, we would immediately arrive at $5A = 0$. Note that we had $3A = 0$. Thus the ansatz does not vanish only when $A = 0$.

We conclude that we obtain only one nearest-neighbor $\mathsf{U}(1)$ mean-field ansatz,

$$\begin{aligned} U_\zeta &= \lambda\tau_z, \quad \zeta \in \{1, \ldots, 12\} \\ a_s &= \omega\tau_z, \quad i \in \{\alpha, \ldots, \delta\}. \end{aligned} \tag{C36}$$

[1] C. Broholm, R. J. Cava, S. A. Kivelson, D. G. Nocera, M. R. Norman, and T. Senthil, Quantum spin liquids, Science **367**, eaay0668 (2020).

[2] L. Savary and L. Balents, Quantum spin liquids: A review, Rep. Prog. Phys. **80**, 016502 (2017).

[3] R. Moessner, Magnets with strong geometric frustration, Can. J. Phys. **79**, 1283 (2001).

[4] J. T. Chalker, *Spin Liquids and Frustrated Magnetism* (Oxford University Press, Oxford, 2017).

[5] R. Moessner and J. T. Chalker, Low-temperature properties of classical geometrically frustrated antiferromagnets, Phys. Rev. B **58**, 12049 (1998).

[6] D. A. Garanin and B. Canals, Classical spin liquid: Exact solution for the infinite-component antiferromagnetic model on the kagomé lattice, Phys. Rev. B **59**, 443 (1999).

[7] S. V. Isakov, K. Gregor, R. Moessner, and S. L. Sondhi, Dipolar spin correlations in classical pyrochlore magnets, Phys. Rev. Lett. **93**, 167204 (2004).

[8] B. Canals and C. Lacroix, Mean-field study of the disordered ground state in the β-Mn lattice, Phys. Rev. B **61**, 11251 (2000).

[9] S. V. Isakov, J. M. Hopkinson, and H.-Y. Kee, Fate of partial order on trillium and distorted windmill lattices, Phys. Rev. B **78**, 014404 (2008).

[10] J. M. Hopkinson, S. V. Isakov, H.-Y. Kee, and Y. B. Kim, Classical antiferromagnet on a hyperkagome lattice, Phys. Rev. Lett. **99**, 037201 (2007).

[11] J. Villain, R. Bidaux, J. P. Carton, and C. R, Order as an effect of disorder, J. Phys. (Paris) **41**, 1263 (1980).

[12] J. T. Chalker, P. C. W. Holdsworth, and E. F. Shender, Hidden order in a frustrated system: Properties of the Heisenberg kagomé antiferromagnet, Phys. Rev. Lett. **68**, 855 (1992).

[13] X.-G. Wen, Quantum orders and symmetric spin liquids, Phys. Rev. B **65**, 165113 (2002).

[14] G. Baskaran and P. W. Anderson, Gauge theory of high-temperature superconductors and strongly correlated Fermi systems, Phys. Rev. B **37**, 580 (1988).

[15] G. Baskaran, Z. Zou, and P. Anderson, The resonating valence bond state and high-Tc superconductivity—A mean field theory, Solid State Commun. **63**, 973 (1987).

[16] I. Affleck, Z. Zou, T. Hsu, and P. W. Anderson, Su(2) gauge symmetry of the large-U limit of the Hubbard model, Phys. Rev. B **38**, 745 (1988).

[17] E. Dagotto, E. Fradkin, and A. Moreo, SU(2) gauge invariance and order parameters in strongly coupled electronic systems, Phys. Rev. B **38**, 2926 (1988).

[18] X.-G. Wen and P. A. Lee, Theory of underdoped cuprates, Phys. Rev. Lett. **76**, 503 (1996).

[19] X. G. Wen, Mean-field theory of spin-liquid states with finite energy gap and topological orders, Phys. Rev. B **44**, 2664 (1991).

[20] Y. Zhou and X.-G. Wen, Quantum orders and spin liquids in Cs_2CuCl_4, arXiv:cond-mat/0210662.

[21] Y.-M. Lu, Symmetric Z_2 spin liquids and their neighboring phases on triangular lattice, Phys. Rev. B **93**, 165113 (2016).

[22] Y.-M. Lu and Y. Ran, $\mathbb{Z}_2$ spin liquid and chiral antiferromagnetic phase in the Hubbard model on a honeycomb lattice, Phys. Rev. B **84**, 024420 (2011).

[23] Y.-Z. You, I. Kimchi, and A. Vishwanath, Doping a spin-orbit Mott insulator: Topological superconductivity from the Kitaev-Heisenberg model and possible application to $(Na_2/Li_2)IrO_3$, Phys. Rev. B **86**, 085145 (2012).

[24] Y.-M. Lu, Y. Ran, and P. A. Lee, $\mathbb{Z}_2$ spin liquids in the $S = \frac{1}{2}$ Heisenberg model on the kagome lattice: A projective symmetry-group study of Schwinger fermion mean-field states, Phys. Rev. B **83**, 224413 (2011).

[25] S. Bieri, L. Messio, B. Bernu, and C. Lhuillier, Gapless chiral spin liquid in a kagome Heisenberg model, Phys. Rev. B **92**, 060407(R) (2015).

[26] S. Bieri, C. Lhuillier, and L. Messio, Projective symmetry group classification of chiral spin liquids, Phys. Rev. B **93**, 094437 (2016).

[27] M. J. Lawler, A. Paramekanti, Y. B. Kim, and L. Balents, Gapless spin liquids on the three-dimensional hyperkagome lattice of $Na_4Ir_3O_8$, Phys. Rev. Lett. **101**, 197202 (2008).

[28] B. Huang, Y. B. Kim, and Y.-M. Lu, Interplay of nonsymmorphic symmetry and spin-orbit coupling in hyperkagome spin liquids: Applications to $Na_4Ir_3O_8$, Phys. Rev. B **95**, 054404 (2017).

[29] L. E. Chern and Y. B. Kim, Theoretical study of quantum spin liquids in $S = \frac{1}{2}$ hyper-hyperkagome magnets: Classification, heat capacity, and dynamical spin structure factor, Phys. Rev. B **104**, 094413 (2021).

[30] J. Sonnenschein, A. Chauhan, Y. Iqbal, and J. Reuther, Projective symmetry group classifications of quantum spin liquids on the simple cubic, body centered cubic, and face centered cubic lattices, Phys. Rev. B **102**, 125140 (2020).

[31] A. Maity, F. Ferrari, R. Thomale, S. Mandal, and Y. Iqbal, Projective symmetry group classification of Abrikosov fermion mean-field ansätze on the square-octagon lattice, Phys. Rev. B **107**, 134438 (2023).

[32] A. Chauhan, A. Maity, C. Liu, J. Sonnenschein, F. Ferrari, and Y. Iqbal, Quantum spin liquids on the diamond lattice, Phys. Rev. B **108**, 134424 (2023).

[33] L. E. Chern, Y. B. Kim, and C. Castelnovo, Competing quantum spin liquids, gauge fluctuations, and anisotropic interactions in a breathing pyrochlore lattice, Phys. Rev. B **106**, 134402 (2022).

[34] C. Liu, G. B. Halász, and L. Balents, Symmetric U(1) and $\mathbb{Z}_2$ spin liquids on the pyrochlore lattice, Phys. Rev. B **104**, 054401 (2021).

[35] B. Huang, W. Choi, Y. B. Kim, and Y.-M. Lu, Classification and properties of quantum spin liquids on the hyperhoneycomb lattice, Phys. Rev. B **97**, 195141 (2018).

[36] L. Capriotti, F. Becca, A. Parola, and S. Sorella, Resonating valence bond wave functions for strongly frustrated spin systems, Phys. Rev. Lett. **87**, 097201 (2001).

[37] Y. Iqbal, F. Becca, and D. Poilblanc, Projected wave function study of $\mathbb{Z}_2$ spin liquids on the kagome lattice for the spin-$\frac{1}{2}$ quantum Heisenberg antiferromagnet, Phys. Rev. B **84**, 020407(R) (2011).

[38] Y. Iqbal, F. Becca, S. Sorella, and D. Poilblanc, Gapless spin-liquid phase in the kagome spin-$\frac{1}{2}$ Heisenberg antiferromagnet, Phys. Rev. B **87**, 060405(R) (2013).

[39] Y. Iqbal, D. Poilblanc, and F. Becca, Vanishing spin gap in a competing spin-liquid phase in the kagome Heisenberg antiferromagnet, Phys. Rev. B **89**, 020407(R) (2014).

[40] R. Shindou, S. Yunoki, and T. Momoi, Projective studies of spin nematics in a quantum frustrated ferromagnet, Phys. Rev. B **84**, 134414 (2011).

[41] W.-J. Hu, F. Becca, A. Parola, and S. Sorella, Direct evidence for a gapless Z_2 spin liquid by frustrating Néel antiferromagnetism, Phys. Rev. B **88**, 060402(R) (2013).

[42] F. Ferrari and F. Becca, Spectral signatures of fractionalization in the frustrated Heisenberg model on the square lattice, Phys. Rev. B **98**, 100405(R) (2018).

[43] Z.-X. Liu, Y. Zhou, and T.-K. Ng, Fermionic theory for quantum antiferromagnets with spin $s > \frac{1}{2}$, Phys. Rev. B **82**, 144422 (2010).

[44] S. Bieri, M. Serbyn, T. Senthil, and P. A. Lee, Paired chiral spin liquid with a Fermi surface in $S = 1$ model on the triangular lattice, Phys. Rev. B **86**, 224409 (2012).

[45] A. Maity, R. Thomale, and Y. Iqbal, Projective symmetry group classification of quantum spin liquid mean field ansatze in spin-1 diamond lattice (unpublished).

[46] F. Wang and A. Vishwanath, Spin-liquid states on the triangular and kagomé lattices: A projective-symmetry-group analysis of Schwinger boson states, Phys. Rev. B **74**, 174423 (2006).

[47] F. Wang, Schwinger boson mean field theories of spin liquid states on a honeycomb lattice: Projective symmetry group analysis and critical field theory, Phys. Rev. B **82**, 024419 (2010).

[48] H.-K. Jin and Y. Zhou, Classical and quantum order in hyperkagome antiferromagnets, Phys. Rev. B **101**, 054408 (2020).

[49] L. Messio, S. Bieri, C. Lhuillier, and B. Bernu, Chiral spin liquid on a kagome antiferromagnet induced by the Dzyaloshinskii-Moriya interaction, Phys. Rev. Lett. **118**, 267201 (2017).

[50] J. M. Hopkinson and H.-Y. Kee, Geometric frustration inherent to the trillium lattice, a sublattice of the B20 structure, Phys. Rev. B **74**, 224441 (2006).

[51] I. Živković, V. Favre, C. Salazar Mejia, H. O. Jeschke, A. Magrez, B. Dabholkar, V. Noculak, R. S. Freitas, M. Jeong, N. G. Hegde, L. Testa, P. Babkevich, Y. Su, P. Manuel, H. Luetkens, C. Baines, P. J. Baker, J. Wosnitza, O. Zaharko, Y. Iqbal, J. Reuther, and H. M. Rønnow, Magnetic field induced quantum spin liquid in the two coupled trillium lattices of $K_2Ni_2(SO_4)_3$, Phys. Rev. Lett. **127**, 157204 (2021).

[52] M. G. Gonzalez, V. Noculak, A. Sharma, V. Favre, J.-R. Soh, A. Magrez, R. Bewley, H. O. Jeschke, J. Reuther, H. M. Rønnow, Y. Iqbal, and I. Živković, Dynamics of $K_2Ni_2(SO_4)_3$ governed by proximity to a 3D spin liquid model, Nat. Commun. **15**, 7191 (2024).

[53] W. Yao, Q. Huang, T. Xie, A. Podlesnyak, A. Brassington, C. Xing, R. S. D. Mudiyanselage, W. Xie, S. Zhang, M. Lee, V. S. Zapf, X. Bai, D. A. Tennant, J. Liu, and H. Zhou, Continuous spin excitations in the three-dimensional frustrated magnet $K_2Ni_2(SO_4)_3$, Phys. Rev. Lett. **131**, 146701 (2023).

[54] K. Boya, K. Nam, K. Kargeti, A. Jain, R. Kumar, S. Panda, S. Yusuf, P. Paulose, U. Voma *et al.*, Signatures of spin-liquid state in a 3D frustrated lattice compound KSrFe2 (PO4) 3 with S= 5/2, APL Mater. **10**, 101103 (2022).

[55] B. Koteswararao, R. Kumar, P. Khuntia, S. Bhowal, S. K. Panda, M. R. Rahman, A. V. Mahajan, I. Dasgupta, M. Baenitz, K. H. Kim, and F. C. Chou, Magnetic properties and heat capacity of the three-dimensional frustrated $S = \frac{1}{2}$ antiferromagnet $PbCuTe_2O_6$, Phys. Rev. B **90**, 035141 (2014).

[56] S. Chillal, Y. Iqbal, H. O. Jeschke, J. A. Rodriguez-Rivera, R. Bewley, P. Manuel, D. Khalyavin, P. Steffens, R. Thomale, A. T. M. N. Islam, J. Reuther, and B. Lake, Evidence for a three-dimensional quantum spin liquid in $PbCuTe_2O_6$, Nat. Commun. **11**, 2348 (2020).

[57] P. Khuntia, F. Bert, P. Mendels, B. Koteswararao, A. V. Mahajan, M. Baenitz, F. C. Chou, C. Baines, A. Amato, and Y. Furukawa, Spin liquid state in the 3D frustrated antiferromagnet $PbCuTe_2O_6$: NMR and muon spin relaxation studies, Phys. Rev. Lett. **116**, 107203 (2016).

[58] F. Wang, A. Vishwanath, and Y. B. Kim, Quantum and classical spins on the spatially distorted kagome lattice: Applications to volborthite $Cu_3V_2O_7(OH)_2 \cdot 2H_2O$, Phys. Rev. B **76**, 094421 (2007).

[59] S. Biswas and K. Damle, Semiclassical theory for liquidlike behavior of the frustrated magnet $Ca_{10}Cr_7O_{28}$, Phys. Rev. B **97**, 115102 (2018).

[60] S. Biswas, Y. H. Kwan, and S. A. Parameswaran, Beyond the freshman's dream: Classical fractal spin liquids from matrix cellular automata in three-dimensional lattice models, Phys. Rev. B **105**, 224410 (2022).

[61] M. J. Lawler, H.-Y. Kee, Y. B. Kim, and A. Vishwanath, Topological spin liquid on the hyperkagome lattice of $Na_4Ir_3O_8$, Phys. Rev. Lett. **100**, 227201 (2008).

[62] Y. Zhou, P. A. Lee, T.-K. Ng, and F.-C. Zhang, $Na_4Ir_3O_8$ as a 3D spin liquid with fermionic spinons, Phys. Rev. Lett. **101**, 197201 (2008).

[63] Y. Okamoto, M. Nohara, H. Aruga-Katori, and H. Takagi, Spin-liquid state in the $S = 1/2$ hyperkagome antiferromagnet $Na_4Ir_3O_8$, Phys. Rev. Lett. **99**, 137207 (2007).

[64] Y. Singh, Y. Tokiwa, J. Dong, and P. Gegenwart, Spin liquid close to a quantum critical point in $Na_4Ir_3O_8$, Phys. Rev. B **88**, 220413(R) (2013).

[65] R. Dally, T. Hogan, A. Amato, H. Luetkens, C. Baines, J. Rodriguez-Rivera, M. J. Graf, and S. D. Wilson, Short-range

correlations in the magnetic ground state of $Na_4Ir_3O_8$, Phys. Rev. Lett. **113**, 247601 (2014).

[66] A. C. Shockley, F. Bert, J.-C. Orain, Y. Okamoto, and P. Mendels, Frozen state and spin liquid physics in $Na_4Ir_3O_8$: An NMR study, Phys. Rev. Lett. **115**, 047201 (2015).

[67] M. I. Aroyo, J. M. Perez-Mato, C. Capillas, E. Kroumova, S. Ivantchev, G. Madariaga, A. Kirov, and H. Wondratschek, Bilbao crystallographic server I: Databases and crystallographic computing programs, Z. Kristallograp. **221**, 15 (2006).

[68] M. I. Aroyo, A. Kirov, C. Capillas, J. M. Perez-Mato, and H. Wondratschek, Bilbao crystallographic server II: Representations of crystallographic point groups and space groups, Acta Cryst. **A62**, 151 (2006).

[69] M. I. Aroyo, ed., *International Tables for Crystallography, Volume A: Space-group Symmetry*, 6th ed. (Wiley, Hoboken, NJ, 2016).

[70] GAP, GAP – Groups, Algorithms, and Programming, Version 4.12.2, The GAP Group (2022).

[71] L. Messio, C. Lhuillier, and G. Misguich, Time reversal symmetry breaking chiral spin liquids: Projective symmetry group approach of bosonic mean-field theories, Phys. Rev. B **87**, 125127 (2013).

[72] B. Schneider, J. C. Halimeh, and M. Punk, Projective symmetry group classification of chiral $\mathbb{Z}_2$ spin liquids on the pyrochlore lattice: Application to the spin-$\frac{1}{2}$ XXZ Heisenberg model, Phys. Rev. B **105**, 125122 (2022).

[73] P. K. Mogensen, K. Carlsson, S. Villemot, S. Lyon, M. Gomez, C. Rackauckas, T. Holy, D. Widmann, T. Kelman, D. Karrasch *et al.*, https://github.com/JuliaNLSolvers/NLsolve.jl (2020).

[74] J. Bezanson, A. Edelman, S. Karpinski, and V. B. Shah, Julia: A fresh approach to numerical computing, SIAM Rev. **59**, 65 (2017).

[75] F. J. Burnell, S. Chakravarty, and S. L. Sondhi, Monopole flux state on the pyrochlore lattice, Phys. Rev. B **79**, 144432 (2009).

[76] R. V. Mishmash, J. R. Garrison, S. Bieri, and C. Xu, Theory of a competitive spin liquid state for weak Mott insulators on the triangular lattice, Phys. Rev. Lett. **111**, 157203 (2013).